

Andreas Undheim Øgreid

Indirect Evaporative- and Desiccant Wheel Cooling for Norwegian Office

Master's thesis in Energy and Environmental Engineering

Supervisor: Laurent Georges

June 2022

NTNU
Norwegian University of Science and Technology
Faculty of Engineering
Department of Energy and Process Engineering

Andreas Undheim Øgreid

Indirect Evaporative- and Desiccant Wheel Cooling for Norwegian Office

Master's thesis in Energy and Environmental Engineering
Supervisor: Laurent Georges
June 2022

Norwegian University of Science and Technology
Faculty of Engineering
Department of Energy and Process Engineering

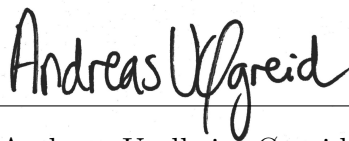
Preface

This master thesis is performed with the Department of Energy and Process Engineering at the Norwegian University of Science and Technology and is written during the spring of 2022. The thesis concludes a two-year MSc degree in Energy and Environmental Engineering and account for 30 ECTS.

I want to thank my supervisor, Associate Professor Laurent Georges, for his great help and guidance during the semester.

Norwegian University of Science and Technology

Trondheim, June 2022



Andreas Undheim Øgreid

Abstract

Global cooling demands are on the rise and actions must therefore be taken to make the operation of HVAC systems more climate-friendly and as energy-efficient as possible. Traditional vapor compression refrigeration cycles possess refrigerants that could be environmentally harmful and require high-grade energy, as electrical energy, for operation. Evaporative cooling techniques dismiss this problem as it does not require any special refrigerants. On the other hand, these evaporative cooling techniques rely on outdoor conditions and may produce insufficient cooling. Rotary desiccant cooling can address these issues as the absolute humidity of the supply air is reduced before being introduced to the evaporative cooler. Desiccant wheels are operated using thermal energy, which can be supplied by lower-grade renewable energy sources like solar energy.

A simplified model of a rotating desiccant wheel has been developed in the building simulation tool IDA ICE. The performance of the desiccant cooling system has been analyzed for a Norwegian office building and compared to indirect evaporative cooling (IEC) and traditional mechanical cooling.

The desiccant wheel model is a continuation of a model that was made in Fall 2021 for a specialization project ahead of this master thesis. The performance of the improved model is dependent on four different parameters rather than two, and the regeneration temperature is now set according to the demand to reduce the energy need. The model is successful in removing moisture while keeping the enthalpy of the air constant, meaning the thermodynamic principles of desiccant wheels are maintained.

Applied systems in Norway are also analyzed to gain knowledge of actual configurations, parameters and control strategies used. Few buildings in Norway possess desiccant cooling, mostly because of high investment costs.

The results of the simulated cases indicated that the AHU configuration with IEC manages to reduce the cooling energy need without influencing the thermal comfort of the building, as the humidity on the supply side remains unchanged. Combining direct- and indirect evaporative cooling resulted in further reduction of cooling energy need, but with slightly reduced thermal comfort. The activation set-point of the desiccant wheel was found to be significant for the energy need due to regeneration of the wheel. Increasing the activation set-point from 16 °C to 20 °C led to a reduction in regeneration energy need of about 51%.

The results of this study is based on net energy need, meaning energy production and losses are not considered. A further study with more focus on delivered energy is therefore suggested to get a more thorough comparison. A such comparison should include the utilization of renewable energy production, as solar thermal collectors, to get the full potential out of the desiccant cooling system.

Sammendrag

Globale kjølebehov er i stadig økning og handlinger må derfor gjøres for å sørge for at driften av VVS-systemer blir mer klimavennlige og så energieffektive som mulig. Tradisjonelle kjølemaskiner inneholder kjølemidler som kan være miljøskadelige og krever energi av høy kvalitet, som elektrisitet, for og driftes. Kjøling ved hjelp av befukning fjerner dette problemet da det ikke krever noen spesielle kjølemidler. På den andre siden avhenger slik kjøling på uteforholdene og kan gi utilstrekkelig kjøling. Kjøling ved hjelp av sorpsjonshjul kan løse disse problemene da den absolutte fuktigheten i tilluften reduseres før befuktningkjølingen skjer. Sorpsjonshjul drives av termisk energi, noe som kan forsynes av fornybare energikilder som solenergi.

En forenklet modell av et sorpsjonshjul er utviklet i bygningssimuleringsverktøyet IDA ICE. Ytelsen av hjulet har blitt analysert for et standard norsk kontorbygg og sammenlignet med adiabatisk kjøling og tradisjonell kjøling med kjølemaskin.

Modellen av sorpsjonshjulet er en fortsettelse på en modell som ble utviklet høsten 2021 ved spesialiseringsemne foran denne masteroppgaven. Ytelsen av den forbedrede modellen er avhengig av fire forskjellige parameter i stedet for to, og regenereringstemperaturen settes nå ut fra det faktiske behovet for å redusere energibehovet. Modellen klarer å fjerne fukt og samtidig holde entalpien konstant, og opprettholder derfor de termodynamiske egenskapene for sorpsjonshjul.

Anvendte systemer i Norge er også analysert for å få kunnskap om konfigurasjoner, parameter og kontrollstrategier brukt i praksis. Få bygninger i Norge benytter sorpsjonskjøling på grunn av høye investeringskostnader.

Resultatet fra simuleringene tyder på at adiabatisk kjøling klarer å senke kjølebehovet uten å påvirke den termiske komforten i bygget, da fuktigheten i tilluften er uendret. Om en adiabatisk befukter legges til på tilluftsiden fører det til enda lavere kjølebehov, men mot noe dårligere termisk komfort og økt PPD. Ved sorpsjonskjøling ble det klart at settpunkt for aktivering av hjulet har stor påvirkning på energibehovet for regenerering. Ved endring av settpunkt fra 16 °C til 20 °C ble energibehovet for regenerering senket med cirka 51%.

Resultatene fra studiet er basert på netto energibehov, hvilket betyr at energiproduksjon og tap ikke er tatt hensyn til. En videre studie med fokus på levert energi er foreslått for å få en mer grundig sammenligning. En slik sammenligning bør inkludere utnyttelsen av fornybare energikilder, som solfangere, for å få det fulle potensialet fra sorpsjonskjøling.

Table of Contents

- List of Figures xii

- List of Tables xv

- Nomenclature xvi

- 1 Introduction 1**
 - 1.1 Goals 2
 - 1.2 Scope 2
 - 1.3 Structure 3

- 2 Theory 4**
 - 2.1 Indoor Climate 4
 - 2.1.1 Thermal Environment 4
 - 2.1.2 Atmospheric Environment 8
 - 2.2 Ventilation 8
 - 2.2.1 Air Flow Rates 8
 - 2.2.2 Control 9
 - 2.3 Energy Needs 10
 - 2.4 Heat Transfer 11
 - 2.4.1 Heat Recovery 11
 - 2.4.2 Power 12
 - 2.5 Air Conditioning Loads 12
 - 2.6 Humid air 13

2.6.1	Absolute Humidity	13
2.6.2	Relative Humidity	13
2.6.3	Dew Point	14
2.6.4	Enthalpy	14
2.6.5	Mollier Diagram	14
2.7	Heat Pump Technology	15
2.7.1	The Heat Pump Process	15
2.7.2	Energy Balance	16
2.7.3	Heat Sources	17
2.8	Desiccants	17
2.9	Dehumidification	18
2.9.1	Cooling Based Dehumidification	18
2.9.2	Desiccant Wheel Dehumidification	18
2.10	Comfort cooling	21
2.10.1	Chiller	21
2.10.2	Direct Evaporative Cooling	22
2.10.3	Indirect Evaporative Cooling	23
2.10.4	Indirect + Direct Evaporative Cooling	24
2.10.5	Desiccant Cooling	25
3	Literature Review	27
3.1	Desiccant Cooling	27
3.2	Indirect Evaporative Cooling	30
4	Applied Systems in Norway	31
4.1	Indirect Evaporative Cooling	31
4.1.1	Fantoftparken	31
4.2	Desiccant Wheel Cooling	35
4.2.1	Søderlundmyra 18	35
4.2.2	Sandnes Helsepark	36
5	Methodology	37

5.1	IDA ICE	37
5.2	Simulation Model	37
5.2.1	Building Structure	38
5.2.2	Weather File	39
5.2.3	Internal Gains	40
5.2.4	Building Services	41
5.3	Desiccant Cooling	43
5.3.1	Wheel Performance	45
5.3.2	IDA ICE Modeling	47
5.3.3	Previous Model	52
5.4	IEC Modeling	53
5.5	Chiller Modeling	54
5.6	Simulations	54
5.6.1	Desiccant Cooling	55
5.6.2	Indirect Evaporative Cooling	56
5.6.3	Chiller	56
6	Results	57
6.1	Base Case	57
6.1.1	Air Flow Review	57
6.1.2	Energy Need	58
6.2	Chiller	59
6.3	Desiccant Cooling	59
6.3.1	Model Validation	59
6.3.2	Energy Need	61
6.3.3	Previous Model	62
6.4	Indirect Evaporative Cooling	63
6.4.1	Model Validation	63
6.4.2	Energy Need	64
6.5	Comparison	66

7 Discussion	67
7.1 Desiccant Wheel Model	67
7.2 Energy Needs	68
7.2.1 Base Case	68
7.2.2 Chiller	68
7.2.3 Indirect Evaporative Cooling	68
7.2.4 Desiccant Cooling	69
7.3 Thermal Comfort	70
7.4 Influencing Factors	70
8 Conclusion	72
8.1 Further Work	74
Bibliography	75
A Appendix	80
A.1 Regression with four independent variables	80
A.1.1 Moisture removal	80

List of Figures

2.1	System boundaries for energy calculations [16].	10
2.2	Sketch of a standard heat pump cycle.	15
2.3	Cooling based dehumidification.	18
2.4	Sketch of desiccant wheel operation.	19
2.5	Sketch of desiccant wheel with purge section.	20
2.6	Section of a desiccant wheel with purge section.	20
2.7	Working principle of a chiller.	21
2.8	Direct evaporative cooling system configuration.	22
2.9	Direct evaporative cooling process in Mollier diagram.	23
2.10	Indirect evaporative cooling system configuration.	23
2.11	Indirect evaporative cooling process in Mollier diagram.	24
2.12	Combined indirect and direct evaporative cooling system configuration.	24
2.13	Indirect + direct evaporative cooling process in Mollier diagram.	25
2.14	Flow chart of Pennington cycle system configuration.	25
2.15	Desiccant cooling process illustrated in Mollier diagram.	26
4.1	Configuration and sensor placement from AHU in Fantoftparken.	32
4.2	Throttle of humidifier LU501 and temperature of intake air.	33
4.3	Throttle of humidifier LU501 and return temperatures before and after humidifier.	33
4.4	Temperatures over heat exchanger on return side.	34
4.5	Throttle of humidifier LU501 and relative humidity of air after humidifier.	34
4.6	Configuration and sensor placement from AHU in S�oderlundmyra.	35

5.1	Visual representation of the modeled ZEB Lab (snipped from IDA ICE).	38
5.2	Schedules for internal gains for office from SN-NSPEK 3031:2020 [17].	40
5.3	Mimic of supply air process in desiccant wheel.	44
5.4	Mollier diagram of desiccant wheel mimic.	45
5.5	Desiccant wheel simulation software [54].	46
5.6	Removed moisture content control in IDA ICE.	48
5.7	Control of set-point moisture content in IDA ICE.	49
5.8	Control of cooling coil in IDA ICE.	49
5.9	Control of heating in IDA ICE.	50
5.10	Activation set-point of the regeneration heater using a Mollier diagram.	51
5.11	Regeneration temperature control.	51
5.12	Configuration of DW AHU in IDA ICE.	52
5.13	Configuration of IEC AHU in IDA ICE.	53
5.14	Configuration of standard air handling unit in IDA ICE.	54
5.15	System boundaries for energy calculation in simulation.	55
5.16	Change in activation set-point for desiccant wheel.	55
6.1	Number of hours above 26 °C for the pre-simulations.	58
6.2	Energy need for simulated period.	58
6.3	Model validation - isenthalpic process.	59
6.4	Temperature change over cooling coil.	60
6.5	Moisture before and after desiccant wheel.	60
6.6	Moisture change in desiccant wheel.	61
6.7	Change in regeneration temperature.	61
6.8	Regeneration energy need and PPD for desiccant cooling system with set-points 16, 18 and 20 C.	62
6.9	Regeneration energy need for desiccant cooling system with various set-point for previous and current model.	62
6.10	Activation of indirect evaporative cooling.	63
6.11	Energy need with indirect evaporative cooling.	64
6.12	Reduced energy need from base case with indirect evaporative cooling. Blue bar is energy need and orange bar is amount reduced from base case scenario.	64

6.13	Energy need with direct and indirect evaporative cooling.	65
6.14	Reduced energy need from base case with indirect and direct evaporative cooling. Blue bar is energy need and orange bar is amount reduced from base case scenario.	65
6.15	Comparison of energy need and PPD of the different systems.	66
A.1	Scatterplot of predicted vs. actual values	88

List of Tables

- 2.1 Thermal comfort factors with belonging category. 5
- 2.2 Recommended operative temperatures for different activity levels from
TEK17 [1]. 7
- 2.3 Heat exchangers with belonging category. 11
- 2.4 Properties found in a Mollier diagram with unit and designation. 14

- 5.1 Zone distribution of ZEB Lab model in IDA ICE. 38
- 5.2 Thermal properties of building parts in IDA ICE model. 39
- 5.3 Window distribution in IDA ICE model per floor and orientation. 39
- 5.4 Internal load at full capacity. 40
- 5.5 Set-points for heating and cooling. 41
- 5.6 Air flows tested in pre-simulations. 42

- 6.1 Pre-simulations of ZEB Lab. 57

- A.1 Inputs and outputs from desiccant wheel simulation. 87
- A.2 Statistics from regression analysis. 88

Nomenclature

\dot{V}	Air flow rate	$[\text{m}^3/h]$
ρ	Density	$[\text{kg}/\text{m}^3]$
C_p	Specific heat	$[\text{J}/\text{kg K}]$
h	Enthalpy	$[\text{J}/\text{kg}]$
Q	Heat	$[\text{W}]$
T	Temperature	$[\text{°C}]$
x	Humidity ratio	$[\text{kg}_w/\text{kg}_{da}]$

Subscripts

amb	Ambient
c	Condenser
da	Dry air
db	Dry bulb
dp	Dew point
e	Evaporator
$regen$	Regeneration
rem	Removed
set	Set-point
w	Water
wb	Wet bulb

List of Abbreviations

AA	Ambient air
AHU	Air handling unit
CC	Cooling coil
COP	Coefficient of performance
DEC	Direct evaporative cooling
DW	Desiccant wheel
EA	Exhaust air
HC	Heating coil
HS	Heat source
HVAC	Heating, Ventilation and Air Conditioning
HX	Heat exchanger
IDA ICE	IDA Indoor Climate and Energy
IEC	Indirect evaporative cooling
NTNU	Norwegian University of Science and Technology
PMV	Predicted mean vote
PPD	Predicted percentage of dissatisfied
RA	Return air
RH	Relative humidity
SA	Supply air
TEK17	Regulations on technical requirements for construction works [1]
VAV	Variable air volume
ZEB	Zero Emission Building

Introduction

Increasing energy consumption and energy efficiency standards have led to buildings becoming more insulated and with less air infiltrations. Increasing insulation leads to buildings having less heating demand and thus quickly warming up. The downside of these new and more insulated buildings is how easily they overheat during summertime, which leads to an increase in cooling demand to keep a healthy indoor climate.

Actions must be taken to make the operation of Heating, Ventilation and Air Conditioning (HVAC) systems more climate-friendly and as energy-efficient as possible. In developed countries, energy for the use of ventilation accounts for 20-40% of the total energy consumption [2]. The global cooling demand in commercial buildings is expected to increase by up to 275% towards 2050 [3]. This increase in cooling demand will likely lead to a tripling in the energy use for air-conditioning by 2050 [4]. Techniques and systems that reduce the energy use for air-conditioning are therefore crucial if targets regarding energy efficiency are to be met [5].

Growing interest in replacing traditional vapor compression refrigeration cycles has occurred over the last few decades. Main reasons for this is the use of refrigerants that could be environmentally harmful and which require high-grade energy, as electrical energy, for compression [6]. Evaporative cooling techniques dismiss the problem as it does not require special refrigerants. Conversely, evaporative cooling techniques rely on outdoor conditions and may produce insufficient cooling [7]. Desiccant cooling can address these issues by reducing the absolute humidity of the supply air before the evaporative cooling takes place. Rotary desiccant technology uses heat to provide cooling and can thus use thermal energy from diverse renewable sources, and also require no special refrigerant. The cooling demand also coincides with the availability of solar energy and allows for the utilization of district heating in the cooling season instead of going to waste.

Several investigations have been done to evaluate the effects of these technologies in various cities and climate zones. Many of these investigations are simulation-based, and some smaller pilot projects have also been conducted. However, no IDA ICE simulation models of desiccant cooling exist, and no investigations have been done on the technologies for a Norwegian office building. This thesis aims to develop a simple rotary desiccant wheel in IDA ICE and to analyze its performance compared to IEC and standard mechanical cooling for a Norwegian office building. The thesis builds upon the findings done in the specialization project performed fall 2021 [8].

1.1 Goals

The assignment is made up of the following sub-goals.

- Review of the existing technologies for cooling based on humidity control (IEC and DW).
- Develop a simple implementation of rotary desiccant wheel cooling in IDA ICE and discuss the advantages and limitations of this implementation.
- Analyze the performance of IEC and rotary desiccant wheel cooling by simulating a Norwegian office building in IDA ICE. Compare the performance in terms energy efficiency and indoor thermal environment with standard mechanical cooling based on heat pump.
- Analyze field measurements from applied systems in Norway if available.
- Propose ideas for further work.

1.2 Scope

This project will be limited to searching the possibilities of creating a simplified desiccant wheel model in IDA ICE for further use. The model is compared with IEC and mechanical cooling for a given office building and will be limited to simulation from May until September and not an entire year. For the simulation, only the net energy need will be compared. This means no losses in the energy system or from pipes will be included. Storage of hot water is also not considered and eventual losses from DHW tank is therefore excluded.

1.3 Structure

The paper starts with presenting background theory and results from a literature review. The theoretic background is stated to establish a theoretical basis regarding indoor environment and HVAC to understand the work presented. After this, the methodology is presented where both the simulation model and the modeling of the cooling systems are presented. Results and discussion of the simulation results are then presented before the conclusion and proposed further work.

The thesis is separated into eight different chapters with content as described below:

Chapter 1 - Introduction

Presents background, goals, scope and structure of the thesis.

Chapter 2 - Theory

Presents necessary theoretical background to establish a basis regarding both indoor environment and HVAC.

Chapter 3 - Literature Review

Presentation of review literature regarding the cooling technologies.

Chapter 4 - Applied Systems in Norway

Introduces existing experience with the investigated cooling systems in Norway.

Chapter 5 - Methodology

Presents the simulation model and the modeling of the cooling systems.

Chapter 6 - Results

Presents the results from simulations.

Chapter 7 - Discussion

Discussion of results from simulations.

Chapter 8 - Conclusion

Conclusion and further work.

Theory

2.1 Indoor Climate

Indoor climate is a term composite of several components influencing different parts of the indoor climate. The five main components of the term are listed below [9].

- Atmospheric environment
- Thermal environment
- Acoustic environment
- Actinic environment
- Mechanical environment

Only the atmospheric- and thermal environment will be discussed further.

2.1.1 Thermal Environment

Thermal Comfort

Thermal comfort is defined in NS-EN ISO 7730 as:

“That condition of mind which expresses satisfaction with the thermal environment.” [10]

Many factors and parameters determine the thermal environment and how occupants perceive it. Professor Fanger [11] established six fundamental factors and their interaction to define the human thermal balance. These are categorized into environmental and behavioral factors, as displayed in Table 2.1.

Environmental	Dry bulb temperature
	Mean radiant temperature
	Relative humidity
	Draught
Behavioral	Clothing
	Metabolic rate

Table 2.1: Thermal comfort factors with belonging category.

Temperature, radiant temperature, humidity, and air movement make up the environmental factors, while clothing and metabolic rate make up the behavioral factors.

Dry-bulb temperature is the measured temperature when radiation from surroundings and moisture are neglected. This temperature is usually referred to as air temperature. According to *Guidance 444*, by the Norwegian Labor Inspection Authority, the air temperature should not exceed 22 °C [12].

Mean radiant temperature is defined by ISO 7730 as *the uniform temperature of an imaginary black enclosure which would result in the same amount of heat loss by radiation from the person as in the actual enclosure* [10]. This temperature is as essential for the heat balance of the human body as the air temperature. It is dependent on the surface temperature of all surrounding surfaces and how the occupant is located relatively to them [9].

Relative humidity has a thermal effect but has a low variation between humidity levels between 20% and 70% [9]. Occupant’s perception of relative humidity is often poor compared to actual measurements. Relative humidity can influence the mucous membrane and static electricity and affect the risk of allergy. The term is explained more in detail in Section 2.6.2.

Draught is the cooling sensation caused by the movement of air. This cooling effect increases with increasing air velocity [9]. Draught can arise when air is cooled by cold surfaces like windows, which cause the air to descend and spread along the floor. This effect can be avoided by placing a heat emitter beneath the cold surface.

Clothing, or clothing insulation, is defined as the thermal resistance of the clothing and is indicated with the unit *clo*. This has a significant influence when evaluating the thermal environment in a room or a building. The *clo* describes the thermal resistance between the skin and the surface of the clothing. For example, a typical summer outfit will equal an insulation level of 0.5 clo, while outerwear will equal 1.5 clo [9].

Metabolic rate is the energy that is developed in the oxidation process of the human body. The energy is expressed per m² body surface area, and a seated resting person will equal about 58 W per m² body surface area. The value for a seated resting occupant is the definition of *met* and thus equals 1 met. If the seated occupant were working and not resting, the metabolic rate would equal about 1.2 met. On average, an occupant with a metabolic rate of 1.2 will give 80.3 W of sensible heat [13].

Heat Balance of the Human Body

The thermal environment consists of the factors that influence the thermal balance of the human body. The inner temperature of the human body is approximately equal to +37 °C with some minor deviations through the day and differs a bit from person to person. Heat production in the body will regulate itself to keep the temperature constant, balancing heat loss and heat production. This relationship between the body's heat production and heat gains/losses can be expressed by the equation below [14].

$$S = M - W - (C_{res} + E_{res} \pm C \pm R + E)$$

where:

- S : Heat storage in the body
- M : Metabolic rate
- W : External work rate
- C_{res} : Respiratory convective heat loss
- E_{res} : Respiratory evaporative heat loss
- C : Convection
- R : Radiation
- E : Evaporation

Operative Temperature

Operative temperature is the combined effect of convection and radiation, making it dependent on air and radiant temperatures. The calculation of operative temperature is given by ISO:7726 and is reproduced in the equation below [15].

$$T_o = \frac{h_c T_a + h_r \bar{T}_r}{h_c + h_r}$$

where:

T_a : Air temperature

\bar{T}_r : Mean radiant temperature

h_c : Convective heat transfer coefficient

h_r : Mean radiant heat transfer coefficient

Suppose the relative air velocity is less than 0.2 m/s and the difference between air temperature and radiant temperature is less than 4 K. In that case, the operative temperature can be calculated as the average of the air temperature and mean radiant temperature as shown in the equation below [9].

$$T_o = \frac{T_a + \bar{T}_r}{2}$$

Regulations on technical requirements for construction works (TEK17) give recommended values for operative temperature based on activity level and are shown in Table 2.2.

Activity	Light	Medium	Heavy
Operative temperature range [°C]	19 - 26	16 - 26	10 - 26

Table 2.2: Recommended operative temperatures for different activity levels from TEK17 [1].

The lower limit should always be fulfilled, but on the warmest days, the upper limit can be exceeded up to 50 hours per year. This means that the indoor temperature can be above 26 °C for no more than 50 hours a year [1].

Thermal Comfort Criteria

In practice, all occupants in a given space will never be fully satisfied with the environment, and there will always be a certain degree of dissatisfaction. To evaluate the deviation from ideal comfort, the PMV- and PPD index was created by danish professor P.O. Fanger in 1970. The thermal comfort indices were later introduced as European standards [9].

PMV is short for “Predicted Mean Vote” and expresses how an occupant feels about the thermal environment and has evolved from experimental data. The index is based on a seven-point scale ranging from -3 to +3, as shown below.

- +3 Very hot
- +2 Hot
- +1 Slightly hot
- 0 Neutral (Comfortable)
- 1 Slightly cold
- 2 Cold
- 3 Very cold

PPD is short for “Predicted Percentage of Dissatisfied” and expresses how many percent of occupants are expected to be dissatisfied with the thermal environment. Since it is not possible for every occupant to be satisfied with the thermal environment, the PPD for a PMV of 0 is 5%.

It is recommended by NS-ISO 7730 [10] to keep the PPD under 10%, which corresponds to a PMV between -0.5 and 0.5.

2.1.2 Atmospheric Environment

CO₂ Concentration

Carbon dioxide is one of the first gases identified in the air. Small amounts of CO₂ are not dangerous, but higher levels affect the perceived air quality. According to *Guidance 444* [12], it is recommended that the concentration of CO₂ is kept under 1000 ppm. Outdoor air has a CO₂ concentration of around 350-400 ppm [9].

2.2 Ventilation

The purpose of ventilation is to maintain a good and healthy indoor environment and is done by the removal of contaminants. These contaminants can, for example, be heat, gases, particles, moisture, and more. The air should be utilized in the best manner possible while avoiding discomfort like draught.

2.2.1 Air Flow Rates

An important detail in ventilation is the air needed to maintain a healthy environment. When deciding the air flow rate for a room or a zone, TEK17 states that the flow should be based on the following three variables [1].

A - Occupants

B - Emissions

C - Processes

The minimum flow rate should be the minimum out of either (A+B) or C. For occupants, TEK17 requires a minimum of 26 m³/h per occupant for light activity. Ventilation based on emissions depends on the amount of emission from both building materials and furniture.

If low emitting materials are used, TEK17 requires a minimum of 2.5 m³/h per m² floor area during occupational hours and 0.7 m³/h per m² floor area outside occupational hours.

2.2.2 Control

In general, there are three ways to control how air flow is regulated in a ventilation system: CAV, VAV, and DCV. These strategies are elaborated in the sections below.

CAV

CAV, or “constant air volume”, is a control strategy where the air flow rate is kept constant. This is the simplest of the control strategies and also the cheapest. A disadvantage of this solution is unnecessary ventilation of rooms not in use, which is a waste of energy [9].

VAV

VAV, or “variable air volume”, is a control strategy where the air flow rate varies with time. It is the most basic demand control but allows the air to be adjusted in response to factors like temperature, CO₂ concentration, or occupancy. This control strategy removes the disadvantage of CAV but requires more expensive equipment [9].

DCV

DCV, or “demand controlled ventilation”, is a control strategy that varies the air flow over time like VAV. However, DCV is a more advanced demand control and adjusts the supplied flow in response to actual demand in a given room or zone. Demand controlled ventilation offers additional energy savings, but for a higher investment cost [9].

2.3 Energy Needs

Figure 2.1 principally illustrates the energy flow through a building. It is normal to differentiate between different types of energy needs in a building, depending on which factors are included in the calculation or not.

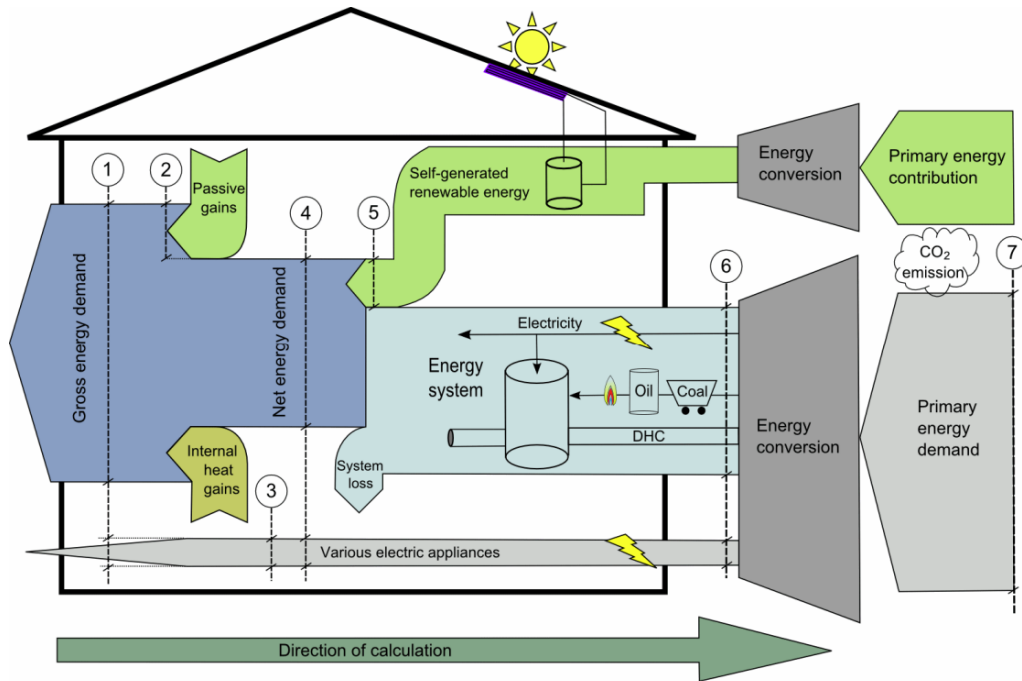


Figure 2.1: System boundaries for energy calculations [16].

Gross Energy Need

The energy need of the building when regardless of both passive gains and internal gains. The gross energy need is shown as point one in Figure 2.1.

Net Energy Need

Net energy needs are the building's energy needs regardless of the energy system's efficiency or losses in the energy chain. It is the same as the gross energy need when passive and internal gains are subtracted. The net energy need is illustrated as point four in Figure 2.1.

Delivered Energy

Delivered energy is shown as point six in Figure 2.1 and refers to the delivered energy to the site before any conversion and therefore includes losses and the energy system's efficiency.

2.4 Heat Transfer

2.4.1 Heat Recovery

Heat exchangers, or heat recovery units, transfer heat from air to air. There are several heat exchangers for ventilation purposes, but they can be split into two categories. These categories are regenerative and recuperative heat exchangers. Table 2.3 below show the most common heat exchangers used in Norway and which category they belong to [9].

Category	Type
Regenerative	Rotating heat exchanger
	Chamber exchanger
Recuperative	Heat pump
	Plate heat exchanger
	Run-around heat exchanger

Table 2.3: Heat exchangers with belonging category.

Regenerative heat exchangers transfer both sensible and latent heat, transferring humidity from return air to supply air.

Recuperative heat exchangers transfer only sensible heat because the air streams are physically separated and never in contact.

The efficiency of a heat exchanger is often given as temperature efficiency, which is the relationship between actual temperature change and maximum temperature change. The equation is shown below [17]:

$$\eta_T = \frac{T_2 - T_1}{T_3 - T_1} * 100\%$$

where:

T_1 : Supply temperature before HX [°C]

T_2 : Supply temperature after HX [°C]

T_3 : Exhaust temperature before HX [°C]

If the return air is cooler than the outside air, the heat exchanger can be used to recover cooling, reducing the cooling demand of the outside air.

2.4.2 Power

The air entering a building or room will affect its state. If the air entering is cooler than the indoor air temperature, the room will be cooled and vice versa. The following equation is used to calculate the amount of power induced by the air. If the power is negative, it means cooling is being done.

$$\dot{Q} = \dot{V} \cdot \rho \cdot C_p \cdot (T_s - T_i) \cdot \frac{1 \text{ h}}{3600 \text{ s}}$$

where:

\dot{Q} : Power [kW]

\dot{V} : Air flow rate [m³/h]

ρ : Air density [kg/m³]

C_p : Specific heat [kJ/kg*K]

T_i : Indoor air temperature [°C]

T_s : Supply air temperature [°C]

2.5 Air Conditioning Loads

There are two different air conditioning loads, namely the sensible and latent loads. The heat that causes a change of state without a temperature change is called latent heat. Sensible heat is the heat that causes a change in temperature in a space or an object and is also called dry heat.

Latent heat is the heat that causes a change of state. When a substance goes from solid to liquid or liquid to gas, it requires heat, which is latent heat. This heat does not affect the substance's temperature, only the state. For example, water will remain at 100 °C when boiling but still require (latent) heat. A latent heat transfer happens at a constant temperature.

For air, a sensible heat transfer is the change of temperature without any change in the absolute moisture content of the air. The heat that is removed or added to the air in the form of moisture is the latent heat.

One can distinguish between sensible and latent capacity. The sensible capacity is the capacity required to change temperature, while the latent capacity is the capacity to remove moisture.

2.6 Humid air

All air contains moisture unless it has been wholly rinsed for water. Dry air is a gas. This moisture content affects how people perceive the climate and the thermal properties of the air. The dry part of the air is constant, and the water content is therefore given in relation to dry air. The unit is given as kilograms of water per kg of dry air. The moisture content can alternatively be given as relative humidity (RH). However, this definition does not say anything about the absolute water content in the air unless the air temperature is stated.

The moisture content of outside air is dependent on temperature and climate. In an average Nordic climate, the water content of outside air can vary from 1 to 12 grams of water per kg of dry air throughout the year.

2.6.1 Absolute Humidity

As mentioned, the humidity ratio of air is given as content per amount of dry air. The ratio is shown in the following equation and does not depend on the temperature of the air.

$$x = \frac{m_w}{m_{da}}$$

It is common to give the value in kg water per kg dry air or grams of water per kg dry air.

2.6.2 Relative Humidity

Unlike absolute humidity, the relative humidity of air depends on the air temperature. The relative humidity is the relationship between the partial pressure of water and the saturation pressure for the same temperature, as indicated by the equation below. This means that the value expresses the content of moisture as a percent of how much it could hold if it were saturated.

$$\phi = \frac{p_w}{p_{sat}}$$

Relative humidity increases with decreasing temperature if the absolute humidity remains constant.

For the value to make sense, it is essential to also know the state's dry-bulb temperature.

2.6.3 Dew Point

The temperature where condensation of air starts is called the dew point. At this point, the partial pressure of water is equal to the saturation pressure for the same temperature, which gives a relative humidity of 100%. The more moisture in the air, the higher the dew-point temperature.

2.6.4 Enthalpy

Enthalpy expresses the total energy in the air. The value increases with increasing temperature and with increasing moisture content. Moisture content increase enthalpy because it takes heat to evaporate moisture into the air [18]. Enthalpy can also be defined as the sum of sensible and latent heat in the air. The change in enthalpy between two states will indicate how much energy it takes to move between them.

2.6.5 Mollier Diagram

The Mollier diagram, also referred to as the psychrometric chart, is a graphical representation of the relationship between the properties of air. Some of the properties represented are temperature, pressure, enthalpy, absolute moisture content, and relative humidity. Relevant properties and their designation is shown in Table 2.4.

Parameter	Unit	Designation
Water content	$\text{kg}_w/\text{kg}_{da}$	x
Relative humidity	%	ϕ
Dry bulb temperature	$^{\circ}\text{C}$	T_{db}
Wet bulb temperature	$^{\circ}\text{C}$	T_{wb}
Dew point	$^{\circ}\text{C}$	T_{dp}
Enthalpy	kJ/kg	i

Table 2.4: Properties found in a Mollier diagram with unit and designation.

2.7 Heat Pump Technology

A heat pump is a machine that uses electric power to transport heat from a heat reservoir with a relatively low temperature to a heat sink with a higher temperature. By extracting energy from a reservoir, the system can deliver more energy than the electrical energy consumed.

Different types of heat reservoirs can be utilized. In Norway, the most common sources are ambient air, sea water, ground heat, and ventilation air.

The heat pump transports heat between two different temperature levels and will therefore have both a “cold” and a “hot” side. This means that the system can be designed for both heating and cooling.

2.7.1 The Heat Pump Process

A heat pump consists of four standard components: a condenser, an expansion valve, an evaporator, and a compressor. These components are coupled together as shown in Figure 2.2. A working fluid circulates between these components and is what transfers the heat between the hot and cold side. The working fluid possesses thermodynamic properties, which are beneficial for the heat transfer, and changing condensation- and evaporation temperature with changing pressure.

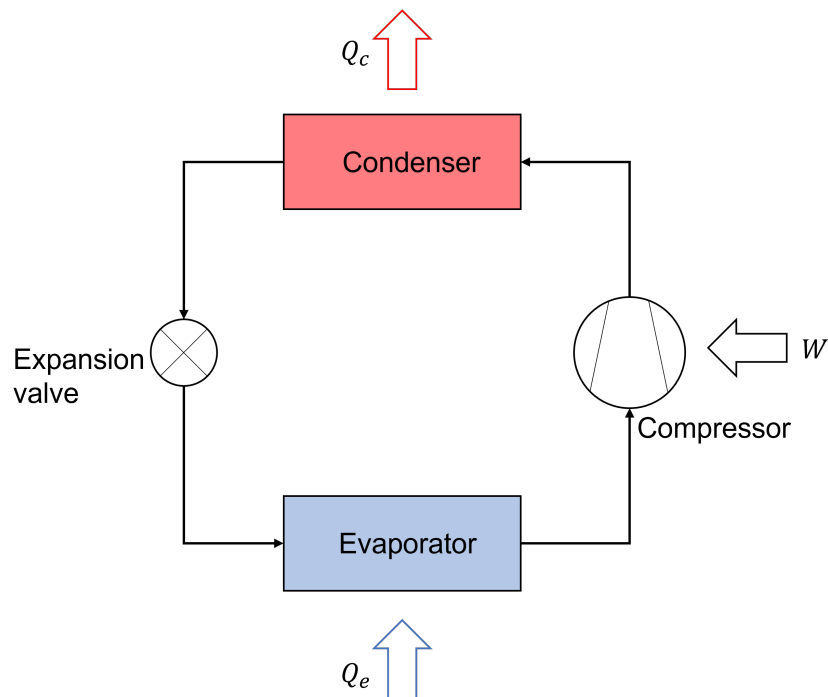


Figure 2.2: Sketch of a standard heat pump cycle.

The **evaporator** works as a heat exchanger, transferring heat from the heat source to the working fluid. The pressure of the working fluid through the evaporator is kept low to keep the evaporating temperature of the fluid lower than the temperature of the heat source. With a lower working fluid temperature, heat (Q_e) will flow from the source, which makes the working fluid evaporate. This means that the source's temperature will decrease while the energy content of the working fluid increases [19].

The **compressor** compresses the gas from the evaporator to a higher pressure, leading to a higher temperature. The compressor is typically driven by an electrical motor and increases the energy content of the gas equal to the consumed electrical energy (W) if losses and efficiency are neglected. This component drives the circulation of the working fluid in the heat pump [19].

The **condenser** also works as a heat exchanger but emits heat from the working fluid to the heat sink. The pressure of the working fluid is so high that the condensation temperature is higher than the temperature of the heat sink. This makes heat (Q_c) flow from the working fluid to the heat sink. The working fluid cools before starting to condensate and will be entirely condensed at the outlet of the condenser. This means that the temperature of the heat sink increases while the energy content of the working fluid decreases, opposite of the evaporator [19].

The **expansion valve** is a pressure reducing component that takes the working fluid from condensation pressure to evaporation pressure. At the valve outlet, the working fluid is a mixture of gas and liquid [19].

2.7.2 Energy Balance

As mentioned, a heat pump utilizes energy from a relatively low-temperature heat source and transforms it into a higher temperature by a compressor to deliver useful energy. The emitted energy from the condenser equals the transferred heat in the evaporator and the consumed energy by the compressor.

$$Q_c = Q_e + W$$

The energy utilized from the heat source is free, making the unit emit more energy than the consumed electrical energy.

The efficiency of a heat pump can be described by the relationship between the delivered energy and the energy consumed by the compressor if heat loss is neglected. This efficiency factor, called COP, or the coefficient of performance, is given by the equation below.

$$\text{COP}_H = \frac{Q_c}{W}$$

2.7.3 Heat Sources

Heat pumps utilize heat with a relatively low temperature that is freely available. The most used sources in Norway are ambient air, ground heat, and sea water [19]. Other sources that can be used are exhaust air, ground water, rivers, industrial wastewater, and greywater.

The source can be used directly in the evaporator, called a direct system, or indirectly through an additional heat exchanger.

2.8 Desiccants

Most solid materials can attract moisture; the difference is the capacity of how much it can attract. Desiccants are hygroscopic substances used as drying agents and are designed for water vapor collection. These substances can hold from 10 to over 10000 percent of their dry weight in water vapor, whereas plastics like nylon only can hold 6 percent [18]. A desiccant typically attracts the most moisture when surrounded by air in a saturated condition (RH=100%). Its moisture absorption capacity is therefore reduced for air with lower relative humidity. By studying a moisture absorption capacity at constant temperature and varying relative humidity, one can derive the moisture sorption isotherm of the substance. The water content of the desiccant can be described by:

W Water capacity of desiccant $[\text{kg}_w/\text{kg}_{desiccant}]$

The most crucial characteristic of desiccants is the surface vapor pressure. A cool and dry desiccant has a low surface vapor pressure and can attract moisture from humid air with higher vapor pressure. After attracting moisture, the desiccant becomes wet and hot, increasing the vapor pressure. In this way, the vapor can move from the air to the desiccant and back depending on the vapor pressure differences [18]. The most commonly used desiccants are silica gel, zeolite molecular sieve, lithium chloride, and activated alumina [20].

2.9 Dehumidification

Dehumidification is a process in which moisture or water vapor is removed from the air. Moisture can be removed from air in three ways: by cooling it to condense the vapor, by increasing its total pressure, or by utilizing desiccants which adsorb moisture from the air by difference in vapor pressures [18].

2.9.1 Cooling Based Dehumidification

The most common strategy for dehumidifying air is to use a cooling coil, followed by a reheating coil to reach the desired temperature [21]. The cooling coil cools ambient air down to the desired moisture content before it is heated up to the desired temperature and, thus, the desired relative humidity. When air is cooled below its dew point, moisture condenses, and the air is dehumidified. The amount of moisture that can be removed is therefore dependent on how cold the air can be cooled.

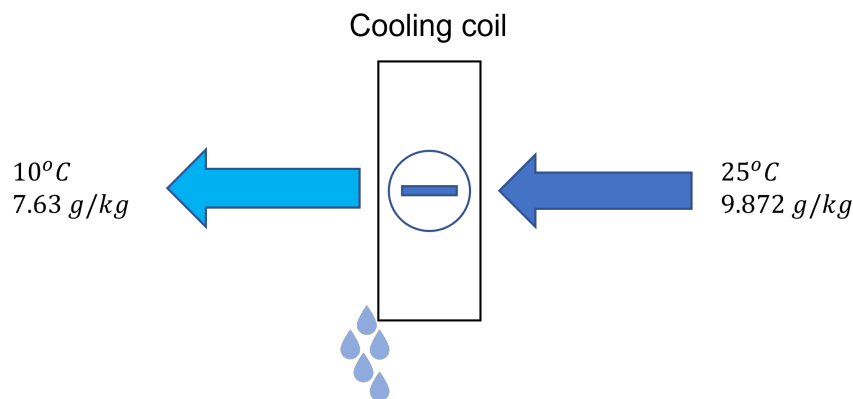


Figure 2.3: Cooling based dehumidification.

2.9.2 Desiccant Wheel Dehumidification

A common type of desiccant dehumidifier is the desiccant wheel, also known as a rotary dehumidifier. This wheel uses a solid desiccant, either coated, impregnated, or formed on the structure of the rotor. Thermal insulation and air barrier are installed in the wheel so that limited energy or mass exchange takes place with surroundings [20].

The rotor is made of a fluted honeycomb structure to make the surface area large. This structure is coated with the desiccant, which makes up 80% of the total weight of the rotor [22].

The wheel treats two separate air streams: the process air and reactivation air. The process air is the air that requires the drying.

Moisture from the stream is adsorbed in the rotor as it passes through the wheel. This happens because the vapor pressure of the process air is higher than the porous openings of the desiccant. The second air stream reactivates the desiccant and is thus called the reactivation air. Meaning that the stream dries the rotor so it can adsorb moisture again. The reactivation air is heated before entering the desiccant wheel, meaning the air will have low relative humidity. This makes the air stream accept the moisture being desorbed from the desiccant [22]. A diagram showing the desiccant wheel's working principle is shown in Figure 2.4 below.

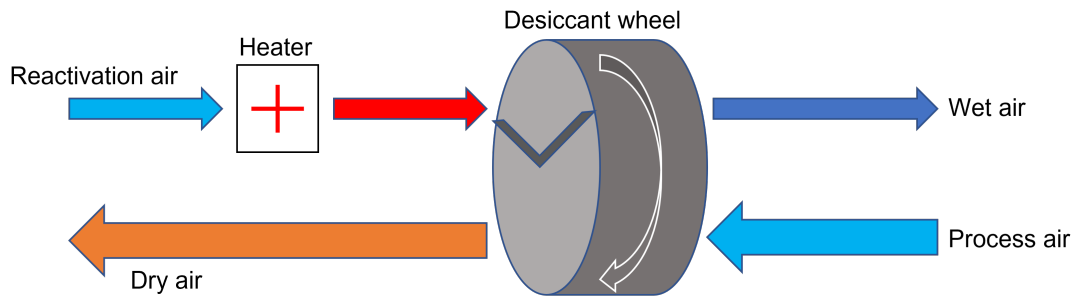


Figure 2.4: Sketch of desiccant wheel operation.

The desiccant dehumidification process is close to and can be treated as an isenthalpic procedure. The process converts latent energy to sensible energy and vice versa. In the reactivation air, the heat of evaporation is taken from the air, which cools the air. The process air will experience a rise in temperature because of the adsorption heat effect.

The performance of the desiccant wheel depends on various parameters which will influence the amount of moisture removed from the process air. The conditions of the process air and reactivation air will influence the performance. In addition, reactivation temperature, regeneration flow rate, rotational speed, and wheel size will influence how the wheel will perform.

Purge Section

The desiccant wheel can also be equipped with three different sections instead of the two previously shown. Here the process air is separated into two streams in the outlet section of the wheel; process air and purge air. With this mechanism, the outlet from the desiccant wheel is partly used as supply air and partly used in the regeneration process. The purge section is introduced because of the low dehumidification efficiency at the beginning of the dehumidification section, mainly because of the wheel's high temperature [23]. The purge section also reduces the risk of carryover between the sides. Extracting air out for use in the regeneration process will typically improve the quality of the process air and lead to increased wheel performance. The configuration of a desiccant wheel with purge air flow is shown in Figure 2.5.

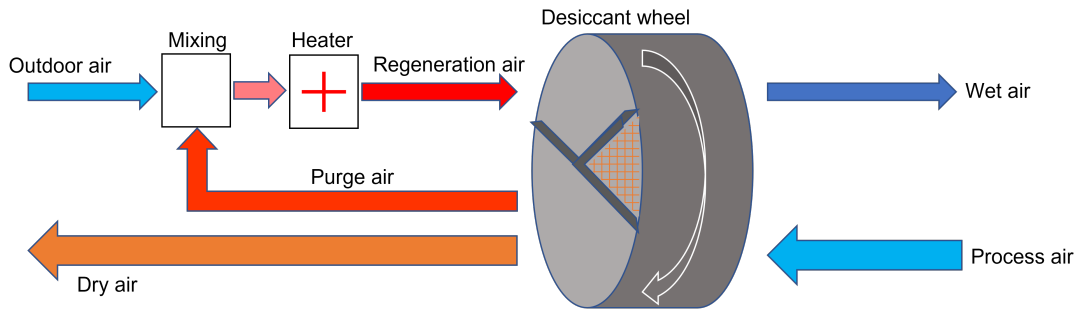


Figure 2.5: Sketch of desiccant wheel with purge section.

When mixing the purge air stream with the outdoor air, the purge will act as an energy source as it has a higher temperature. The purge air stream also has a lower humidity ratio compared to the outdoor conditions, which makes the mixed stream end up with a lower vapor pressure than it would have with only outdoor air. The lower vapor pressure in the regeneration stream is beneficial because it increases the mass transfer between the stream and the desiccant material.

As the wheel rotates, the regenerated desiccants will first meet the purge section before it rotates through the dehumidification section. A section of the desiccant wheel with purge section is shown in Figure 2.6 below.

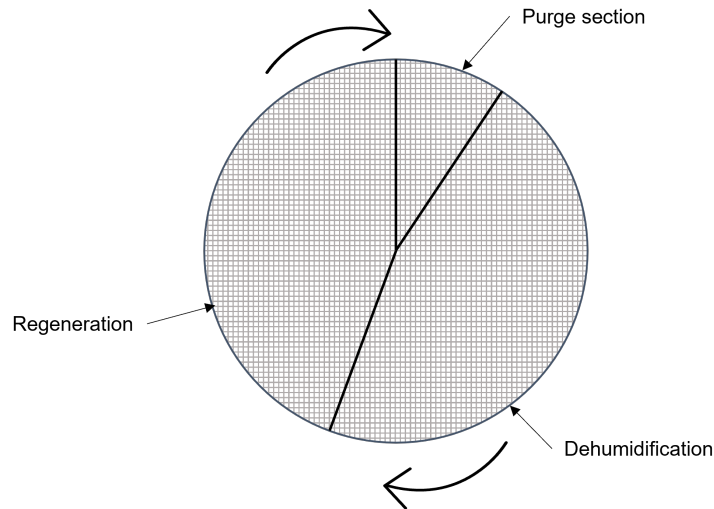


Figure 2.6: Section of a desiccant wheel with purge section.

2.10 Comfort cooling

Comfort cooling is the cooling needed to remove the excess heat in a room or a building. Several technical solutions and strategies are present to overcome this, and some will be presented in this section.

2.10.1 Chiller

When a heat pump is used for cooling purposes, it is called a chiller. It contains the same components but the heat removed by the evaporator is the point of interest. Heat is removed by the evaporator and must be moved somewhere else by the condenser. This heat can either be discarded in ambient air or be utilized. The evaporator receives return water from the cooling coil in the air handling unit. The working fluid, having a lower temperature than the return water, will receive heat from the water, which makes the water cool down. Normal temperature levels for these cooling coils in the air handling unit is 7 °C supply temperature and 12 °C return temperature. This means that the evaporator must cool down from 12 °C to 7 °C. Figure 2.7 shows the working principle of a chiller used to chill water from a cooling coil.

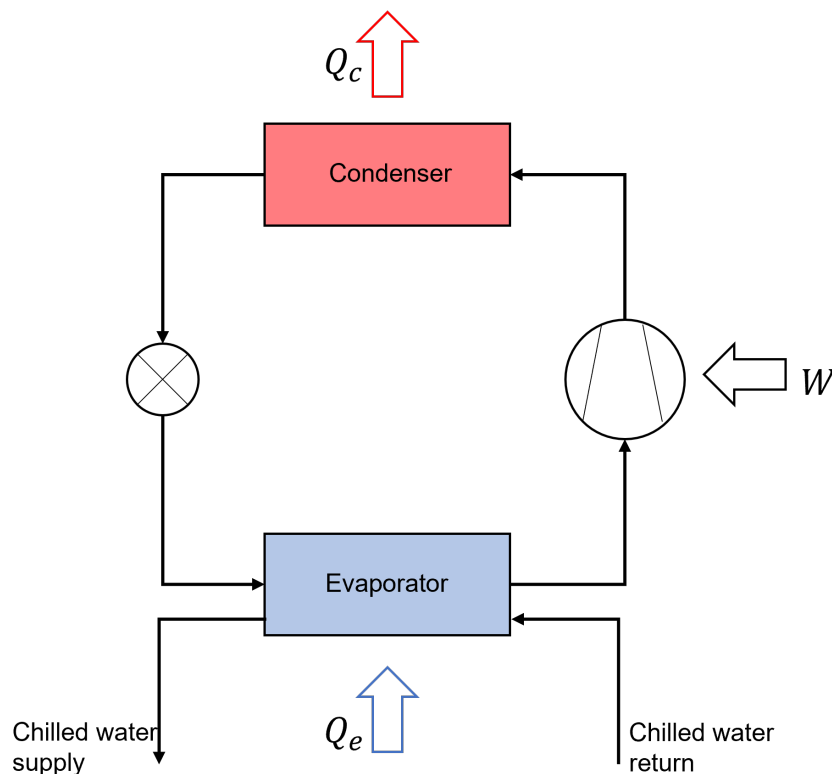


Figure 2.7: Working principle of a chiller.

As COP_H expresses the heating efficiency of a heat pump, the refrigeration efficiency for a chiller can be expressed as the relationship between the energy drawn in the evaporator and the consumed energy in the compressor.

$$COP_R = \frac{Q_e}{W}$$

where:

Q_e : Energy drawn in evaporator.

W : Energy used by compressor.

2.10.2 Direct Evaporative Cooling

With direct evaporative cooling, DEC, outside air is cooled directly through humidification. The air is humidified with water spray that evaporates in the air. The heat of evaporation is taken from the air, decreasing the air temperature. The enthalpy of the air remains approximately constant because the heat of evaporation is added to the air but bound in the water [9]. This makes the process approximately isenthalpic.

The limit of cooling is dependent on the outside air conditions. Air with lower absolute humidity can be cooled more than air with higher absolute humidity as the air has more space for additional humidification. Figure 2.8 shows the system configuration for direct evaporative cooling.

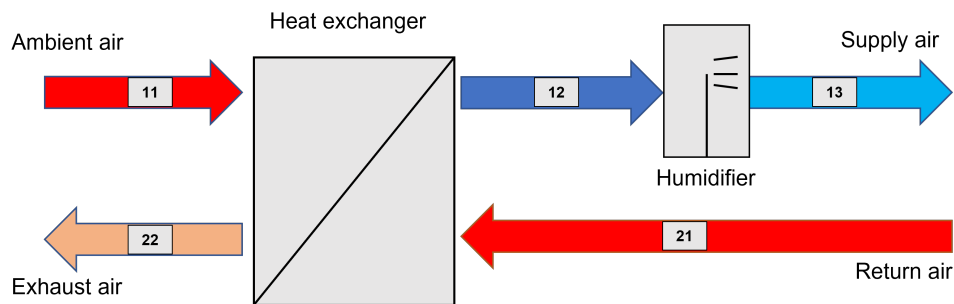


Figure 2.8: Direct evaporative cooling system configuration.

The process is illustrated with a Mollier diagram in Figure 2.9. The diagram is only sketched for the supply side. The labels in the Mollier diagram correspond to the numbers from Figure 2.8.

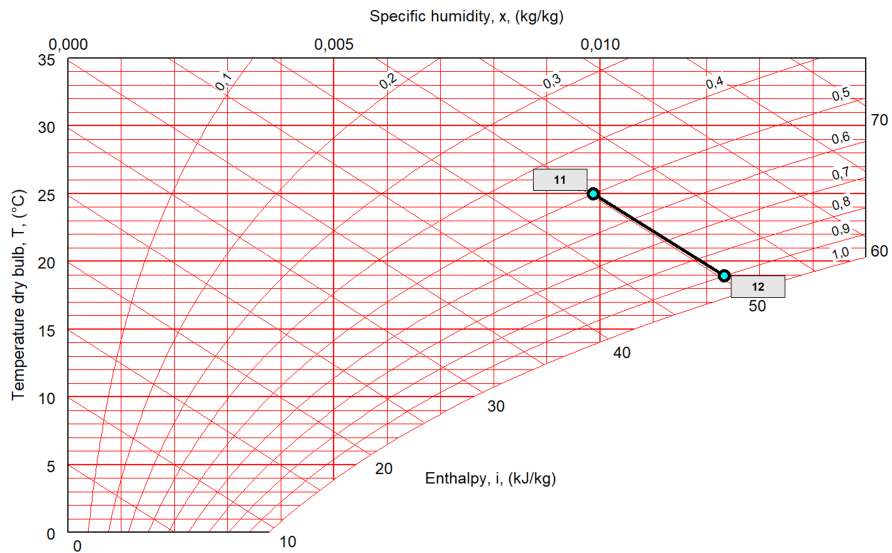


Figure 2.9: Direct evaporative cooling process in Mollier diagram.

In the sketched process, outside air of 25 °C and 50% RH is humidified until the RH reaches 90%, resulting in an air temperature of 18.9 °C.

2.10.3 Indirect Evaporative Cooling

With indirect evaporative cooling, IEC, the return air is humidified. Return air is humidified and thus cooled before using a recuperative heat exchanger for cooling recovery of the supply air. A recuperative heat exchanger avoids transmitting the humidity over to the supply air. As for direct evaporative cooling, the air is humidified with water spray that evaporates in the air, resulting in an isenthalpic process.

The system configuration for indirect evaporative cooling is shown in Figure 2.10.

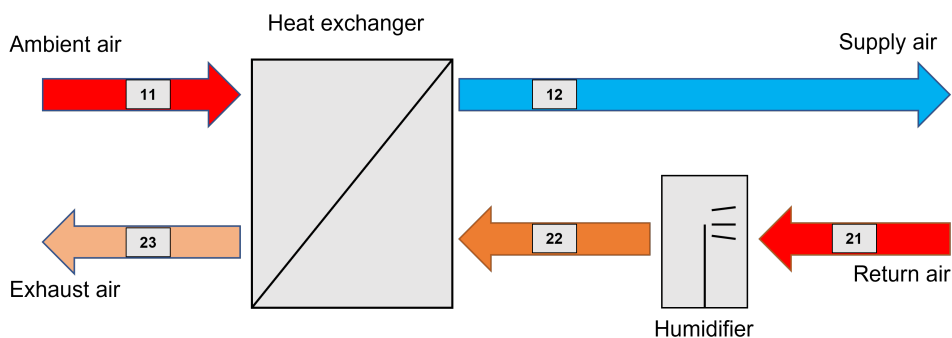


Figure 2.10: Indirect evaporative cooling system configuration.

Figure 2.11 shows an example of an indirect evaporative cooling process in a Mollier diagram. The labels in the Mollier diagram correspond to the numbers from Figure 2.10.

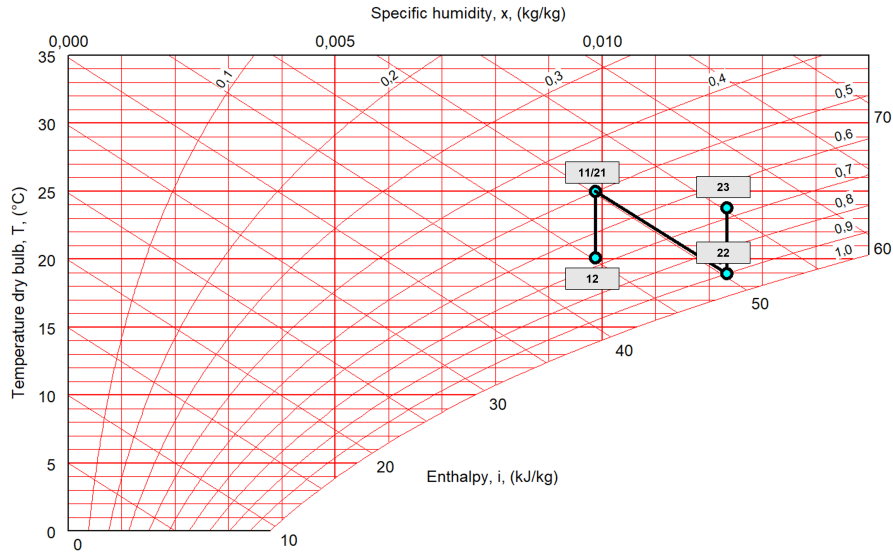


Figure 2.11: Indirect evaporative cooling process in Mollier diagram.

The return air is cooled by humidification along an isenthalpic line before exchanging heat with the outside air in a heat exchanger. The outside air will be cooled through the heat exchanger as the return air after humidification has a lower temperature.

In Figure 2.11, return air of 25 °C and 50% RH is humidified until the RH is 90% which cools the air to about 18.9 °C. Assuming that the outside air has the same conditions as the return air, cooling recovery in a heat exchanger will cool the supply air to 20.1 °C if 80% temperature efficiency is assumed [24].

2.10.4 Indirect + Direct Evaporative Cooling

The two strategies described above can be combined into what will be called Indirect + direct evaporative cooling here. This solution can reach lower temperatures than what IEC and DEC can reach alone. Figure 2.12 shows the configuration for the combination of IEC and DEC.

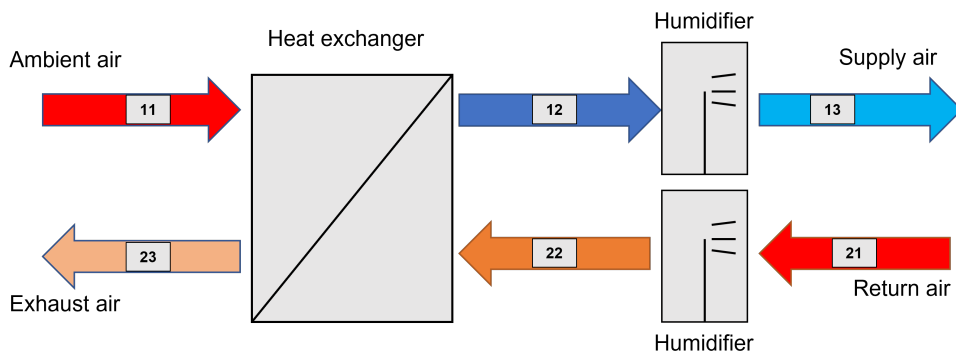


Figure 2.12: Combined indirect and direct evaporative cooling system configuration.

As for the other strategies, the combined process has been sketched in a Mollier diagram in Figure 2.13. The labels in the Mollier diagram correspond to the numbers from Figure 2.12.

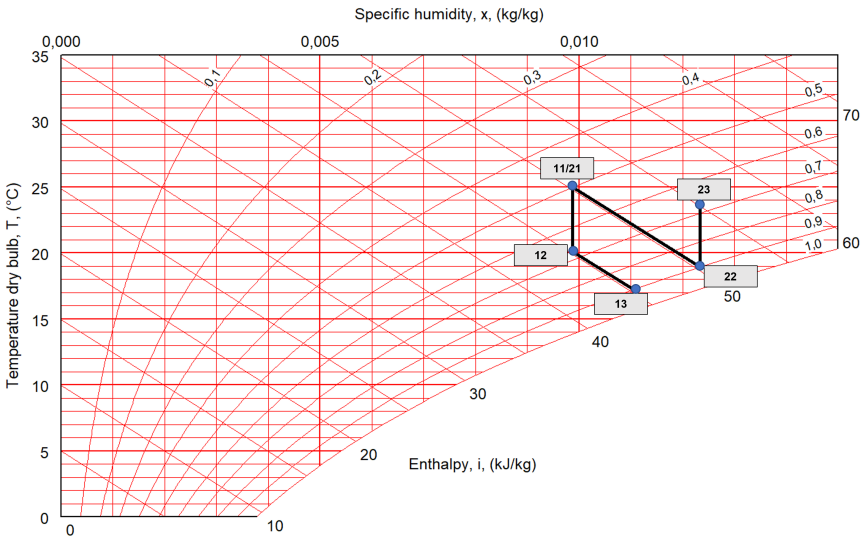


Figure 2.13: Indirect + direct evaporative cooling process in Mollier diagram.

In Figure 2.13, the same conditions as for IEC and DEC is used. Return air and outside air of 25 °C and 50% RH is the starting point. Where DEC was able to deliver supply air of 18.9 °C and IEC 20.1 °C, the combined solution can reach a supply temperature of 17.2 °C.

2.10.5 Desiccant Cooling

Desiccant cooling is a cooling system based on using a desiccant wheel, described in Section 2.9.2. The wheel dehumidifies the air before being sensibly cooled by a heat exchanger and an evaporative cooler. The first patent on rotary desiccant air conditioning was invented by Pennington back in 1955 [25]. Figure 2.14 shows a flow chart of the Pennington cycle.

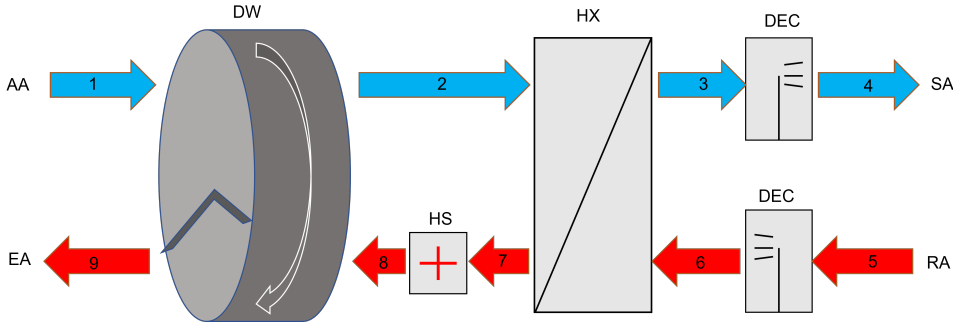


Figure 2.14: Flow chart of Pennington cycle system configuration.

The Mollier diagram in Figure 2.15 illustrates an example of the Pennington cycle process.

The numbers in the Mollier diagram are according to the numbers in Figure 2.14.

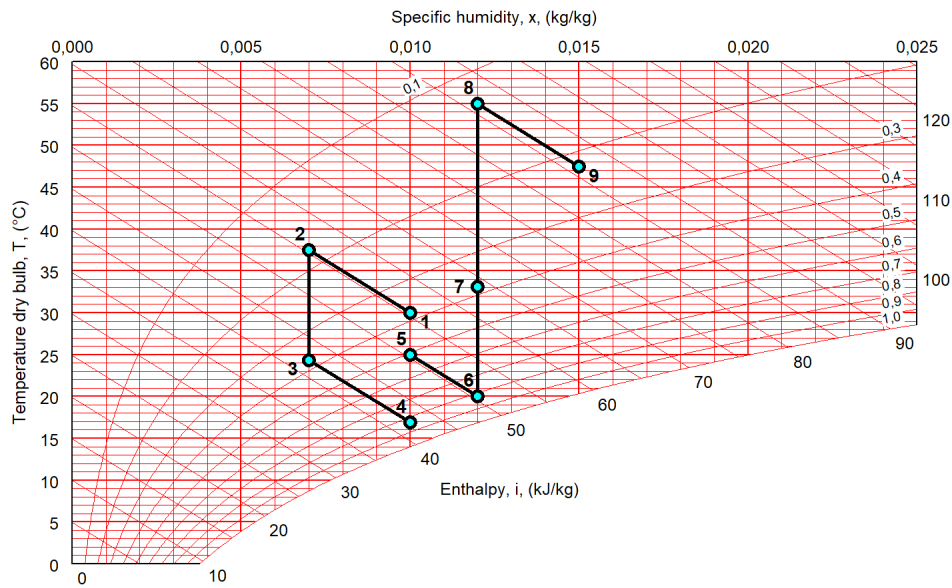


Figure 2.15: Desiccant cooling process illustrated in Mollier diagram.

The system can be looked at as a combination of the desiccant dehumidification and the indirect evaporative cooling techniques. The desiccant wheel is used to dehumidify the ambient air, which makes the air increase in temperature. The return air is cooled by a direct evaporative cooler to increase the temperature difference between the two air streams, increasing the cooling recovery in the supply air and utilizing indirect evaporative cooling. The final step is evaporative cooling of the supply air to the desired supply temperature.

Literature Review

In this section previous studies of the cooling technologies are presented.

3.1 Desiccant Cooling

Most of the research that has been done in the area is built on either numerical simulations, experimental investigations, practical applications, thermodynamic analysis, or a combination. Research also aims to establish new innovative cycles for improved efficiency and design. In the following section, the state-of-the-art research for desiccant wheels and desiccant wheel cooling will be presented.

A theoretical study on the design parameters for a solar desiccant wheel was conducted by Ahmed et al. [26]. Factors like wheel speed, thickness, and area ratio were investigated to find the optimal value. It was concluded that for a smaller regeneration section, an increased regeneration temperature should be used.

Su et al. [27] carried out a number of investigations into regeneration temperatures from 40 °to 80 °C with varying regeneration section angles. Results from the examination indicated that increasing thickness of the wheel will increase dehumidification performance. At constant thickness, an increase in regeneration angle will also lead to increased dehumidification performance.

One study by Yu et al. [28] examined the effect of temperature and humidity ratio on a low-temperature regenerated desiccant dehumidification system. Experiments were performed for regeneration temperatures from 40 °to 70 °C. Results showed that air with higher humidity ratio required higher regeneration temperatures, indicating that low-temperature desiccant cooling is most suitable in areas with less absolute humidity.

Henning et al. [29] evaluated a one-stage desiccant cooling system for three different climates. The results from the evaluation showed that the one-stage system was insufficient for a hot and humid climate with no additional cooling devices in the system. Integrating the desiccant cooling system with a conventional cooling system turns out to be feasible from both an economic and an energetic point of view, with primary energy savings of up to 50%.

Ge et al. [30] proposed a two-stage system that utilized desiccant dehumidification over two steps rather than one. Here it was found that the performance was greatly influenced by regeneration temperature and outdoor conditions.

Both liquid and solid desiccants exist and can both be used in air conditioning systems. Research conducted by Factor and Grossman [31] shows that the solid desiccant has the greatest dehumidification potential and is used in desiccant wheels.

Studies by Kang and Maclain-Cross [32] concluded that the dehumidifier is crucial for a desiccant cooling system, and its performance can be improved with improved performance of the component. Studies by Farooq and Ruthven [33] concluded with the same findings.

Nia et al. [34] created a model of a desiccant wheel in MATLAB Simulink to simulate the combined heat and mass transfer occurring in the wheel and predict the temperature and humidity of the outlet air.

Ronghui et al. [35] conducted a study on desiccant air conditioning for the climatic conditions of Singapore, Boulder, Houston, Beijing, and Los Angeles. Results from the study show that electrical savings increase with higher humidity and lower sensible heat ratio. The ideal climatic condition was Singapore, while Beijing had the least ideal conditions.

Studies of solar-driven desiccant cooling systems across Europe have been conducted by Halliday et al. [36] and Mavroudaki et al. [37] Both find potential primary energy savings by utilizing desiccant cooling systems with solar heat in all the climatic zones tested. However, higher relative humidity leads to excessive regeneration temperatures making desiccant cooling impracticable. Halliday et al. [36] also found solar-driven desiccant cooling feasible in the United Kingdom, which is located in the same climate zone as Norway.

Zhou [38] investigated the thermal and energy performance of a solar-driven desiccant cooling system with low-temperature regeneration air. The same system was then compared to a conventional vapor-compression air conditioning system for the same building. For tropical areas, it was found that the desiccant system could not maintain acceptable thermal comfort in the building for over 25% of the working time.

Daou et al. [39] reviewed air conditioning systems with desiccant cooling. By reviewing different desiccant cooling systems, it was clear that desiccant cooling is a simple technology that can supplement traditional cooling systems to improve overall efficiency. The desiccant cooling requires energy for heating regeneration air, but overall energy saving potential was found. Energy saving is especially potent if free energy from waste heat or solar is utilized.

Company Munters delivers complete air handling units with desiccant cooling. Their system can cool from 30 °C to 15 °C by using regeneration heat and cold tap water. Comparing the system to a conventional system with mechanical cooling, the desiccant cooling system requires 50% of the installed electric power. The system will also achieve a higher temperature efficiency by using the desiccant wheel as a rotating heat exchanger outside the heating season [40].

Different studies have also been conducted regarding energy-efficient heat sources for desiccant regeneration. One of the advantages of desiccant wheels is the possibility of utilizing low-grade energy as a source of regeneration energy. Several studies on low-grade energy sources such as solar energy [41, 42, 43, 44, 7] and thermal waste energy [45, 46] have been conducted.

3.2 Indirect Evaporative Cooling

Sweco has been part of several projects where indirect evaporative cooling has been tested in Bergen. Theoretically calculated temperatures on a warm day showed that supply air temperature is kept under 20 °C even when outdoor air reaches 27 °C [24].

Lab tests done by Nehasil et al. [47] using an air handling unit with a water humidification chamber showed increasing cooling power with increasing outdoor temperature. It was found that the size of the heat exchanger surface had a significant effect on the final temperature. As a result, proper nozzles and heat exchangers showed that a 16 to 19 °C supply temperature was reachable when outdoor temperatures vary from 21 to 36 °C.

Maheshwari et al. [48] studied the energy-saving potential of an indirect evaporative cooler. An analytical evaluation of field performance results of an IEC unit in Kuwait was performed to see the benefits of the technology. Results showed that performance and benefits offered by indirect evaporative cooling are strongly site-related. However, a reduction in both cooling energy demand, cooling peak power demand, and electricity savings can be achieved. Pros with IEC is that the maximum cooling capacity reduction coincides with the peak cooling demand.

A review by Porumb et al. [49] presents knowledge about indirect evaporative cooling. The IEC technology is found to be suitable in different applications. The technology is entirely energy environmental friendly and has a meager global warming potential. The main disadvantage of IEC is that the cooling is limited by the wet bulb temperature of the return air.

Dean and Metzger [50] conducted a study to demonstrate the potential of IEC technology in dry climates. The study's primary objective was to see how IEC technology can reduce energy use and improve thermal comfort. Three different cooling units were tested to see a comparison over the three summer months, June to August. Results showed that the IEC achieved an 80% reduction in energy compared to the typical unit.

Amer et al. [51] performed an extensive literature review to map evaporative cooling systems. The review concludes that evaporative cooling technology is among the most environmentally friendly and effective cooling systems.

Applied Systems in Norway

In this chapter, existing experience with the investigated cooling techniques is presented. Some are actual projects where the technique is used, and some are projects where the technique was investigated as a possible solution.

4.1 Indirect Evaporative Cooling

4.1.1 Fantoftparken

Fantoftparken is an office building located in Bergen that was built in February 2021 and has a total floor area of 6500 m². When the building was built, it had high ambitions regarding energy efficiency and being climate friendly. The goal was to reach a BREEAM Outstanding certification with several innovative solutions. Among these solutions are the air handling units installed with indirect evaporative cooling that use rain water as the water source. The building consists of two separate air handling units with this configuration. The AHU configuration is shown in Figure 4.1.

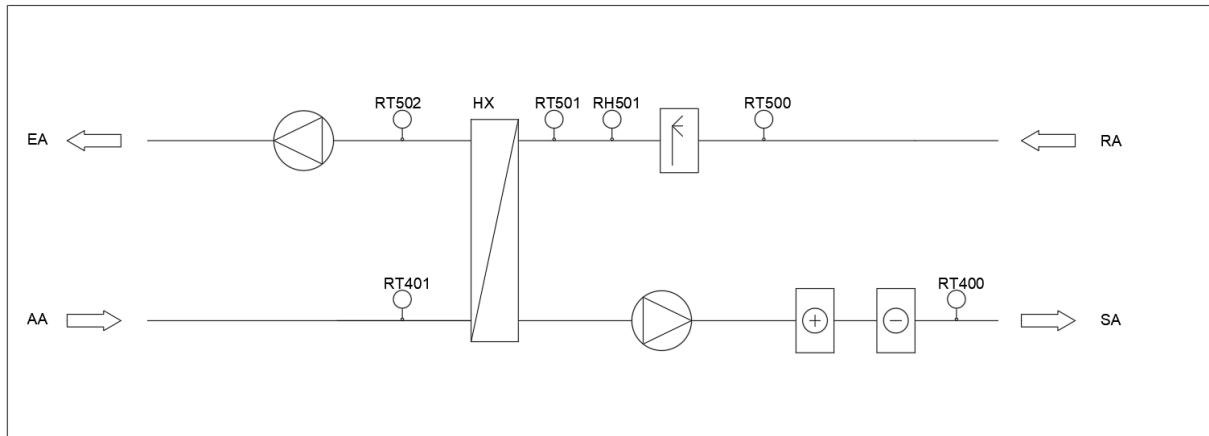


Figure 4.1: Configuration and sensor placement from AHU in Fantoftparken.

An overview of actual parameters that are available for historical data exporting is shown in the list below.

RT401	Intake temperature.
RT400	Supply temperature.
RT500	Return temperature.
RH500	Relative humidity of return air.
RT501	Return temperature after evaporator.
RT502	Exhaust temperature.
LU501	Humidifier throttle.
LX501	Temperature efficiency HX.
RF401	Supply air flow.
RF501	Return air flow.

Historical data

Historical data are presented here to show how the system is operated and to validate the theoretical background on IEC systems. The data presented is taken from the 31st of May till the 5th of June in 2021.

Figure 4.2 shows the humidifier's operation and the intake air's temperature. As seen, the throttle of the humidifier increases with higher air temperatures. The humidifier is activated as soon as there is a cooling demand of the air and is not active for lower temperatures.

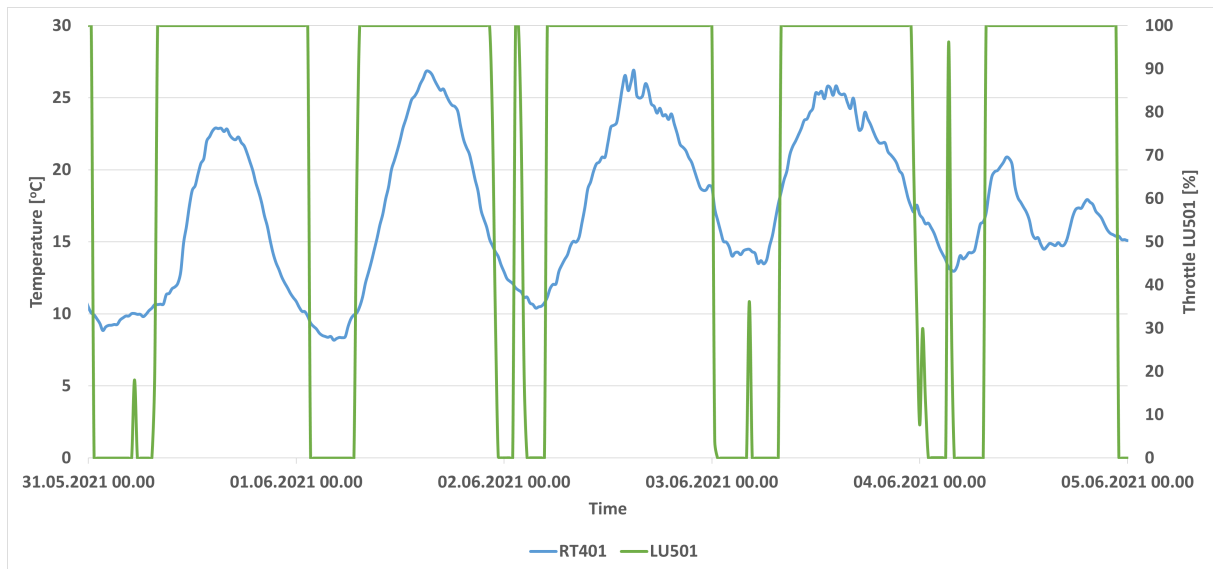


Figure 4.2: Throttle of humidifier LU501 and temperature of intake air.

Figure 4.3 shows the humidifier's throttle and the air's return temperature before and after the humidifier. The graphs show that the return temperature is significantly reduced when the humidifier is active.

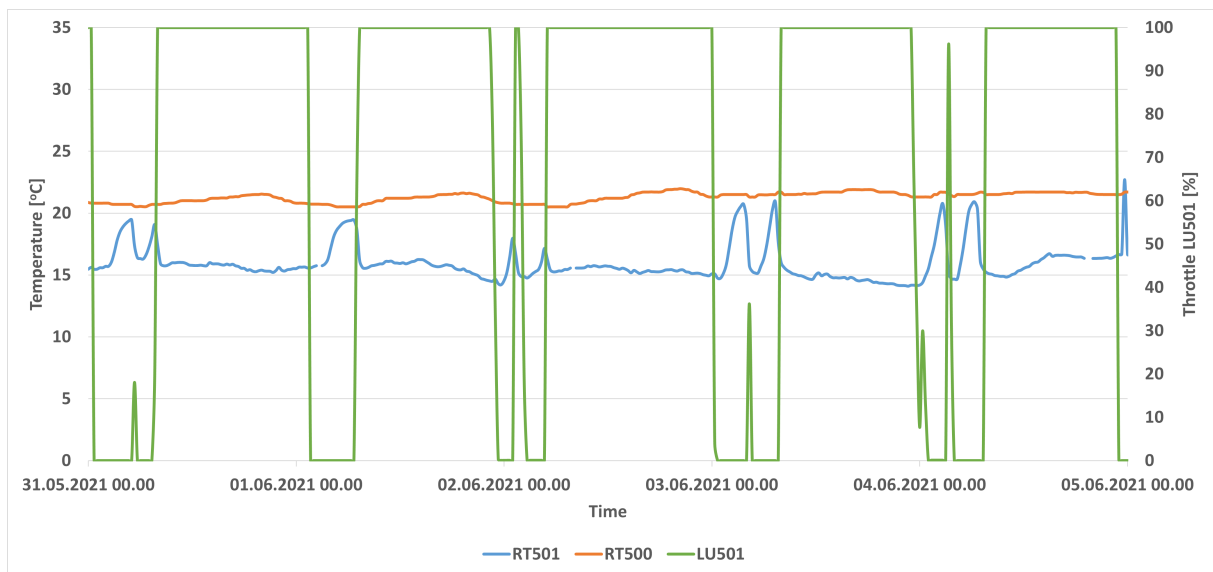


Figure 4.3: Throttle of humidifier LU501 and return temperatures before and after humidifier.

Figure 4.4 shows the temperatures over the heat exchanger on the return side. RT501 is before the heat exchanger, and RT502 is after, and as seen, the temperature flow varies over the day. When the humidifier is active, the temperature after the heat exchanger is larger than before, meaning that cooling is being recovered on the supply side. When the humidifier is inactive, the supply side is recovering heat from the return air as the temperature after the exchanger is lower than before.

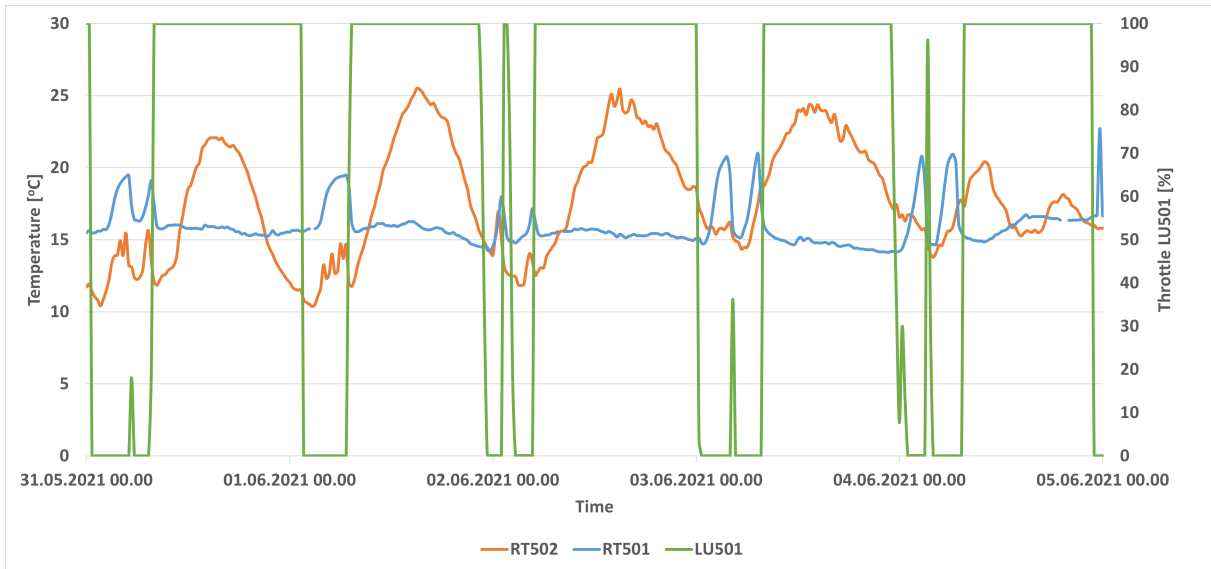


Figure 4.4: Temperatures over heat exchanger on return side.

Figure 4.5 shows the relative humidity of the air after the humidifier. The figure shows that the relative humidity is significantly increased when the humidifier is active. Leaving relative humidity out of the humidifier caps at about 95% RH.



Figure 4.5: Throttle of humidifier LU501 and relative humidity of air after humidifier.

4.2 Desiccant Wheel Cooling

4.2.1 Søderlundmyra 18

Haaland AS has provided access to the building energy management system of their office building in Søderlundmyra 18, located in Mo i Rana in the northern part of Norway. The building is 2142 m² and consists of offices, a warehouse, a workshop, and a cafeteria. One of the air handling units in the building use desiccant cooling to cover the cooling need.

The configuration of the air handling unit is shown in Figure 4.6.

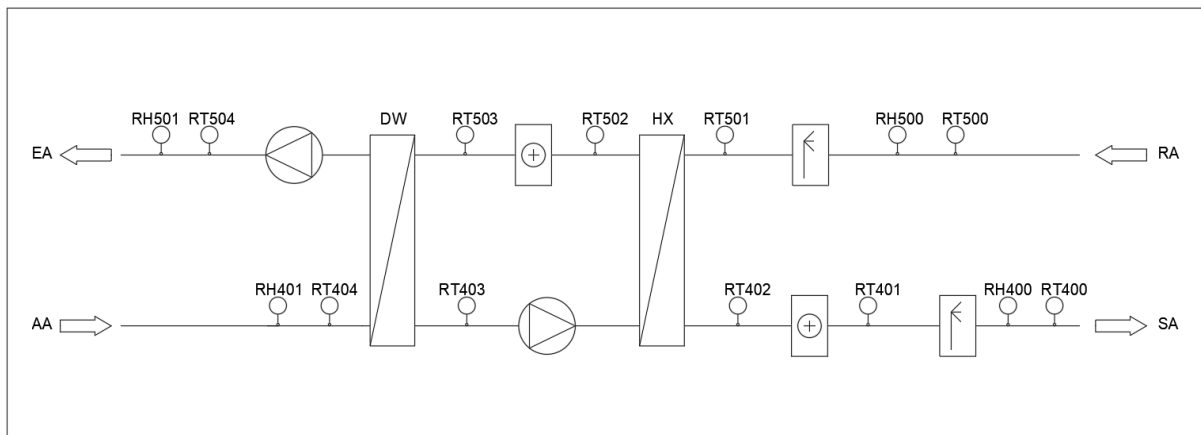


Figure 4.6: Configuration and sensor placement from AHU in Søderlundmyra.

The location of the sensors are explained below.

RH401	Relative humidity of intake.
RT404	Intake temperature.
RT403	Supply temperature after DW.
RT402	Supply temperature after HX.
RT401	Supply temperature after heating coil.
RT400	Supply temperature.
RH400	Relative humidity of supply air.
RT500	Return temperature.
RH500	Relative humidity of return air.
RT501	Return temperature after evaporator.
RT502	Return temperature after HX.
RT503	Regeneration temperature.
RT504	Exhaust temperature.
RH504	Relative humidity of exhaust air.
RF401	Supply air flow.
RF501	Return air flow.

4.2.2 Sandnes Helsepark

Sweco has investigated the potential use of desiccant wheel cooling in a building under construction located in Sandnes, in the southern part of Norway. The intended idea was to utilize district heating to heat regeneration air. Desiccant wheel cooling is not used a lot in Norway but was considered for this project.

The following parameters were the basis for the consideration.

Air flow rate	80 000 m ³ /h
Climate data	Stavanger
Cooling season	100 hours
Total operating time	3120 hours
Supply temperature	16 °C
Electricity price*	1.18 NOK/kWh
District heating price*	0.15 NOK/kWh
Regeneration temperature	55 °C
COP _R	3

* Including all fees

Maintenance costs and costs linked to water usage and floor area were not taken into account in the consideration.

There were several different options that desiccant wheel cooling was compared. The compared alternatives are shown below.

- Alternative 1 - Desiccant cooling
- Alternative 2 - Desiccant cooling + cooling coil
- Alternative 3 - Cooling coil
- Alternative 4 - Indirect evaporative cooling + cooling coil

The considered desiccant cooling system was not chosen for the given building. The system was not beneficial for the project, even for low energy prices. The main reasons for the decision were high investment costs, low cooling demands, insufficient cooling for certain outside air conditions, and legionella challenges.

Methodology

This chapter presents the methods used in the master thesis. The simulation model from IDA ICE is explained together with essential input values. Modeling of the different cooling technologies is also presented in the chapter.

5.1 IDA ICE

IDA ICE, or IDA Indoor Climate & Energy, is a dynamic whole-year detailed and multi-zone simulation tool used to study and evaluate thermal indoor climate and energy use for buildings. The program covers many applications, such as thermal models and air flow networks, calculations of CO₂ and moisture, and more. The tool is transparent and every underlying equation and variable is available and can be logged. IDA ICE can produce output about any data with a given time resolution, which can be exported to Microsoft Excel [52].

The disadvantage of the tool is its complexity, which takes time to understand and master. Running complex and detailed building simulations requires much computational power and can lead to prolonged simulation times.

5.2 Simulation Model

A simplified model of the ZEB Laboratory in Trondheim was acquired from a previous master thesis [53]. In order to simulate the different cooling strategies, three different AHUs will be conducted in the model to compare the results. The original model was created to investigate the potential of ventilative cooling in the ZEB Laboratory and was created using construction drawings of the actual building.

The modeled building is shown in Figure 5.1 below.

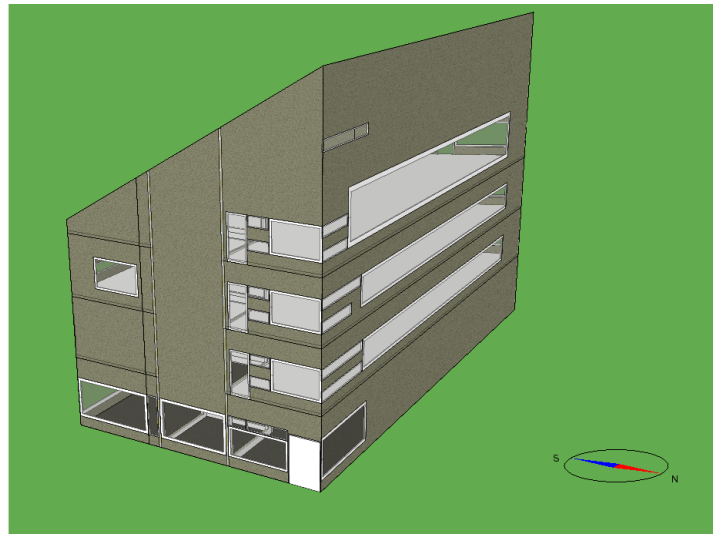


Figure 5.1: Visual representation of the modeled ZEB Lab (snipped from IDA ICE).

5.2.1 Building Structure

The building is a four-story living office laboratory with a total height of 22.77 m. Martin Sande constructed the building model following plan drawings of the actual building, located at Gløshaugen in Trondheim [53]. The model is divided into four main zones, each representing a building floor, with a staircase zone reaching from the ground floor to the third floor. Table 5.1 shows the zone distribution with area and elevation above ground level.

Zone name	Area [m ²]	Elevation [m]
Ground floor	441.9	0
First floor	441.9	4.45
Second floor	441.9	8.3
Third floor	441.9	12.15

Table 5.1: Zone distribution of ZEB Lab model in IDA ICE.

The different building parts are designed to achieve the ZEB-COM requirements. The U-values of the building parts are summarized in Table 5.2. All the windows have the U-value as presented, a frame factor of 0.2, and a solar gain coefficient g_{tot} of 0.45.

Building part	Magnitude	Unit
External wall	0.15	W/m ² K
External roof	0.09	W/m ² K
Floor towards ground	0.1	W/m ² K
Window	0.77	W/m ² K
Normalized thermal bridge	0.04	W/mK

Table 5.2: Thermal properties of building parts in IDA ICE model.

About 18% of the whole facade is made up of windows and spread across the different sides. Due to extensive computational time for the simulations, all windows placed on the same facade are merged into one bigger window. As IDA ICE is used as the simulation tool, this will have a negligible effect as the conditions are the same for the whole facade. Table 5.3 gives the window distribution per floor and facade orientation.

Floor number	Window area [m²]			
	North	East	South	West
Ground floor	25.35	36.05	55.18	10.32
First floor	51.48	11.02	41.2	12.29
Second floor	51.47	17.05	39.18	20.21
Third floor	90.7	13.26	0	13.03

Table 5.3: Window distribution in IDA ICE model per floor and orientation.

The ZEB Laboratory is assumed to be semi-exposed, and the pressure coefficients at the building surface are set to the default values for semi-exposed in IDA ICE.

5.2.2 Weather File

The weather file used for the simulations is made from actual weather data recorded at the top of “Varmeteknisk Laboratorium” at Gløshaugen. This is the closest known location where climate data is recorded.

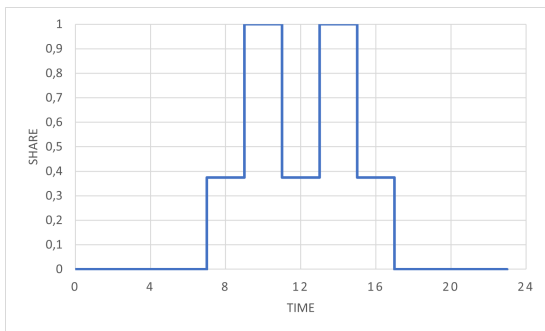
5.2.3 Internal Gains

As one of the purposes of cooling is to remove excess heat from the building, the sources of this excess heat need to be implemented in the model to make it as realistic as possible. Internal gains from equipment, lighting, and occupancy are set to the normative values given in SN-NSPEK 3031:2020 for office buildings [17]. At full operation or occupancy, the loads are as shown in Table 5.4.

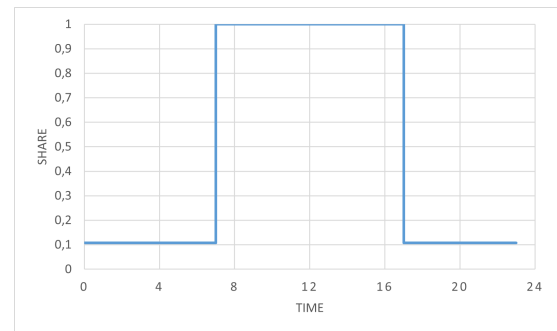
Load type	Energy [W/m ²]
Occupancy	8.0
Lighting	3.7
Equipment	8.6

Table 5.4: Internal load at full capacity.

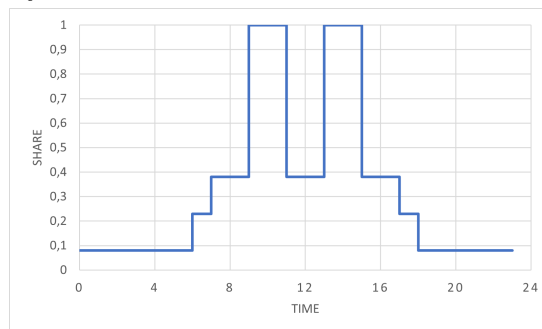
The schedules for the loads are also set according to the standard and can be seen in Figure 5.2. Here the schedules are given as a share of the maximum load given in Table 5.4.



(a) Occupancy



(b) Lighting



(c) Equipment

Figure 5.2: Schedules for internal gains for office from SN-NSPEK 3031:2020 [17].

In IDA ICE, the number of occupants and their metabolic rate must be selected for each floor. To find the number of occupants, the sensible heat emitted from an average person needs to be known. From the Norwegian standard, we know that the maximum heat gain from people is set to 8.0 W/m². A study by Ahmed et al. [13] shows that a person, on average, emits 80.3 W of sensible heat at a metabolic rate of 1.2. Knowing this, the number of occupants corresponding to the Norwegian standard’s value can be calculated and put into the model.

If we use the ground floor as an example, which has a floor area of 441.9 m², the number of people present at full capacity becomes as follows:

$$n = \frac{8.0 \text{ W/m}^2 \cdot 441.9 \text{ m}^2}{80.3 \text{ W/pers}}$$

$$n = 44 \text{ pers}$$

Since all floors have the same floor area, 44 occupants are assumed to be the maximum capacity for each floor.

5.2.4 Building Services

Heating and Cooling

The heating and cooling set-points are set according to the normative values from SN-NSPEK 3031:2020 to get a resemblance to other office buildings. These values differ whether the building is occupied or not. The operating hours are set from 06:00 to 18:00 on weekdays. Set-point values for both occupied and unoccupied hours are shown in Table 5.5.

Building type	Heating set-point [°C]		Cooling set-point [°C]	
	Occupied	Unoccupied	Occupied	Unoccupied
Office	21	19	24	22

Table 5.5: Set-points for heating and cooling.

Ventilation

The office building is cooled entirely by mechanical ventilation and is operated as a VAV system. The VAV system works as described in Section 2.2.2 and is controlled by CO₂- and temperature sensors. Air is supplied at a constant temperature of 16 °C, and the cooling power from ventilation will vary with the rate at which it is supplied as recalled from the equation in Section 2.4.2.

As there are requirements for the thermal environment, shown in Section 2.1.1, the ventilation rate that fulfills these requirements needs to be found before the cooling technologies can be integrated. Therefore, several pre-simulations are conducted to find the upper air flow rate where the thermal requirements are still being fulfilled. The lower rate where the VAV system will operate is the minimum requirement given in Section 2.2.1, which equals a rate of 0.7 m³/h per m² floor area. As the VAV is operated both on temperature and CO₂, the upper limit of CO₂ concentration is set to 900 ppm, below the recommended value from Section 2.1.2.

The pre-simulations were performed for a standard air handling unit equipped with a heat exchanger, heating coil, cooling coil, and fans for supply and return. The temperature efficiency of the heat exchanger was set to 75%. The passive cooling strategies given below were also implemented before completing the pre-simulations. The air flows tested are given in Table 5.6. Note that the air flows are given in liters per second per square meter of floor area.

Air flow [$\frac{L}{s \cdot m^2}$]	
Lower rate	Upper rate
0.19	1.00
0.19	1.20
0.19	1.25
0.19	1.35
0.19	1.50
0.19	1.67

Table 5.6: Air flows tested in pre-simulations.

Results from the simulation can be seen in Section 6.1. As seen, several of the tested rates are within the thermal requirements from Section 2.1.1. TEK17 also gives requirements regarding air flow rates, shown in Section 2.2.1, which must be fulfilled. In Section 5.2.3, calculations showed an estimate of 44 occupants on each floor. This means that the maximum air flow must cover the required air flow rate for all the occupants. Assuming that low-emitting materials are used, the required air flow rate for the building becomes as shown in the below calculation.

$$\dot{V} = 4 \text{ floors} \cdot 44 \text{ pers} \cdot 26 \frac{m^3}{h * pers} + 1767.7 m^2 \cdot 2.5 \frac{m^3}{h * m^2}$$

$$\dot{V} = 8995.25 \frac{m^3}{h}$$

Normalizing and converting units give:

$$\dot{V} = \frac{8995.25 \frac{m^3}{h}}{1767.7 m^2} \cdot \frac{1000 L}{1 m^3} \cdot \frac{1 h}{3600 s}$$

$$\dot{V} = 1.41 \frac{L}{s * m^2}$$

The air flow rate used for the simulations of the cooling technologies is therefore set to $1.50 \frac{L}{s * m^2}$ for all floors.

Passive Cooling

In order to reduce the amount of ventilation needed to keep the building within the requirements for thermal comfort, two passive cooling strategies were implemented in the building. These passive cooling strategies are external window shading controlled by the sun and night cooling of the building.

External window shading is applied to reduce the amount of unwanted radiant heat gain. This will reduce the cooling needed inside as there is less heat to remove.

Night cooling is done by reducing the cooling set-point of the building during the night to pre-cool the building, utilizing the building's thermal inertia. The thermal mass of the building will then work as a heat sink the following day, reducing the cooling load. As seen in Table 5.5, the cooling set-point when the building is unoccupied is lower than when the building is occupied.

5.3 Desiccant Cooling

Desiccant wheels are not selectable in IDA ICE, meaning that the technology's work process needs to be emulated. This is done by implementing a cooling- and heating coil with a fitting custom control system. The custom control is shown as a block diagram in Figure 5.3.

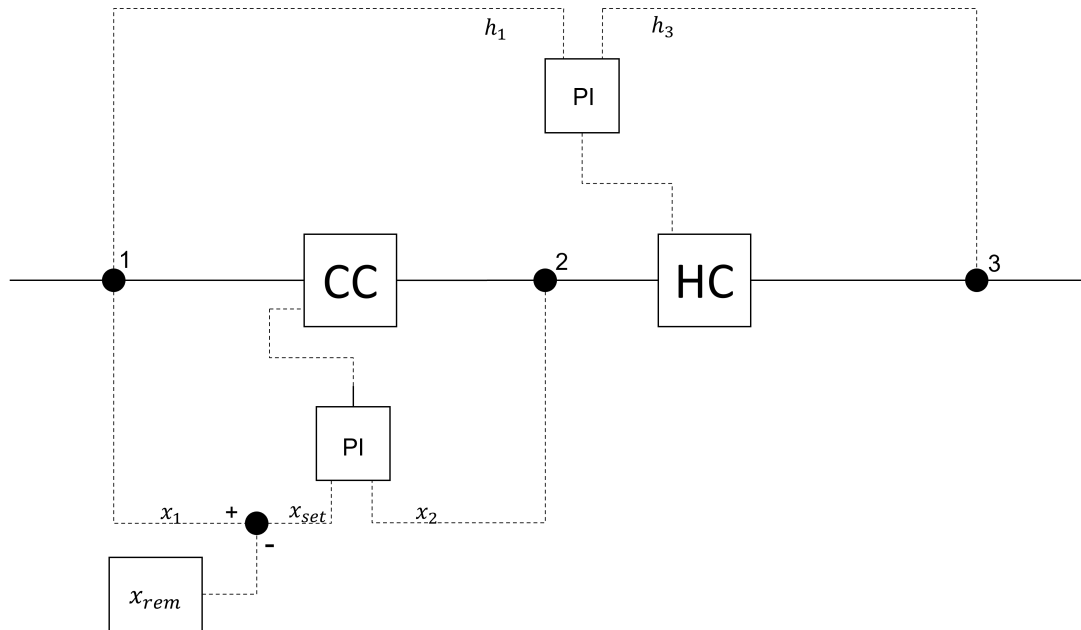


Figure 5.3: Mimic of supply air process in desiccant wheel.

At point 1, the ambient air's absolute humidity and enthalpy content are measured. A given content of the measured humidity content is removed, which is the set-point for the cooling coil. The cooling coil is there to emulate the dehumidification process of the desiccant wheel and is controlled by a PI controller. It is set to cool the air until the humidity ratio at point 2 equals the reduced value from point 1. The expression below shows that the set-point is the removal amount subtracted from the ambient condition.

$$x_{set} = x_1 - x_{rem}$$

As the desiccant wheel is an isenthalpic process, the final state after the wheel should be at the same enthalpy level as the initial. This is where the heating coil comes in, as its purpose is to heat until the enthalpy level equals the initial state. This is also controlled with a PI controller but with enthalpy measurements at points 1 and 3. An example of how the emulated process could look in a Mollier diagram is shown in Figure 5.4.

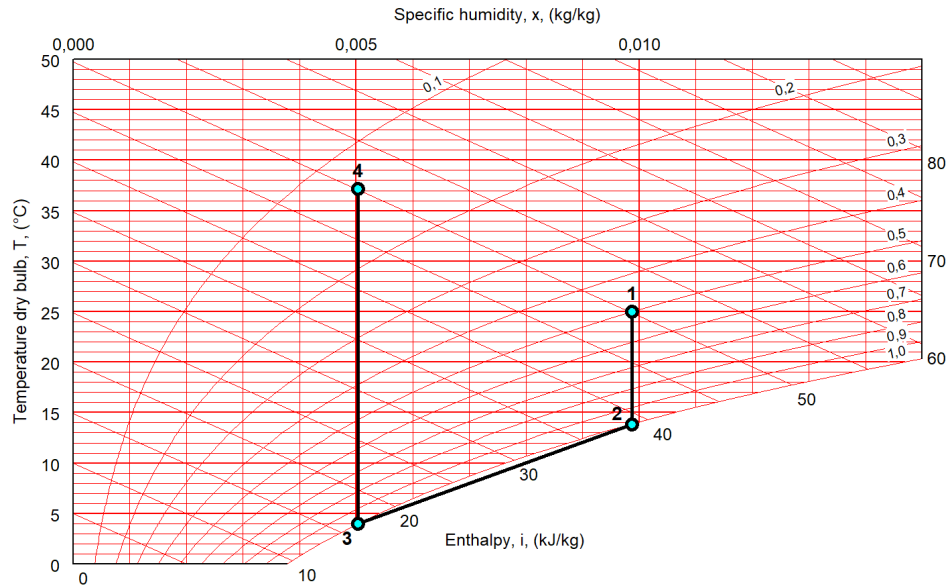


Figure 5.4: Mollier diagram of desiccant wheel mimic.

Instead of a desiccant wheel, where the process would go directly from state 1 to 4., the emulated process uses cooling-based dehumidification by the cooling coil from point 1 to 3 before it is heated from point 3 to 4 in the heating coil.

Figure 5.3 only shows the process happening at the supply air side, where the desiccant wheel is replaced by a cooling coil followed by a heating coil. The process happening on the return side of the wheel is irrelevant as long as the energy consumption due to regeneration of the desiccant is considered.

5.3.1 Wheel Performance

To evaluate the performance of a desiccant wheel under different conditions, a desiccant wheel simulation program provided by NovelAire is used with various input parameters. The program allows for inputs for outdoor conditions, indoor conditions, regeneration temperature, and air flow rate. The interface of the simulation software is shown in Figure 5.5.

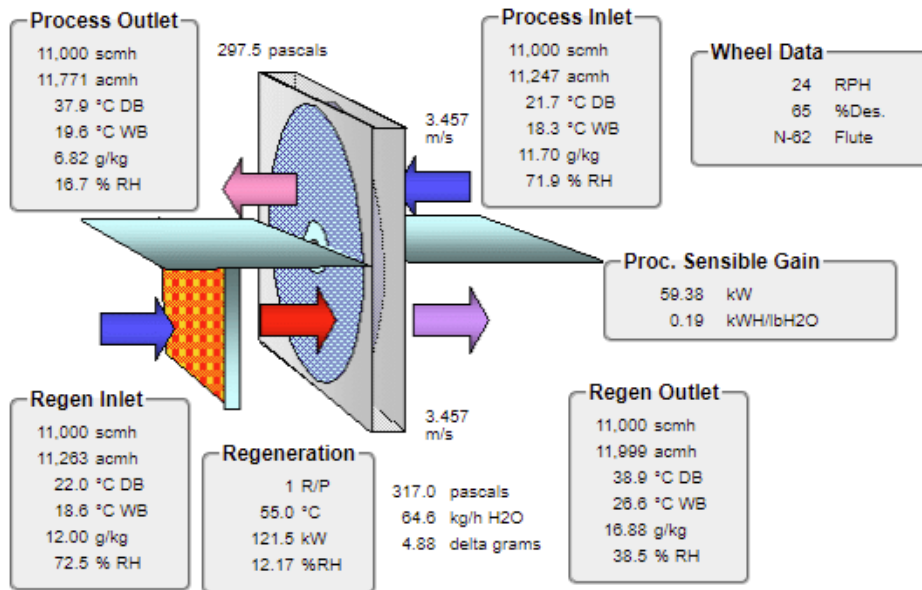


Figure 5.5: Desiccant wheel simulation software [54].

In order to find how the wheel performs under different conditions, several simulations are done to find how each parameter influences the wheel's performance. Simulations with the software are done for various outdoor and indoor conditions and regeneration temperatures.

The outdoor conditions tested in the simulation are adapted from the Gloschaugen weather file used in IDA ICE. The maximum and minimum points for outdoor moisture content and temperature are tested for temperatures 16 °C and above. From this, it is tested how an increase/decrease by one of the parameters while keeping the other constant will influence the wheel's performance. These values are also tested with a change in indoor moisture content and regeneration temperature. For every simulation, the removed moisture content is registered.

These simulations are used to make a regression equation for how the moisture removal rate changes with the four parameters, which will be used to control the desiccant wheel performance in IDA ICE.

The tested values and results from the NovelAire software simulations, along with the regression equation calculation, are shown in Appendix Section A.1.

The regression equation ends up being:

$$Y' = -3.21 \cdot 10^{-3} + (-1.21 \cdot 10^{-4}) \cdot X_1 + (4.70 \cdot 10^{-1}) \cdot X_2 + (-9.90 \cdot 10^{-2}) \cdot X_3 + (1.13 \cdot 10^{-4}) \cdot X_4$$

where:

Y' : Removed moisture content [$\text{kg}_w/\text{kg}_{da}$]

X_1 : Outdoor temperature [$^{\circ}\text{C}$]

X_2 : Outdoor moisture content [$\text{kg}_w/\text{kg}_{da}$]

X_3 : Indoor moisture content [$\text{kg}_w/\text{kg}_{da}$]

X_4 : Regeneration temperature [$^{\circ}\text{C}$]

From Figure A.1 in the Appendix, one can see that the predicted values for moisture removal match the actual values quite well.

As indicated by the equation, here is how the four variables affect the removal amount:

- Removed moisture content **decreases** with increasing outdoor temperature.
- Removed moisture content **increases** with increasing outdoor moisture content.
- Removed moisture content **decreases** with increasing indoor moisture content.
- Removed moisture content **increases** with increasing regeneration temperature.

5.3.2 IDA ICE Modeling

Using the block diagram in Figure 5.3 and the regression equation provided above, the air handling unit with the desiccant wheel mimic can be modeled in IDA ICE. As the supply temperature is set to 16 $^{\circ}\text{C}$, the desiccant wheel is set to only operate when the ambient air is over 16 $^{\circ}\text{C}$.

Supply Side

The supply side process includes removing moisture in a cooling coil and heating until it reaches the same enthalpy as the initial condition in a heating coil.

As the removed moisture content varies with regeneration temperature and both indoor and outdoor conditions, the regression equation shown in Section 5.3.1 is implemented in the control. The control is shown in Figure 5.6 and resembles how it looks in IDA ICE.

Value b_1 is multiplied by the measured ambient temperature, b_2 is multiplied by the ambient moisture content, b_3 is multiplied by the indoor moisture content, and b_4 is multiplied by the regeneration temperature. The sum of these factors, and value a , make up the removed moisture content for the given condition.

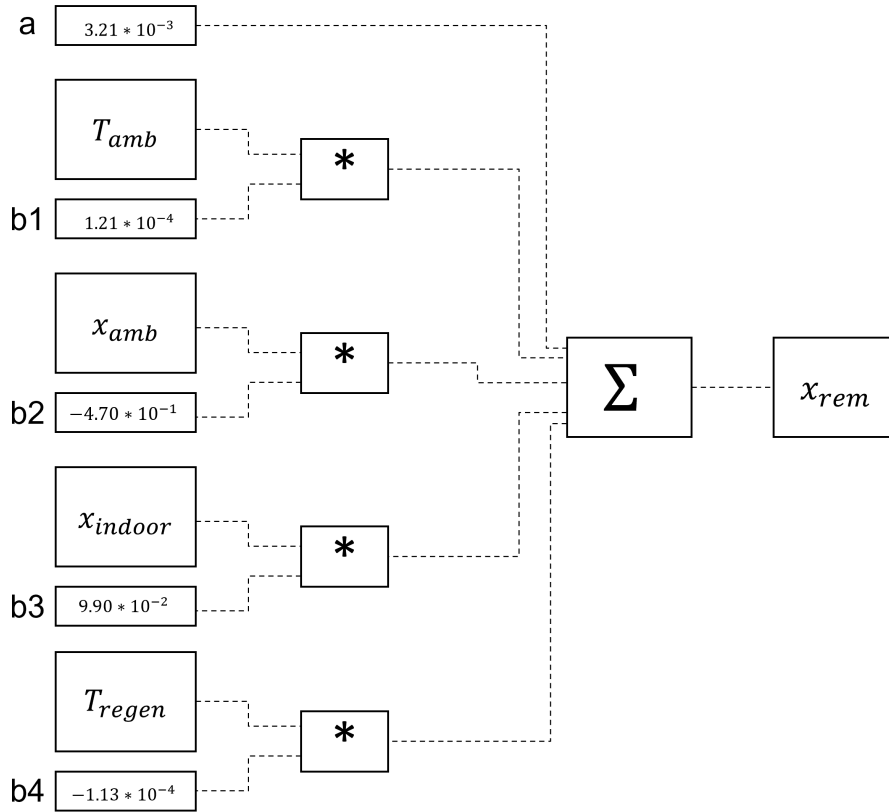


Figure 5.6: Removed moisture content control in IDA ICE.

As the supply temperature is set to 16 °C, the wheel is set to operate only when the outside air temperature is above this. The control implemented in IDA ICE is shown in Figure 5.7. The ambient temperature is checked in a box before sending a signal to be multiplied with the removed moisture content. If the ambient temperature is under 16 °C, the removed moisture content signal will be multiplied by a zero. This means that the set-point moisture content will equal the outdoor conditions as long as the outdoor temperature is under 16 °C.

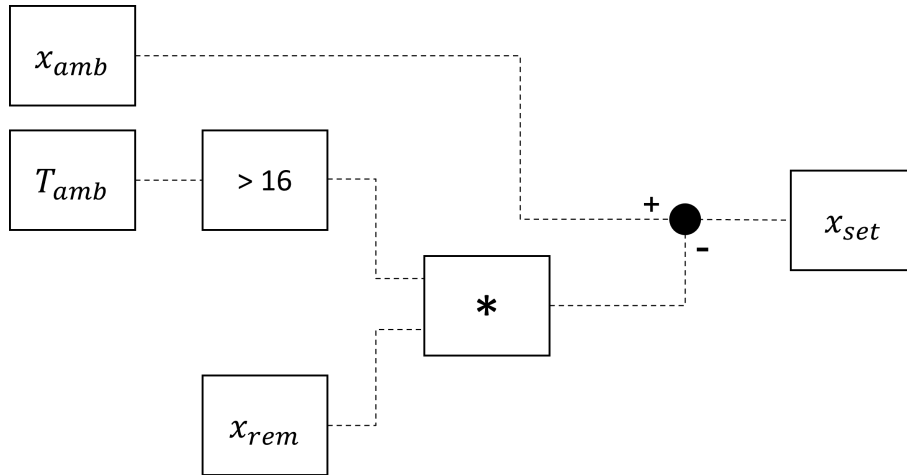


Figure 5.7: Control of set-point moisture content in IDA ICE.

The set-point from Figure 5.7 is used to control the cooling coil as seen in Figure 5.8. The set-point moisture content is compared to the moisture content after the cooling coil in a PI controller. The signal from the PI controller is set-point in a linear transformation from the ambient temperature to a lower limit. The linear transformation sets the set-point temperature for the cooling coil. If the set-point moisture content is equal to the moisture content after the cooling coil, the coil will be turned off as the set-point is equal to the ambient conditions.

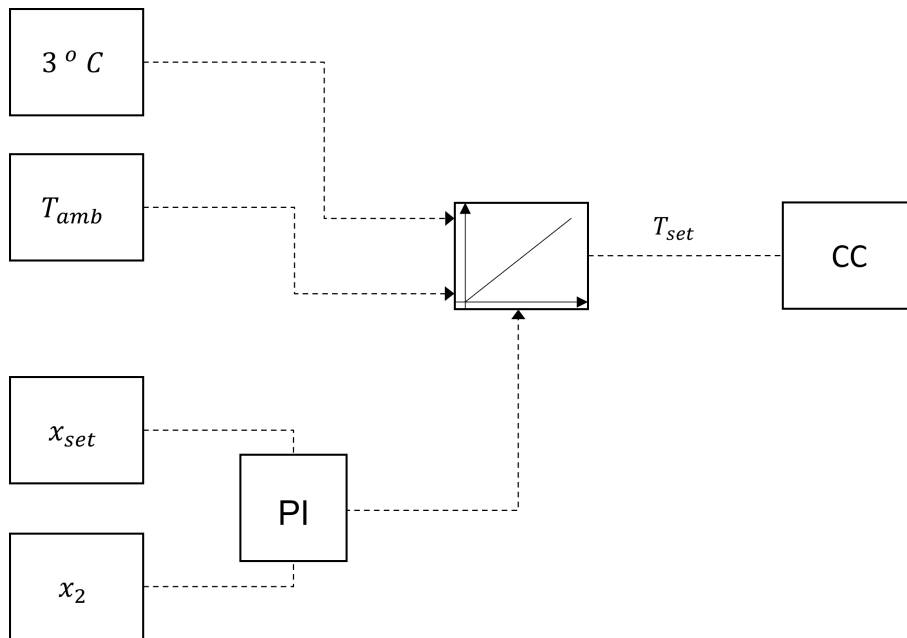


Figure 5.8: Control of cooling coil in IDA ICE.

The heating coil is present to heat the air until it reaches the same enthalpy level as the air had before the cooling coil. The control is shown in Figure 5.9. The control uses a PI controller, which compares the outdoor enthalpy level and the enthalpy level after the heating coil.

Similar to the cooling coil, the set-point is decided by a linear transformation with the signal from the PI controller as the input signal. The heating coil will turn off if the two enthalpy levels are equal.

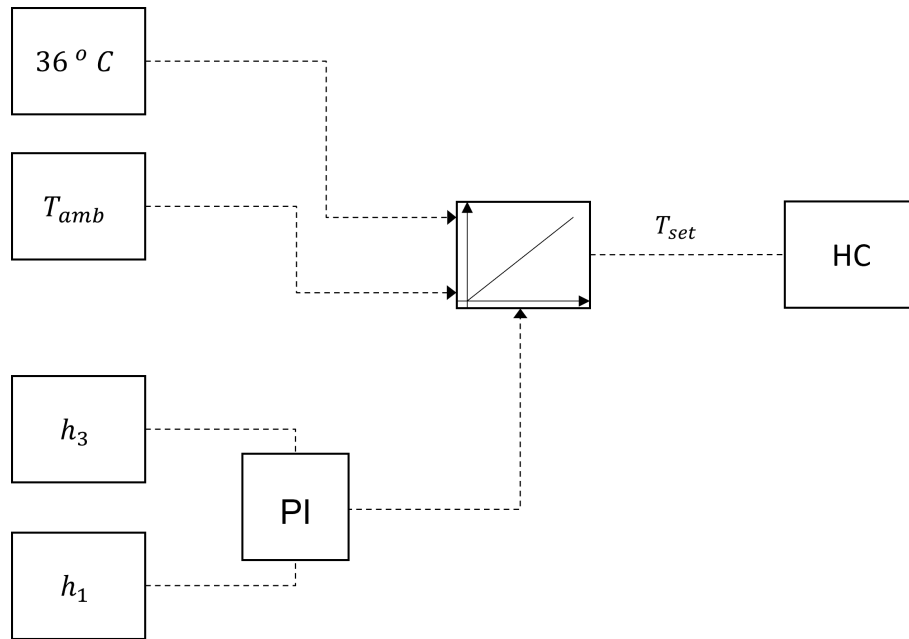


Figure 5.9: Control of heating in IDA ICE.

Regeneration Temperature

As the regeneration heater is used to regenerate the desiccant wheel, it is only needed when the wheel is operated. As the wheel only operates when the outside air is above 16 °C, this also applies to the regeneration heater.

To avoid unnecessary energy use due to heating of regeneration air, the regeneration temperature is controlled, so the wheel never removes more moisture than necessary. This is done by comparing the enthalpy level of the supply air with the enthalpy level of air at 16 °C and 75% relative humidity in a PI controller. The idea is that the adiabatic humidifier will cover the remaining sensible cooling. Suppose the enthalpy level of the supply air is too high. In that case, the regeneration temperature will be increased to remove more moisture in order to reach the desired set-point temperature out of the AHU.

A visual representation using the Mollier diagram is shown in Figure 5.10. If the enthalpy level of the supply air is above the line, the regeneration temperature will increase.

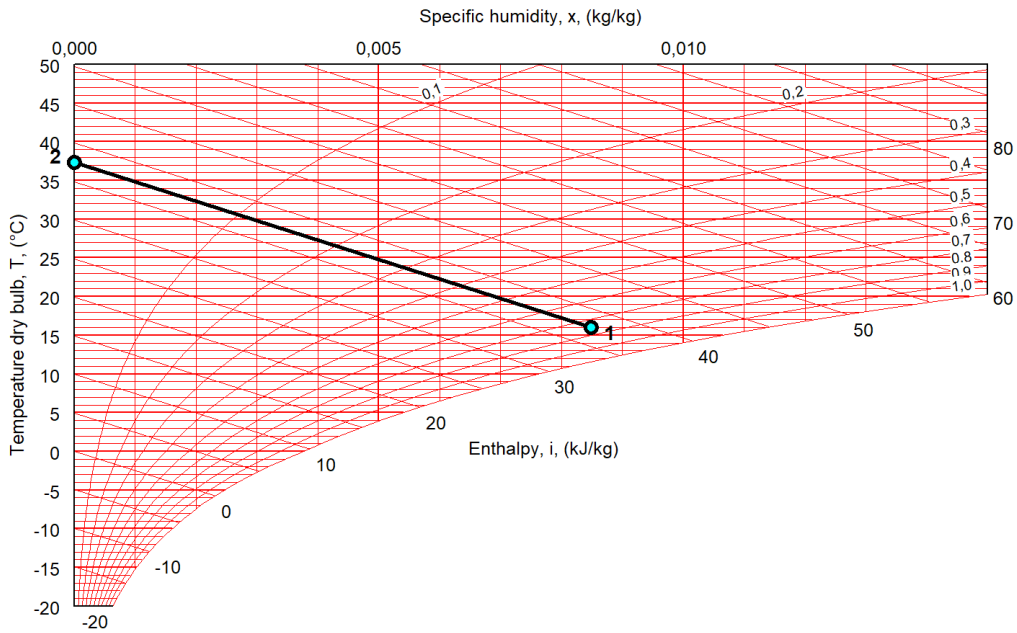


Figure 5.10: Activation set-point of the regeneration heater using a Mollier diagram.

The output from the PI controller is used in a linear transformation to varying temperatures between the return temperature and 55 °C. The upper regeneration temperature is set to 55 °C, as this is the same temperature used in the DesiCool system provided by Munters [55].

The described control is shown in Figure 5.11, where the value of 36877 J/kg is the enthalpy of air at 16 °C and 75% relative humidity.

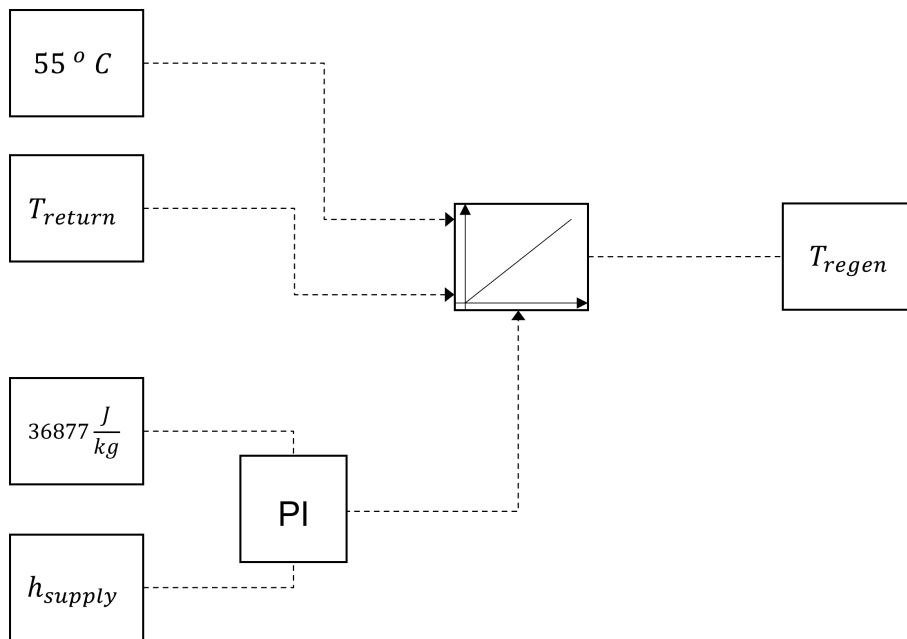


Figure 5.11: Regeneration temperature control.

Direct Evaporative Cooler

The direct evaporative cooler on the supply side is present to cool the supply air to the desired state and is thus controlled by a 16 °C input signal. In order to avoid too high relative humidity, a maximum amount of 75% is set, which corresponds to the enthalpy level used to control the regeneration temperature. As this component can only cool the air, it does not have to be controlled according to the outdoor conditions like the desiccant wheel and the regeneration heater.

As the direct evaporative cooler on the return is present to utilize indirect evaporative cooling through the heat exchanger by cooling the return air, it is necessary to implement more control. Cooling the return air is only necessary when there is a cooling demand, making the evaporative cooler controlled by the ambient air temperature. For outside air temperatures above 16 °C, the evaporative cooler will cool the air, and for temperatures below, it will be turned off. The evaporative cooler on the return side is set to a maximum RH of 95%, as this is the same limit observed in Section 4.1.1. In this way, the heat exchanger will recover heat when the temperature is under 16 °C and recover cooling when the temperature is over 16 °C.

Overview

The controls described above are implemented with the AHU configuration shown in Figure 5.12, and are used for the desiccant cooling simulations. Configuration matches the unit installed in S oderlundmyra 18 shown in Section 4.2.1. The heat exchanger is set to a temperature efficiency of 75%.

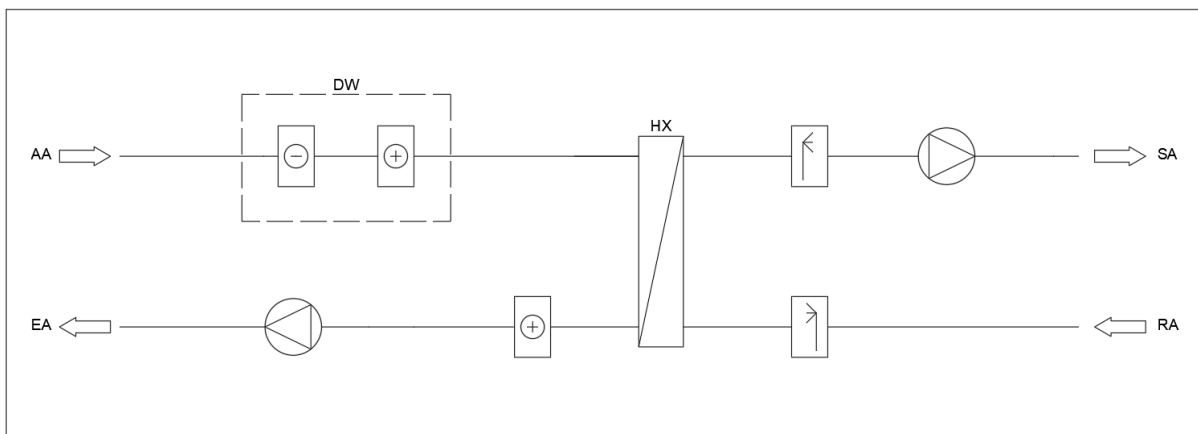


Figure 5.12: Configuration of DW AHU in IDA ICE.

5.3.3 Previous Model

The model presented is an extension of a previously built model, which was also made using the desiccant wheel simulation program provided by NovelAire.

The difference between the two models is the number of parameters used to evaluate the performance. The previous model kept both regeneration temperature and indoor conditions constant for simplicity. Here the regeneration temperature was set to 55 °C as long as the wheel was active.

The performance equation for the previous model was as follows:

$$Y' = 1,57 * 10^{-3} + (-6,30 * 10^{-5}) \times X_1 + (2,95 * 10^{-1}) \times X_2$$

where:

Y' : Removed moisture content [kg_w/kg_{da}]

X_1 : Outdoor temperature [°C]

X_2 : Outdoor moisture content [kg_w/kg_{da}]

5.4 IEC Modeling

The indirect evaporative cooling works as explained in Section 2.10.3. A direct evaporative humidifier is installed on the return side of the air handling unit and is controlled by the outside air temperature. The humidifier is active as long as the ambient air temperature is greater than 16 °C. Maximum relative humidity out of the evaporative humidifier is, as for the desiccant cooling, set to 95%. If additional air cooling is necessary, the cooling coil fulfills the demand. The air handling unit contains a heat exchanger with a temperature efficiency of 75%.

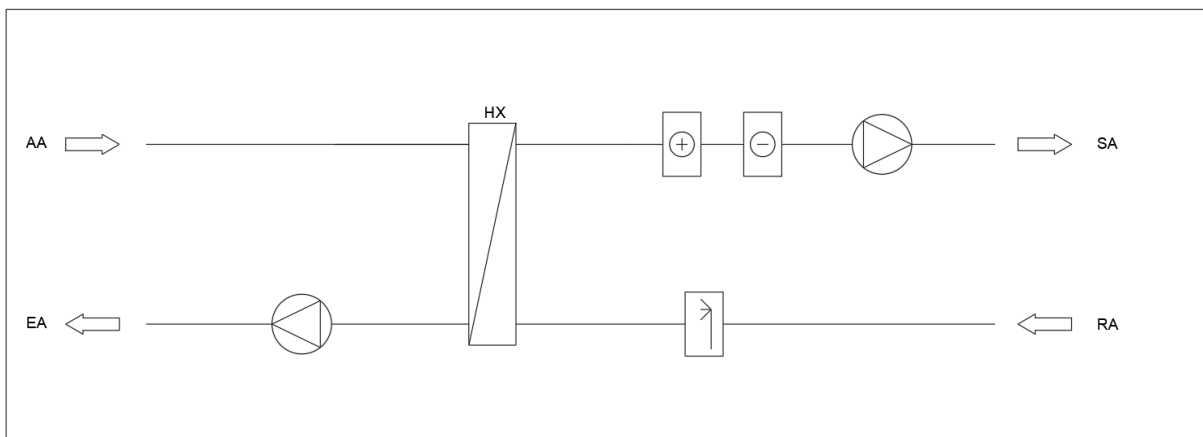


Figure 5.13: Configuration of IEC AHU in IDA ICE.

5.5 Chiller Modeling

For the case of standard mechanical cooling, a generic electric chiller is installed together with a standard air handling unit. A COP_R of 3.1 is selected for the electric chiller, which is a reasonable value for an air-cooled chiller [56]. This means the system provides just over three times the cooling power for the electric power consumed, as explained in Section 2.10.1.

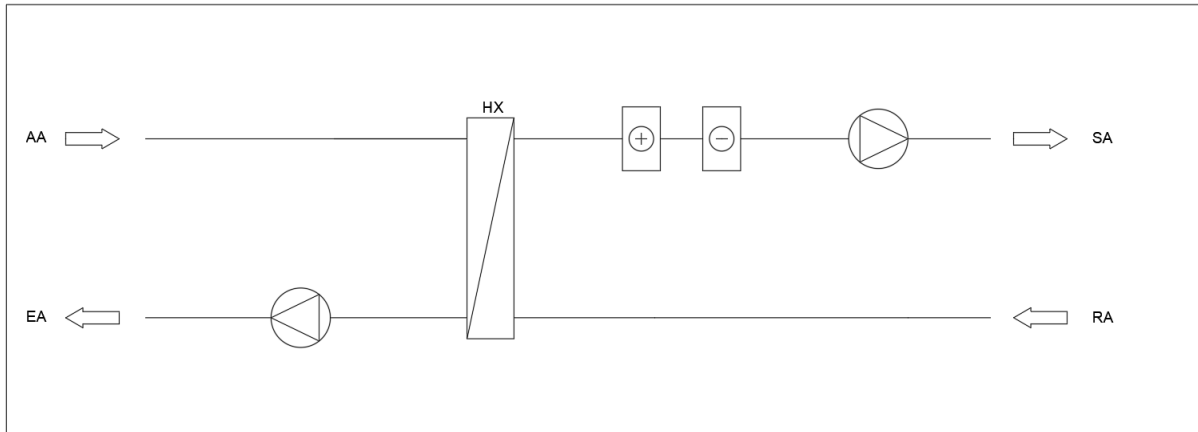


Figure 5.14: Configuration of standard air handling unit in IDA ICE.

The air handling unit contains a heat exchanger with a temperature efficiency of 75%.

5.6 Simulations

All the simulated cooling technologies are implemented with the simplified model of the ZEB Laboratory. Since the study's objective is cooling, the simulation period is set from May 1st to September 30th, which is the cooling season in Norway. As explained in the scope of the study, efficiencies and losses in the energy system are not included in the simulations, meaning only the energy supplied to the AHU is considered. A simplified sketch of the system boundaries is shown in Figure 5.15. As seen, the boundary in blue is the considered area for the comparison between the cooling technologies.

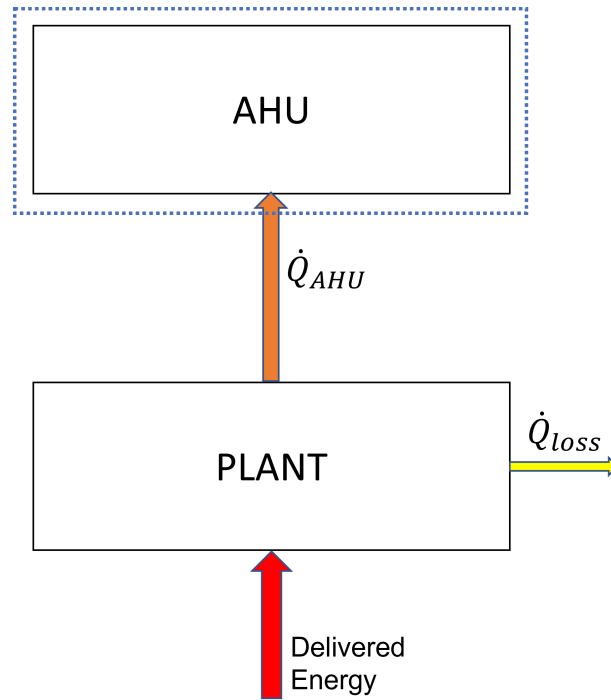


Figure 5.15: System boundaries for energy calculation in simulation.

5.6.1 Desiccant Cooling

The set-point temperature in which the desiccant wheel is activated is also investigated. For lower temperatures, it is expected that the heat exchanger and the evaporative humidifiers can cover the load without needing the desiccant wheel. This is done by changing the set-point temperature shown in Figure 5.16 which controls the activation of the wheel. The red box from the figure illustrates the activation set-point and is the one being changed to vary the activation set-point. In addition to the 16 °C set-point, setting the wheel to activate at 18 °C and 20 °C is tested and compared based on energy need and thermal comfort.

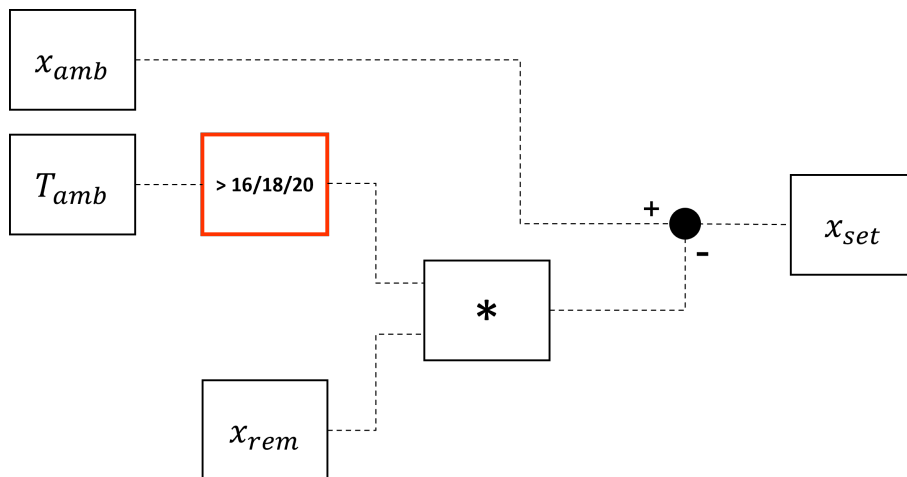


Figure 5.16: Change in activation set-point for desiccant wheel.

5.6.2 Indirect Evaporative Cooling

Simulations are performed for the system shown in Figure 5.13. The effect of adding a direct evaporative humidifier to the supply is also investigated. For the case of DEC in supply, the same settings as the DEC in desiccant cooling are used.

5.6.3 Chiller

Simulations are run for the standard air handling unit shown in Figure 5.14.

Results

6.1 Base Case

6.1.1 Air Flow Review

Results of the pre-simulations of the ZEB Lab are shown in Table 6.1. Six different values for normalized ventilation rate were tested to see how the operative temperatures and cooling load would change. This is to eventually find a reasonable air flow rate that would fulfill the thermal requirements of the building code.

Table 6.1 shows the max operative temperature measured for each floor for the different tests, along with the annual cooling load per floor area for the building.

Air flow [$\frac{L}{s \cdot m^2}$]	Max operative temperature [$^{\circ}C$]				Cooling load [W/m^2]
	Ground fl.	First fl.	Second fl.	Third fl.	
1.00	27.71	27.31	27.35	26.91	19.92
1.20	26.69	26.28	26.32	25.91	22.62
1.25	26.48	26.07	26.11	25.7	23.27
1.35	26.19	25.72	25.79	25.4	24.56
1.50	25.83	25.36	25.41	25.07	26.53
1.67	25.51	25.04	25.09	24.78	28.56

Table 6.1: Pre-simulations of ZEB Lab.

Figure 6.1 gives the number of hours the temperature of the floors exceed 26 °C for the pre-simulations with the different air flow rates.

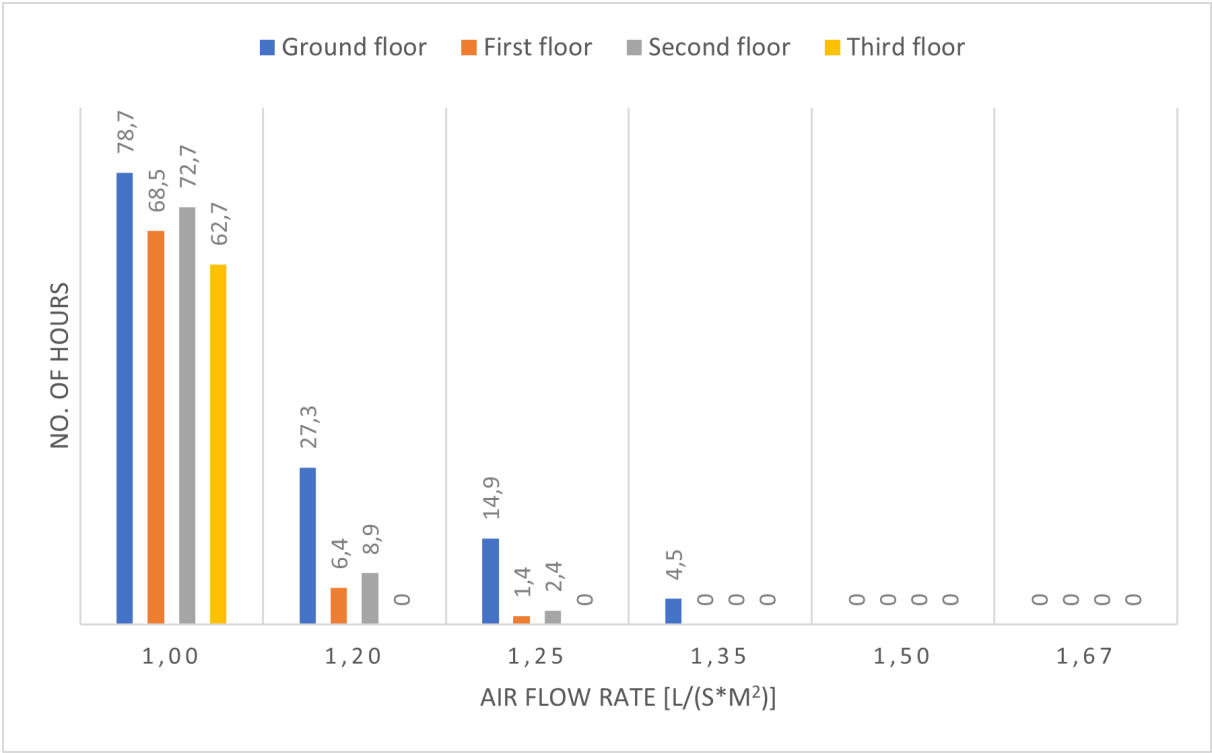


Figure 6.1: Number of hours above 26 °C for the pre-simulations.

6.1.2 Energy Need

Figure 6.2 shows the AHU cooling energy needed to keep the supply air at 16 °C for the simulated period.

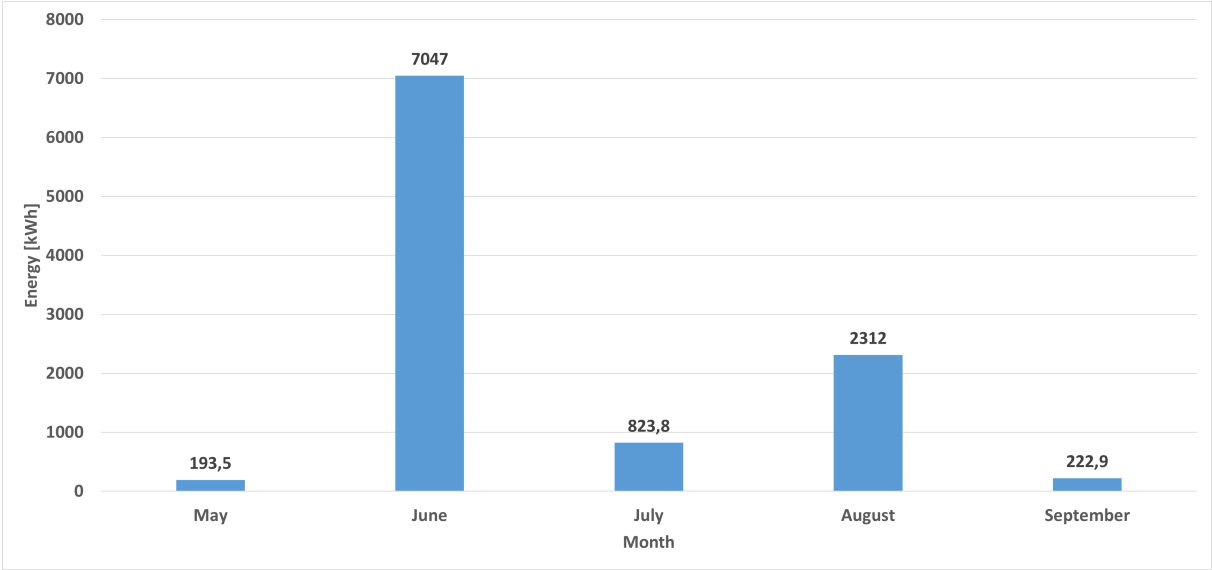


Figure 6.2: Energy need for simulated period.

The total comes out at 10599.2 kWh of cooling supplied by the cooling coil.

6.2 Chiller

Using a chiller, the energy need of the system becomes equal to the base case. However, the consumed electrical energy to provide this need is considerably lower. The chiller has a COP_R of 3.1, which means the consumed electrical energy will be $1/3.1$ of the energy need.

6.3 Desiccant Cooling

6.3.1 Model Validation

To verify that the model works as intended, and follows the correct physical principles, results that authenticate the model are presented below.

The process happening inside the desiccant wheel is approximately isenthalpic, and the enthalpy level of the air prior to and after the wheel is shown in Figure 6.3. As seen, the two enthalpy levels coincide at all times.

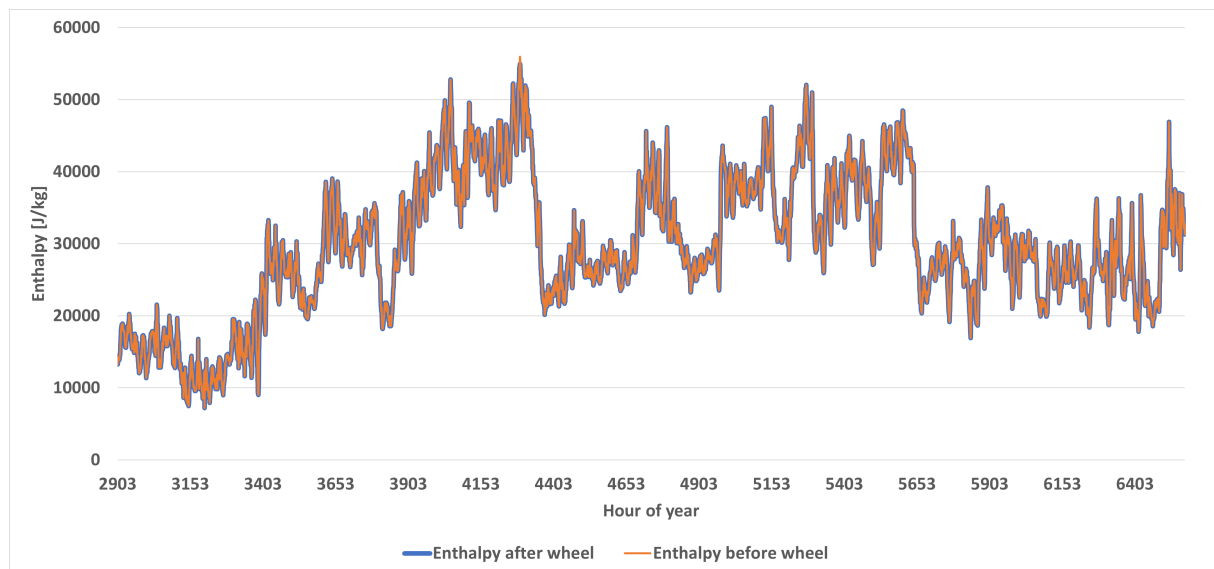


Figure 6.3: Model validation - isenthalpic process.

Figure 6.4 shows the temperature of the air prior to and after the cooling coil in the desiccant model. The coil cools the air when outside air exceeds $16\text{ }^{\circ}\text{C}$. The graphs coincide when the ambient temperature is under the set-point of 16 ° , meaning no cooling is being done.

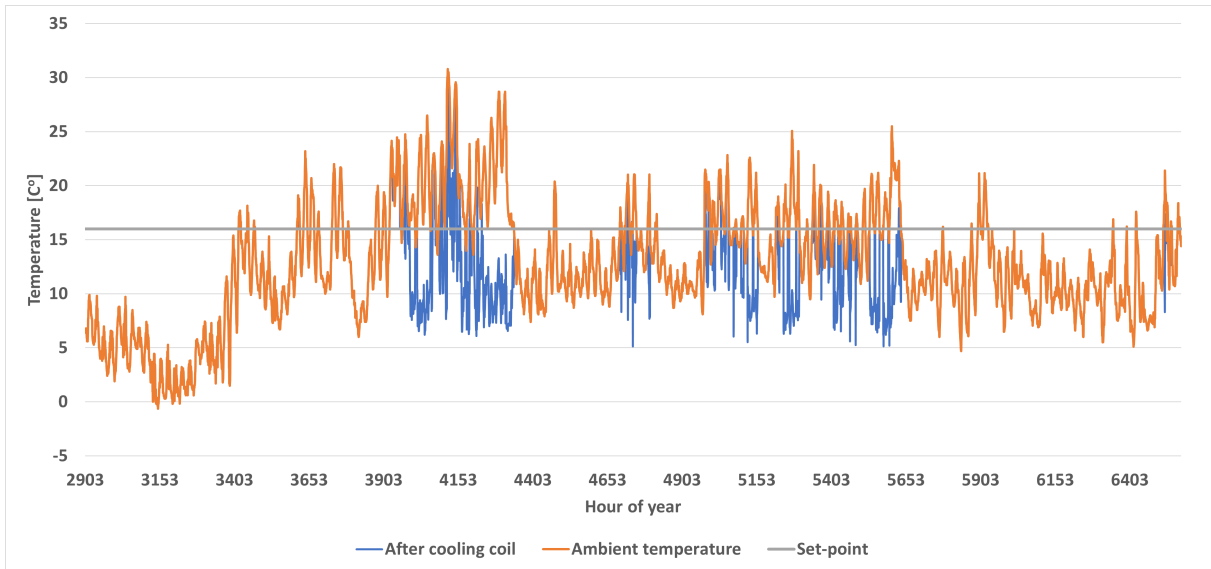


Figure 6.4: Temperature change over cooling coil.

Figure 6.5 shows the moisture content of the air prior to and after the desiccant wheel. As seen, the deviations increase with increasing moisture content.

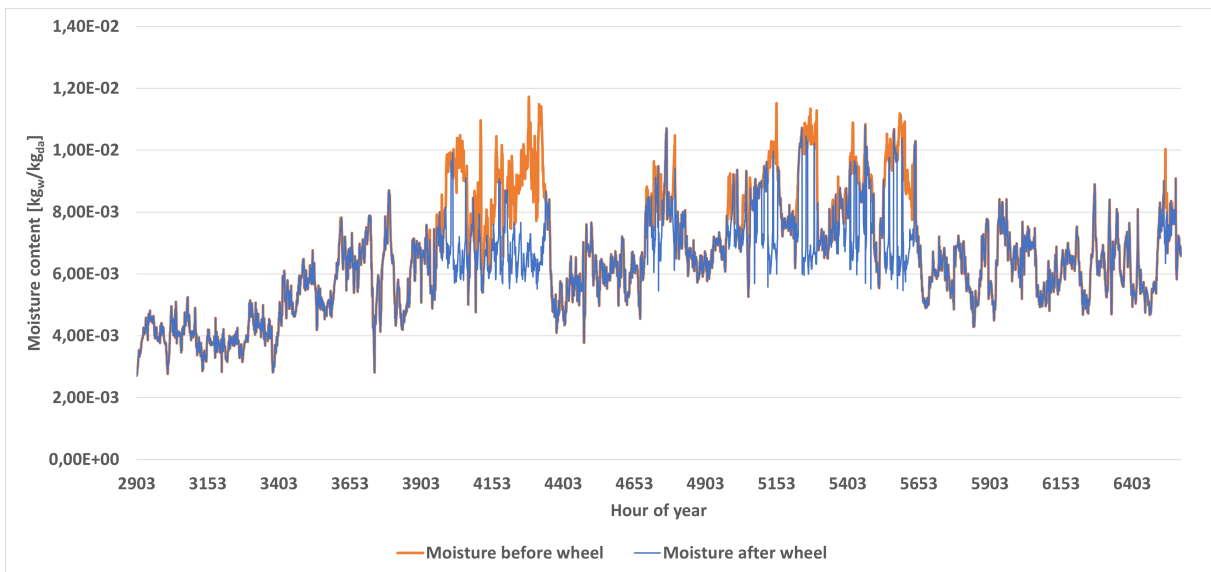


Figure 6.5: Moisture before and after desiccant wheel.

Figure 6.6 shows the change in moisture through the air, meaning the content before minus the content after.

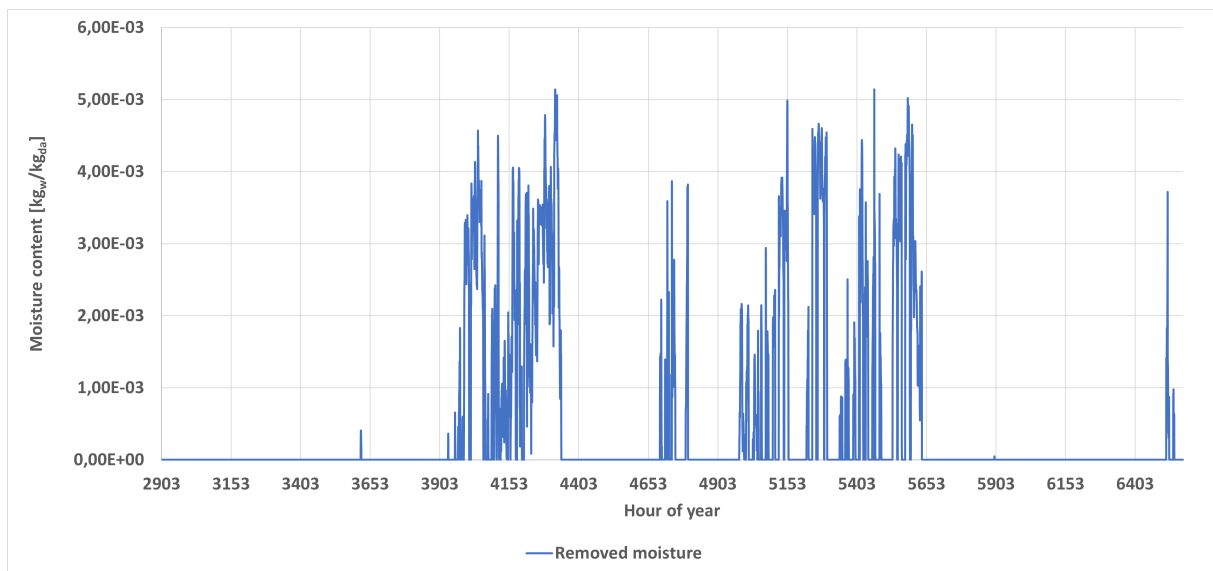


Figure 6.6: Moisture change in desiccant wheel.

The change in regeneration temperature is shown in Figure 6.7. If compared with Figure 6.6, it is clear that the higher regeneration temperatures coincide with the greater changes in moisture.

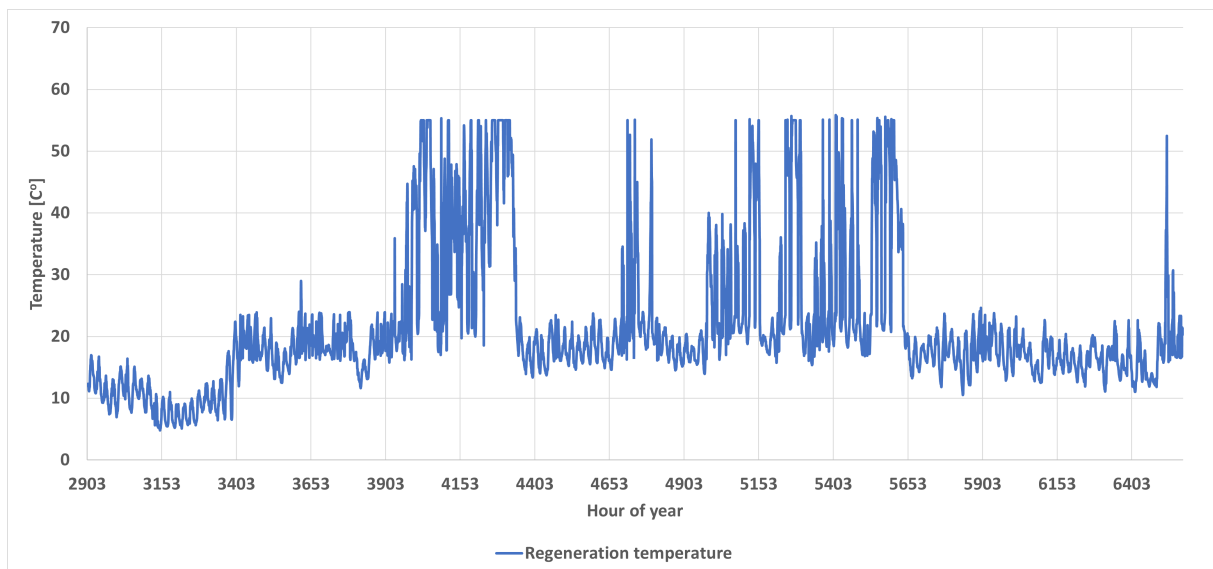


Figure 6.7: Change in regeneration temperature.

6.3.2 Energy Need

The energy used for cooling with the desiccant wheel system is the energy due to the regeneration of the desiccant. Since the system also uses IEC and DEC, different activation set-points for the desiccant wheel have been tested and compared based on energy use and thermal comfort. Figure 6.8 presents the energy use for regeneration and the highest PPD value for three different activation set-points. Note that the number behind DW is

the set-point for where the wheel is activated.

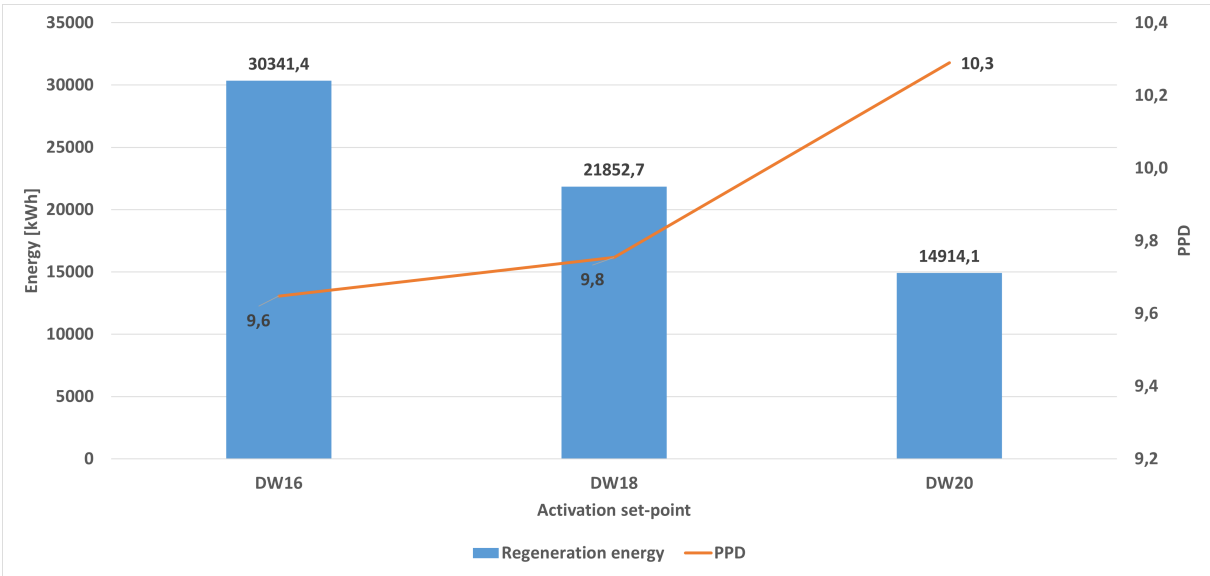


Figure 6.8: Regeneration energy need and PPD for desiccant cooling system with set-points 16, 18 and 20 C.

6.3.3 Previous Model

Comparing the energy need due to regeneration for the previous model with the current model gives the distribution shown in Figure 6.9.

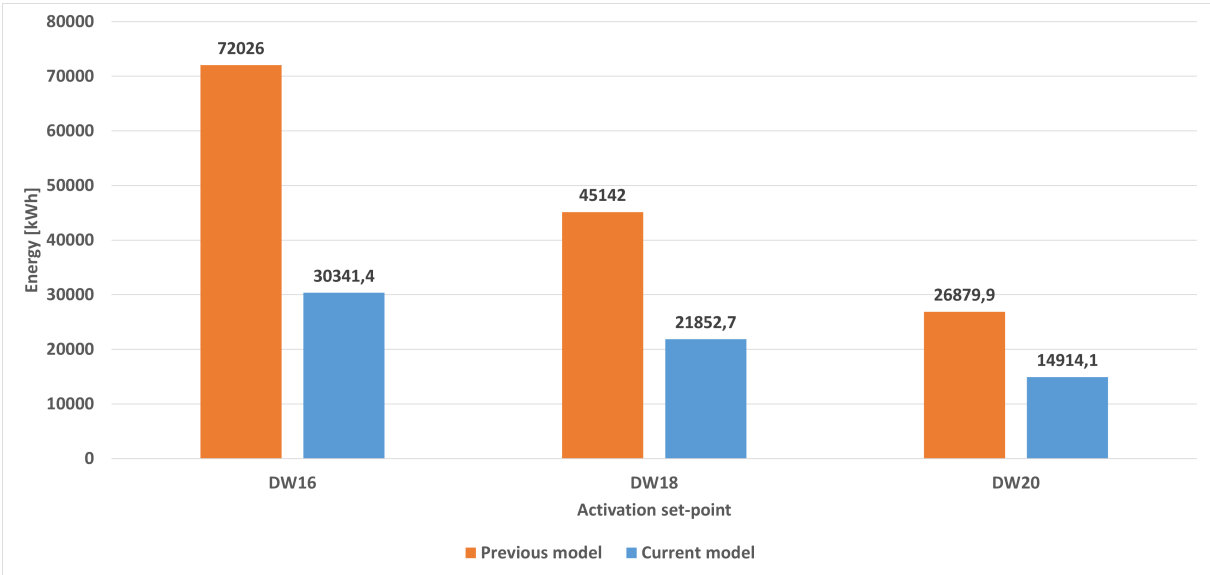


Figure 6.9: Regeneration energy need for desiccant cooling system with various set-point for previous and current model.

6.4 Indirect Evaporative Cooling

6.4.1 Model Validation

In Figure 6.10, ambient temperature is compared with temperatures from the air handling unit. As seen, the return temperature after the humidifier is reduced as soon as the ambient air temperature exceeds 16 °C, which is the set-point for activation.

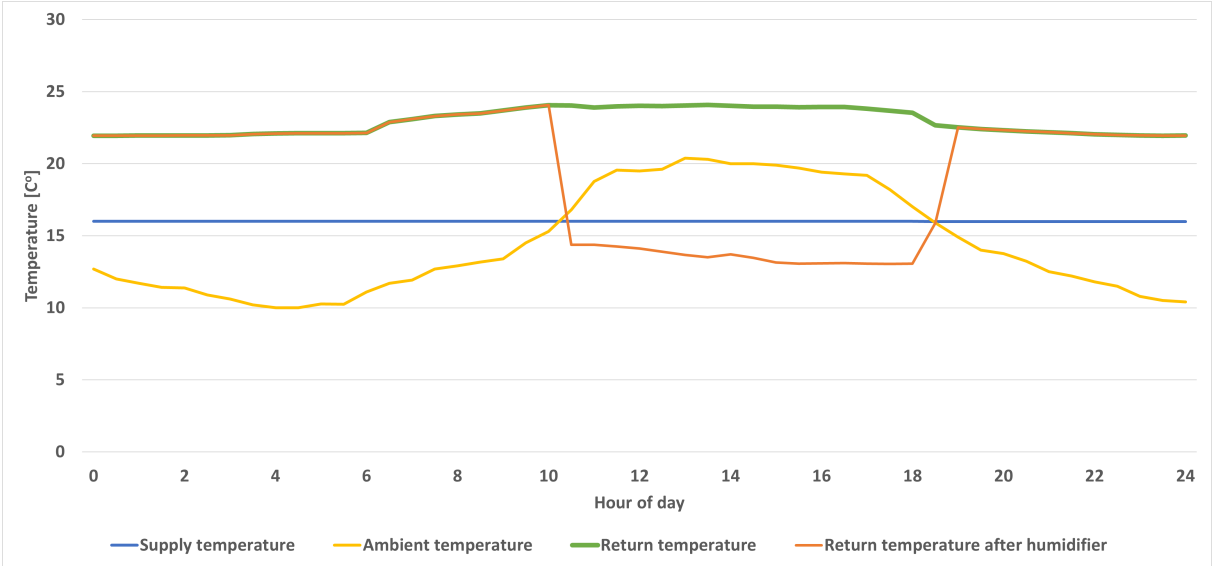


Figure 6.10: Activation of indirect evaporative cooling.

6.4.2 Energy Need

The energy need for the system containing indirect evaporative cooling is shown in Figure 6.11.

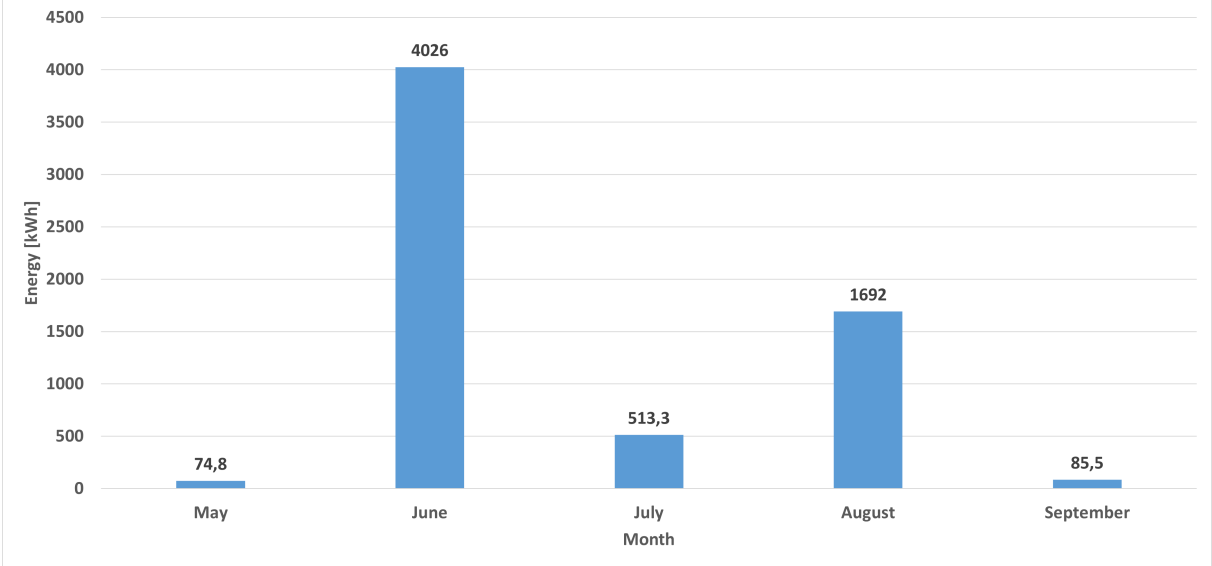


Figure 6.11: Energy need with indirect evaporative cooling.

In order to visually compare the energy need of the IEC system with the case without IEC, both the energy need with IEC and the reduced energy need are shown in Figure 6.12. The blue bars represent the energy need with IEC, while the orange bars represent the amount of energy reduced from the base case. Summing up the two bars for each month gives the base case results shown in Figure 6.2.

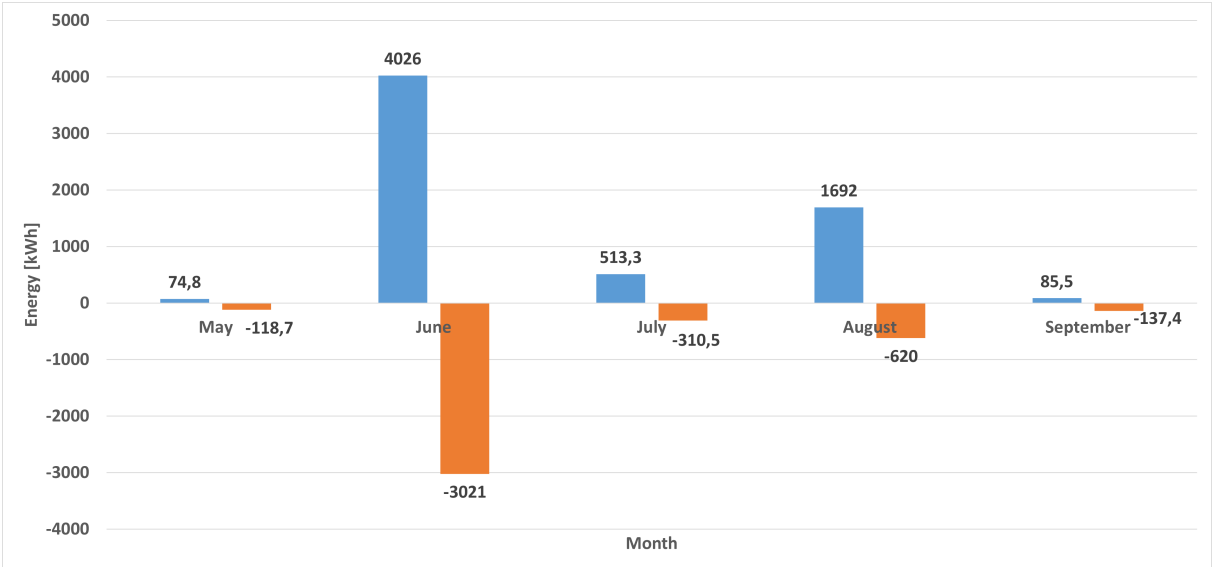


Figure 6.12: Reduced energy need from base case with indirect evaporative cooling. Blue bar is energy need and orange bar is amount reduced from base case scenario.

The total energy need is 6391.6 kWh, a reduction of 4207.6 kWh from the energy need of the base case.

Adding an evaporative cooler in the supply, making the system contain both direct and indirect evaporative cooling, makes the energy need end up as shown in Figure 6.13.

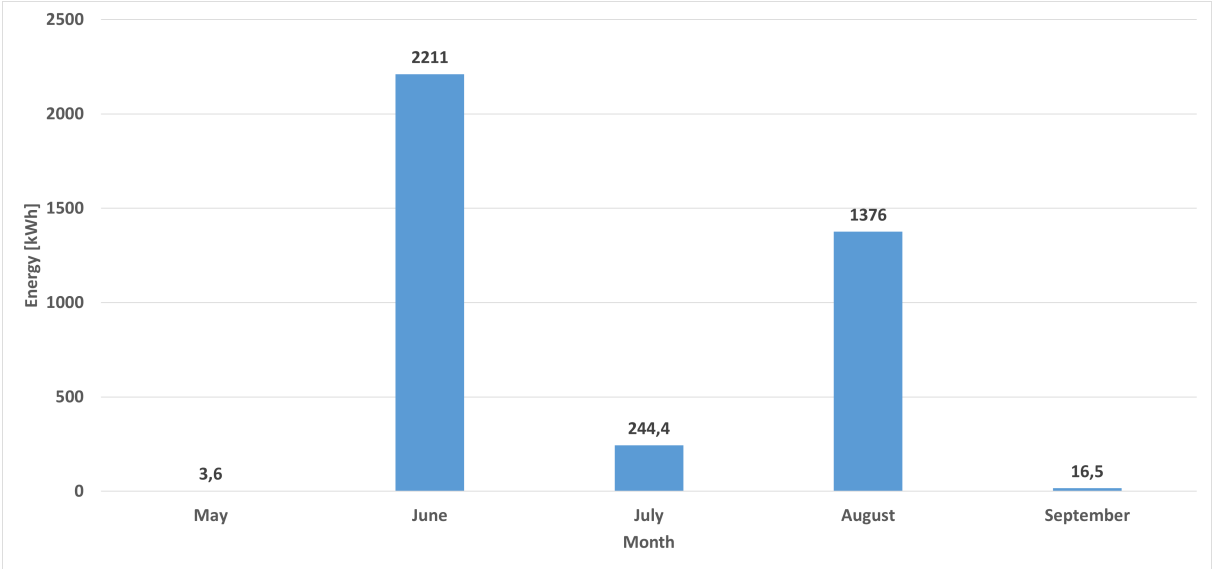


Figure 6.13: Energy need with direct and indirect evaporative cooling.

As for the IEC system, the combined IEC and DEC are compared to the energy need of the base case. The comparison is shown in Figure 6.14, where the orange bars represent the reduction and the blue bars represent the energy need for the configuration.

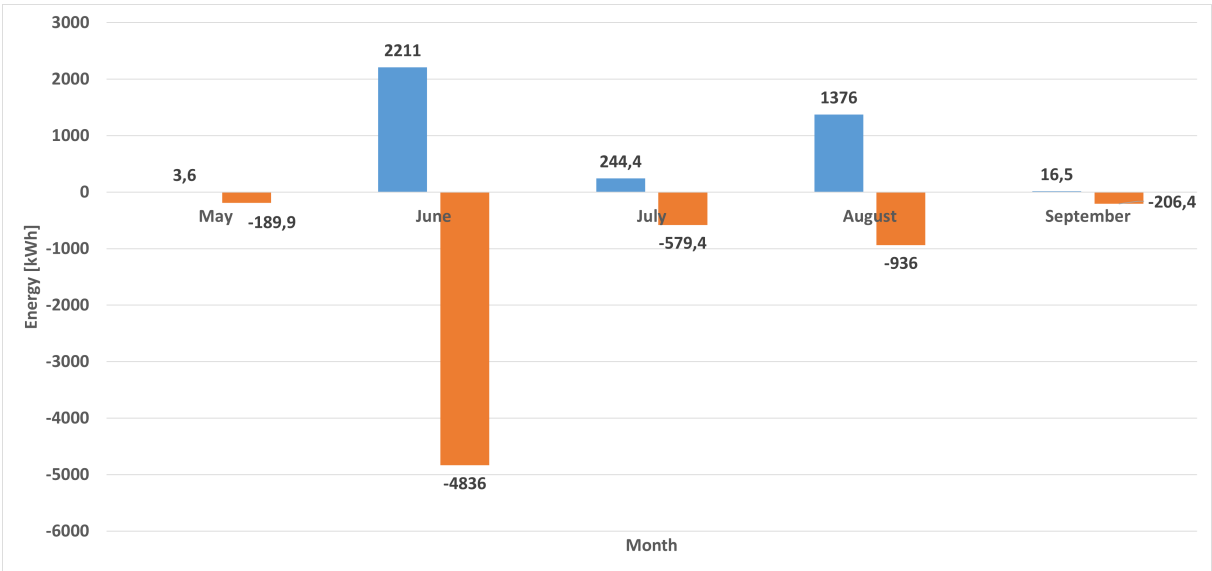


Figure 6.14: Reduced energy need from base case with indirect and direct evaporative cooling. Blue bar is energy need and orange bar is amount reduced from base case scenario.

The total energy need is 3851.5 kWh, a reduction of 6747.7 kWh from the energy need of the base case.

6.5 Comparison

Comparing the simulated system configurations on both energy need and the PPD of the worst zone gives the distribution shown in Figure 6.15. For all the system configurations, the ground floor is the zone with the highest PPD.

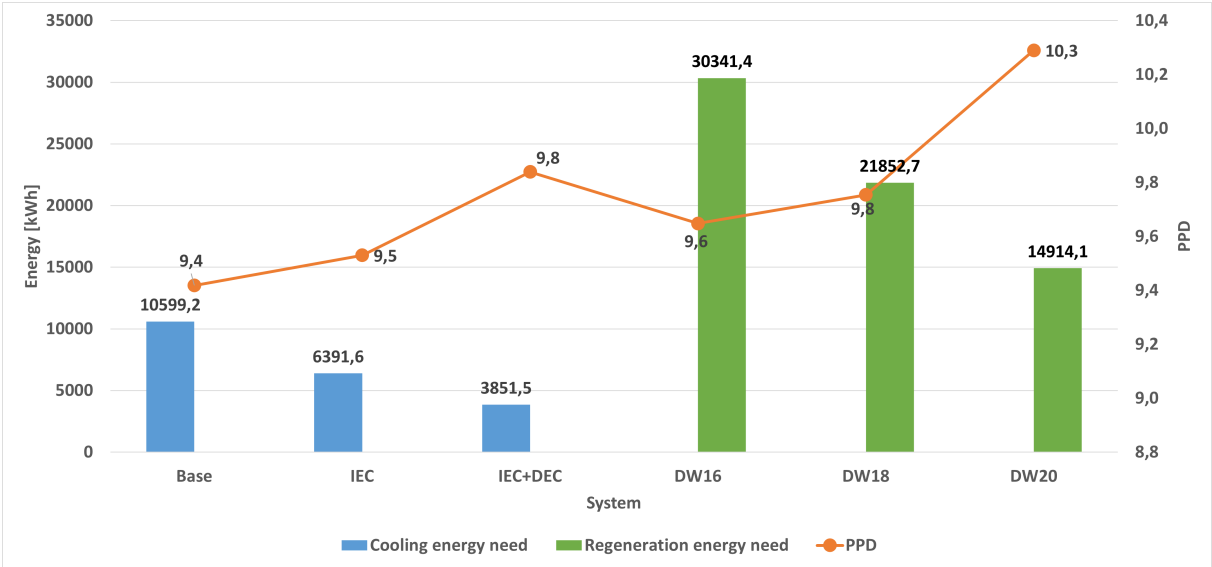


Figure 6.15: Comparison of energy need and PPD of the different systems.

Discussion

In this chapter, the findings and results from the simulations are discussed.

7.1 Desiccant Wheel Model

An initial objective of the master thesis was to improve the simplified model of the desiccant wheel in IDA ICE which was created for the specialization course. As explained, the performance of the previous model of the desiccant wheel was influenced only by two factors, namely outdoor temperature and moisture content. The performance of the improved model is influenced by four factors, namely the outdoor temperature, outdoor moisture content, indoor moisture content, and regeneration temperature. The control of the wheel is also set to only remove as much moisture as necessary, and thus only as much energy need due to regeneration as necessary.

The process happening in the desiccant wheel is isenthalpic, meaning the enthalpy both before and after the wheel should remain constant. Figure 6.3 presents the enthalpy level of the supply air prior to and after the wheel. The figure clearly shows that the two enthalpy levels coincide at all times, meaning that the process is isenthalpic.

Figure 6.5 and Figure 6.4 shows the change in moisture and temperature over the cooling coil, respectively. There is no change when the ambient temperature is under the set-point temperature for activation. The temperature and moisture change when the ambient temperature exceeds the set point. The period for these graphs is equal, and as seen, both changes in temperature and moisture happen at the same time.

As mentioned, the improved model aims to minimize energy need by controlling the regeneration temperature by the current demand in the system. The regeneration temperature is shown in Figure 6.7, and from here, it is observed that the temperature varies

throughout the simulated period. Rather than heating the air to 55 °C all times the wheel is active, the temperature is controlled based on the enthalpy of the supply air. Using this control, the system prioritizes cooling by indirect and direct evaporative cooling and uses the desiccant wheel when additional cooling is necessary.

7.2 Energy Needs

7.2.1 Base Case

The base case gives the net energy need for a standard air handling unit for the simulated period and is used to compare the effects of the different cooling technologies.

7.2.2 Chiller

The net energy need remains the same with a chiller since the system configuration remains unchanged. The energy use, which is the electrical energy consumed by the compressor in the chiller, is significantly reduced when introducing the chiller as it has a cooling efficiency of 3.1.

For the simulated cases, both SFP and the efficiency of the heat exchanger have remained constant. In the case of the chiller, the humidity of the air is not changed, making using a recuperative heat exchanger unnecessary. Regenerative heat exchangers usually offer improved efficiency and would decrease the net energy need and thus the electrical energy consumed.

7.2.3 Indirect Evaporative Cooling

For the system configuration with indirect evaporative cooling, where a humidifier is installed in the return air to increase the cooling recovery, the net energy need is significantly reduced compared to the base case configuration. The net energy need is shown in Figure 6.11 and is reduced by about 40% compared to the base case. This is also visually represented in Figure 6.12.

Adding a humidifier in the supply in addition to the one in the return to utilize both direct and indirect evaporative cooling leads to an even lower energy need. The net energy need is for this system shown in Figure 6.13 and is about 64% lower than the base case. However, the system increases the PPD because it influences the supply air relative humidity, but it is still under 10%.

The consumption of water and the energy need due to the humidifier operation is not considered for the simulated case. This would likely make the solution less beneficial than what is shown but is expected to be less than the offered benefit. The water for the humidifiers is regular cold tap water which is not costly compared to the reduced energy need. One could argue that the use of tap water is a waste of drinking water. As presented in Section 4.1.1, Fantoftparken uses rainwater for indirect evaporative cooling, removing the controversy.

The use of both indirect and direct evaporative cooling looks to be a good addition to an air handling unit as it reduces the energy need significantly. If a chiller covered the remaining cooling need, the energy use would be diminished significantly compared to the original energy need.

7.2.4 Desiccant Cooling

From the simulated cases, it is clear that desiccant cooling is sufficient and manages to cool the air by altering the humidity.

The AHU configuration with desiccant cooling contains the desiccant wheel and both direct and indirect evaporative cooling. Direct and indirect evaporative cooling is operated simply by water; it is favorable to utilize the full potential of this technology before using the desiccant wheel. Simulations were run with different activation temperatures for the desiccant wheel to see the effect on energy need and thermal comfort. The activation set-point was set to 16, 18, and 20 °C. The three cases' results are shown in Figure 6.8, and as expected, the energy need is significantly reduced with increasing activation set-point. This is because fewer hours of heating are necessary, and the system utilizes direct and indirect evaporative cooling as much as possible. It is also noticed that the thermal comfort is reduced with increasing set-point due to higher humidity in the supply.

The model was also compared to its predecessor, which was only affected by the outdoor conditions. As the previous model only had one set-point for the regeneration temperature, it was expected that the energy need would be significantly reduced for the improved model. Figure 6.9 compares the previous and current model for all three activation set-points. As seen from the distribution, the energy need for the current model was as expected. This is because of the improved control of the current model, where the regeneration temperature is changed with the system's demand, decreasing the amount of heating needed.

An advantage of desiccant cooling is removing moisture without excessive cooling below the dew point. It has the ability of addressing sensible and latent heat portions separately. For the simulated case, no strict requirements were set for the relative humidity of the

supply air. A case with more strict requirements could lead to different conclusions as it would utilize the benefit of the technology.

7.3 Thermal Comfort

Figure 6.15 shows how the PPD changes with the system configuration. The systems where the relative humidity is affected on the supply side experience increased PPD. As explained in Section 2.1.1, thermal comfort is dependent on relative humidity, which explains the increase. Increasing the activation set-point for desiccant cooling also led to increased PPD. Increased set-point leads to increased use of the humidifiers, which may cause an increase in PPD. The increased set-point can also lead to more unmet hours of cooling, increasing the PPD, but the level of thermal comfort is acceptable for all set-points.

7.4 Influencing Factors

The supply temperature was kept at a constant 16 °C for all cases, which would be an interesting parameter to change and see how it would affect the results. The building was cooled using only mechanical ventilation, meaning a higher supply temperature would need an increased air flow rate to supply the same cooling power. It also means fewer hours with cooling need, which could influence the technology comparison.

Most parameters were unchanged from the default in IDA ICE, creating uncertainty when comparing the technologies. The pressure rise over both fans was kept constant for all technologies, even though the configurations contain different components. Desiccant cooling contains the desiccant wheel, which offers an additional pressure drop that the fans must cover. This expected increase in pressure drop leads to increased energy use by the fans. For the case of desiccant cooling, a recuperative heat exchanger is used to avoid the transport of moisture from return to supply. Recuperative heat exchangers like plate heat exchangers generally give a lower temperature efficiency than regenerative heat exchangers like rotating heat exchangers. For the simulated cases, the efficiency was set equal for all cases which would have an influence on the net energy need.

The efficiency of desiccant cooling depends on the outdoor conditions, which means the geographical location is significant for the results. Simulations conducted in multiple locations could give different conclusions and should be investigated further. The weather file used for this case was made from measurements for a meteorological year, which could explain why the energy need in June was so dominant compared to the other summer months.

The comparison is carried out using the energy need of the system, meaning no losses or energy produced on site is taken into account. One of the benefits of desiccant cooling is that low-grade energy like solar energy can be utilized. Further investigations on the subject would be to compare the delivered energy needed so that solar thermal collectors may be utilized. A more detailed simulation where all factors were included and the actual energy use was compared would be interesting to see how the systems perform in their entirety. The utilization of renewable energy sources for the desiccant cooling system should also be investigated.

Conclusion

An improved model of a cooling system based on a rotary desiccant wheel technology has been developed in IDA ICE. A desiccant wheel simulation tool has been used to make a regression of the wheel's performance based on four different parameters rather than two: outdoor moisture content, outdoor temperature, indoor moisture content, and regeneration temperature. The model utilizes a cooling coil to remove moisture and a heating coil for reheating to the correct enthalpy level. The implementation successfully removes moisture while keeping the enthalpy of the air constant, making the process isenthalpic as it should.

The improved model is controlled so that the regeneration temperature varies with the system's demand, minimizing the energy use and maximizing the utilization of the evaporative coolers. The original model had a constant regeneration temperature set-point, leading to unnecessary heating and poor energy efficiency compared to traditional cooling. This improved control of the regeneration heater makes the desiccant cooling system more competitive than the original. The simulations on desiccant cooling was ran for different activation set-points to fully utilize the potential of the evaporative coolers in the system. For the simulations, set-points of 16, 18, and 20 °C were considered, resulting in decreasing energy use due to regeneration with increasing set-point. Changing set-points to 18 °C and 20 °C led to a decrease in regeneration energy need of about 28% and 51% compared to the 16 °C set-point, respectively. If waste heat of distributed power generation systems or solar thermal collectors, the cooling technology can save electric energy.

Indirect evaporative cooling has also been investigated as an addition to air handling units to reduce the energy need for cooling. Altering the humidity of the return air to increase the cooling recovery showed great potential as it reduced the energy need by about 40%. Research on applied systems in Norway also showed the possibility of using rain water as the source for the humidifiers, removing both costs and drinking water concerns. Integrating a humidifier on the supply side in addition to the one in return led

to even more energy need reduction, about 64%. Water and energy costs to operate the humidifiers were not considered for this undertaking.

Regarding thermal comfort, it was clear that systems where the humidity of the supply was altered experienced slightly worse thermal comfort in terms of PPD. The maximum PPD was, however, acceptable. For the desiccant cooling system, the simulations with higher activation set-point experienced higher PPD, which could be caused by both relative humidity and unmet cooling during some conditions.

Comparing the systems, it is clear that the system with combined direct and indirect evaporative cooling showed great potential in reducing the original energy need. The improved model of desiccant cooling made the system more competitive. Further investigation should be done to compare the energy use when including both energy production on site and losses in the system. Using a chiller to supply the remaining energy need for the system with IEC and DEC will lead to significantly low energy use for cooling compared to the original energy need.

8.1 Further Work

The tested cooling technologies have been compared using simulations in IDA ICE of an office building in Trondheim. For the tests, only the net energy need has been compared for simplicity. More thorough simulations and comparisons would require a lot more work. The list below proposes ideas for further work that could be considered.

- Analyze field measurements for a desiccant cooling system to compare and improve the model.
- Compare the performance of the DW model with other manufactured products.
- Compare the different technologies for multiple locations.
- Conduct simulations for a whole meteorological year.
 - With restrict humidity levels of supply air.
- Investigate renewable energy supply for regeneration of DW.
- Compare the delivered energy needed for all technologies.
 - Include system losses and efficiencies.
 - Include water consumption and costs.

Bibliography

1. Direktoratet for byggkvalitet. Byggteknisk forskrift (TEK17). 2017. Available from: <https://dibk.no/byggereglene/byggteknisk-forskrift-tek17/>
2. Pérez-Lombard L, Ortiz J and Pout C. A review on buildings energy consumption information. *Energy and buildings* 2008; 40:394–8
3. Santamouris M. Cooling the buildings—past, present and future. *Energy and Buildings* 2016; 128:617–38
4. Birol F. The future of cooling: opportunities for energy-efficient air conditioning. International Energy Agency 2018
5. EC A. Roadmap for moving to a competitive low carbon economy in 2050. European Commission, Brussels 2011
6. Kim MH, Pettersen J and Bullard CW. Fundamental process and system design issues in CO₂ vapor compression systems. *Progress in energy and combustion science* 2004; 30:119–74
7. Jani D, Mishra M and Sahoo PK. A critical review on application of solar energy as renewable regeneration heat source in solid desiccant – vapor compression hybrid cooling system. *Journal of Building Engineering* 2018; 18:107–24. DOI: <https://doi.org/10.1016/j.jobbe.2018.03.012>. Available from: <https://www.sciencedirect.com/science/article/pii/S2352710218301050>
8. Øgreid AU. Indirect Evaporative- and Desiccant Wheel Cooling for Norwegian Office. Project report in TEP4560. Department of Energy, Process Engineering, NTNU – Norwegian University of Science and Technology, 2021 Dec
9. Ingebrigtsen S. Ventilasjonsteknikk - Del 1. Skarland press AS, 2019
10. International Standard Organization. Ergonomics of the thermal environment — Analytical determination and interpretation of thermal comfort using calculation of the PMV and PPD indices and local thermal comfort criteria. 2005

-
11. Fanger PO et al. Thermal comfort. Analysis and applications in environmental engineering. Thermal comfort. Analysis and applications in environmental engineering. 1970
 12. Arbeidstilsynet. Klima og luftkvalitet på arbeidsplassen. 2016. Available from: <https://www.arbeidstilsynet.no/contentassets/3f86f6d2038348d18540404144f76a22/luftkvalitet-pa-arbeidsplassen.pdf>
 13. Ahmed K, Akhondzada A, Kurnitski J and Olesen B. Occupancy schedules for energy simulation in new prEN16798-1 and ISO/FDIS 17772-1 standards. *Sustainable cities and society* 2017; 35:134–44
 14. Roghanchi P, Sunkpal M and Kocsis C. Understanding the human thermal balance and heat stress indices as they apply to deep and hot US mines. *Proceedings of 15th Northern American Mine Ventilation Symposium, Blacksburg VA*. 2015 :1–6
 15. International Standard Organization. Ergonomics of the thermal environment — Instruments for measuring physical quantities. 1998
 16. Høseggen RZ. Dynamic use of the building structure-energy performance and thermal environment. 2008
 17. Standard Norge. SN-NSPEK 3031:2020 Energy performance of buildings. Calculation of energy needs and energy supply. 2020
 18. Munters. The Dehumidification Handbook - Third edition. 2019
 19. Stene J. Prenøk 4.7. Revised 2016. Skarland Press AS, 1997
 20. Narayanan R. Chapter Seven - Heat-Driven Cooling Technologies. *Clean Energy for Sustainable Development*. Ed. by Rasul MG, Azad A kalam and Sharma SC. Academic Press, 2017 :191–212. DOI: <https://doi.org/10.1016/B978-0-12-805423-9.00007-7>. Available from: <https://www.sciencedirect.com/science/article/pii/B9780128054239000077>
 21. Pillai J, P.E., BEMP and Desai R. Dehumidification Strategies and their Applicability based on Climate and Building Typology. 2018
 22. Climate by Design International. Dr. Dry - Active Desiccant Dehumidification. 2017. Available from: <https://www.youtube.com/watch?v=4HzlP44M8BQ>
 23. Motaghian S and Pasdarsahri H. Regeneration energy analysis and optimization in desiccant wheels using purge mechanism. *Journal of Building Engineering* 2020; 27:100980. DOI: <https://doi.org/10.1016/j.jobe.2019.100980>. Available from: <https://www.sciencedirect.com/science/article/pii/S2352710219303584>
 24. Vårdal DV and Hvidevold HK. Fuktig luft kan erstatte kostbare kjølemaskiner. 2019. Available from: <https://nemitek.no/dan-vegard-wardal-hilde-kristine-hvidevold-kjoleanlegg/fuktig-luft-kan-erstatte-kostbare-kjolemaskiner/115601>
 25. Pennington N. Humidity changer for air conditioning. 1955
-

-
26. Ahmed M, Kattab N and Fouad M. Evaluation and optimization of solar desiccant wheel performance. *Renewable Energy* 2005; 30:305–25. DOI: <https://doi.org/10.1016/j.renene.2004.04.010>. Available from: <https://www.sciencedirect.com/science/article/pii/S0960148104001752>
 27. Su X, Tian S, Shao X and Zhang X. Experimental and numerical study on low temperature regeneration desiccant wheel: Parameter analysis with a comprehensive energy index. *International Journal of Refrigeration* 2020; 120:237–47
 28. Yu H, Mikšik F, Thu K, Miyazaki T, Ng KC et al. Effects of temperature and humidity ratio on the performance of desiccant dehumidification system under low-temperature regeneration. *Journal of Thermal Analysis and Calorimetry* 2022 :1–14
 29. Henning HM, Erpenbeck T, Hindenburg C and Santamaria I. The potential of solar energy use in desiccant cooling cycles. *International Journal of Refrigeration* 2001; 24:220–9. DOI: [https://doi.org/10.1016/S0140-7007\(00\)00024-4](https://doi.org/10.1016/S0140-7007(00)00024-4). Available from: <https://www.sciencedirect.com/science/article/pii/S0140700700000244>
 30. Ge T, Li Y, Wang R and Dai Y. Experimental study on a two-stage rotary desiccant cooling system. *International Journal of Refrigeration* 2009; 32:498–508
 31. Factor HM and Grossman G. A packed bed dehumidifier/regenerator for solar air conditioning with liquid desiccants. *Solar energy* 1980; 24:541–50
 32. Kang T and Maclaine-Cross I. High performance, solid desiccant, open cooling cycles. *J. Sol. Energy Eng.:(United States)* 1989; 111
 33. Farooq S and Ruthven D. Numerical simulation of a desiccant bed for solar air conditioning applications. 1991
 34. Nia FE, van Paassen D and Saidi MH. Modeling and simulation of desiccant wheel for air conditioning. *Energy and Buildings* 2006; 38:1230–9. DOI: <https://doi.org/10.1016/j.enbuild.2006.03.020>. Available from: <https://www.sciencedirect.com/science/article/pii/S0378778806000740>
 35. Qi R, Lu L and Huang Y. Energy performance of solar-assisted liquid desiccant air-conditioning system for commercial building in main climate zones. *Energy conversion and Management* 2014; 88:749–57
 36. Halliday S, Beggs C and Sleigh P. The use of solar desiccant cooling in the UK: a feasibility study. *Applied Thermal Engineering* 2002; 22:1327–38. DOI: [https://doi.org/10.1016/S1359-4311\(02\)00052-2](https://doi.org/10.1016/S1359-4311(02)00052-2). Available from: <https://www.sciencedirect.com/science/article/pii/S1359431102000522>
 37. Mavroudaki P, Beggs C, Sleigh P and Halliday S. The potential for solar powered single-stage desiccant cooling in southern Europe. *Applied Thermal Engineering* 2002; 22:1129–40. DOI: [https://doi.org/10.1016/S1359-4311\(02\)00034-0](https://doi.org/10.1016/S1359-4311(02)00034-0). Available from: <https://www.sciencedirect.com/science/article/pii/S1359431102000340>
-

-
38. Zhou X. Thermal and energy performance of a solar-driven desiccant cooling system using an internally cooled desiccant wheel in various climate conditions. *Applied Thermal Engineering* 2021; 185:116077
 39. Daou K, Wang R and Xia Z. Desiccant cooling air conditioning: a review. *Renewable and Sustainable Energy Reviews* 2006; 10:55–77
 40. Granstrand A. Munters: Sorptiv kjøling - DesiCool. 2021
 41. Ge T, Dai Y and Wang R. Review on solar powered rotary desiccant wheel cooling system. *Renewable and Sustainable Energy Reviews* 2014; 39:476–97. DOI: <https://doi.org/10.1016/j.rser.2014.07.121>. Available from: <https://www.sciencedirect.com/science/article/pii/S1364032114005735>
 42. Angrisani G, Minichiello F, Roselli C and Sasso M. Experimental analysis on the performances of a desiccant wheel regenerated by low grade thermal energy. *International Sorption Heat Pump Conference*. Vol. 2. 1. IIR/AICARR. 2011 :733–44
 43. Zhang J, Ge T, Dai Y, Zhao Y and Wang R. Experimental investigation on solar powered desiccant coated heat exchanger humidification air conditioning system in winter. *Energy* 2017; 137:468–78
 44. Dezfouli M, Mat S, Pirasteh G, Sahari K, Sopian K and Ruslan M. Simulation analysis of the four configurations of solar desiccant cooling system using evaporative cooling in tropical weather in Malaysia. *International Journal of Photoenergy* 2014; 2014
 45. Angrisani G, Roselli C, Sasso M and Tariello F. Dynamic performance assessment of a micro-trigeneration system with a desiccant-based air handling unit in Southern Italy climatic conditions. *Energy conversion and management* 2014; 80:188–201
 46. De Antonellis S, Joppolo CM, Molinaroli L and Pasini A. Simulation and energy efficiency analysis of desiccant wheel systems for drying processes. *Energy* 2012; 37:336–45
 47. Nehasil O and Adamovsk D. Experimental Verification of Indirect Adiabatic Cooling by Ventilation Air. *IOP Conference Series: Earth and Environmental Science*. Vol. 290. 1. IOP Publishing. 2019 :012104
 48. Maheshwari G, Al-Ragom F and Suri R. Energy-saving potential of an indirect evaporative cooler. *Applied Energy* 2001; 69:69–76
 49. Porumb B, Ungureşan P, Tutunaru LF, Şerban A and Bălan M. A Review of Indirect Evaporative Cooling Technology. *Energy Procedia* 2016; 85. EENVIRO-YRC 2015 - Bucharest:461–71. DOI: <https://doi.org/10.1016/j.egypro.2015.12.228>. Available from: <https://www.sciencedirect.com/science/article/pii/S1876610215028933>
 50. Dean J and Metzger I. Multistaged indirect evaporative cooler evaluation. National Renewable Energy Laboratory, 2014
-

-
51. Amer O, Boukhanouf R and Ibrahim H. A review of evaporative cooling technologies. *International journal of environmental science and development* 2015; 6:111
 52. EQUA Simulation AB. IDA Indoor Climate and Energy. Available from: <https://www.equa.se/en/ida-ice>
 53. Sande M. Ventilative Cooling Potential of the ZEB Laboratory. MA thesis. NTNU, 2021
 54. NovelAire. DW Web Application. Available from: <https://novtools.novelaire.com/DWWebApp.aspx>
 55. Munters. DesiCool product brochure. Available from: https://www.munters.com/globalassets/inriver/resources/desicool_product_brochure.pdf
 56. Yu F and Chan K. Experimental determination of the energy efficiency of an air-cooled chiller under part load conditions. *Energy* 2005; 30:1747–58. DOI: <https://doi.org/10.1016/j.energy.2004.11.007>. Available from: <https://www.sciencedirect.com/science/article/pii/S0360544204004876>

Appendix **A**

Appendix

A.1 Regression with four independent variables

A regression equation with four independent variables may be written as:

$$Y = a + b_1X_1 + b_2X_2 + b_3X_3 + b_4X_4$$

where:

Y : Observed score

a : Intercept

b : Slope

X : Observed score on independent variable

A.1.1 Moisture removal

Removed moisture [kg/kg]	Outdoor temperature [C]	Outdoor moisture [kg/kg]	Indoor moisture [kg/kg]	Regeneration temperature [C]
2,45E-03	16,5	5,79E-03	1,20E-02	55
2,35E-03	17,5	5,79E-03	1,20E-02	55
2,24E-03	18,5	5,79E-03	1,20E-02	55
2,13E-03	19,5	5,79E-03	1,20E-02	55
2,03E-03	20,5	5,79E-03	1,20E-02	55
1,92E-03	21,5	5,79E-03	1,20E-02	55
1,81E-03	22,5	5,79E-03	1,20E-02	55
1,70E-03	23,5	5,79E-03	1,20E-02	55
1,59E-03	24,5	5,79E-03	1,20E-02	55

Removed moisture [kg/kg]	Outdoor temperature [C]	Outdoor moisture [kg/kg]	Indoor moisture [kg/kg]	Regeneration temperature [C]
1,48E-03	25,5	5,79E-03	1,20E-02	55
1,36E-03	26,5	5,79E-03	1,20E-02	55
1,25E-03	27,5	5,79E-03	1,20E-02	55
1,13E-03	28,5	5,79E-03	1,20E-02	55
1,02E-03	29,5	5,79E-03	1,20E-02	55
9,00E-04	30,5	5,79E-03	1,20E-02	55
4,45E-03	21,7	1,07E-02	1,20E-02	55
3,99E-03	21,7	9,70E-03	1,20E-02	55
3,50E-03	21,7	8,70E-03	1,20E-02	55
2,97E-03	21,7	7,70E-03	1,20E-02	55
2,42E-03	21,7	6,70E-03	1,20E-02	55
1,85E-03	21,7	5,70E-03	1,20E-02	55
4,88E-03	21,7	1,17E-02	1,20E-02	55
5,40E-04	21,3	3,57E-03	1,20E-02	55
2,82E-03	16,5	5,79E-03	1,00E-02	55
2,72E-03	17,5	5,79E-03	1,00E-02	55
2,63E-03	18,5	5,79E-03	1,00E-02	55
2,53E-03	19,5	5,79E-03	1,00E-02	55
2,43E-03	20,5	5,79E-03	1,00E-02	55
2,33E-03	21,5	5,79E-03	1,00E-02	55
2,23E-03	22,5	5,79E-03	1,00E-02	55
2,12E-03	23,5	5,79E-03	1,00E-02	55
2,00E-03	24,5	5,79E-03	1,00E-02	55
1,90E-03	25,5	5,79E-03	1,00E-02	55
1,79E-03	26,5	5,79E-03	1,00E-02	55
1,68E-03	27,5	5,79E-03	1,00E-02	55
1,58E-03	28,5	5,79E-03	1,00E-02	55
1,46E-03	29,5	5,79E-03	1,00E-02	55
1,35E-03	30,5	5,79E-03	1,00E-02	55
4,89E-03	21,7	1,07E-02	1,00E-02	55
4,43E-03	21,7	9,70E-03	1,00E-02	55
3,92E-03	21,7	8,70E-03	1,00E-02	55
3,40E-03	21,7	7,70E-03	1,00E-02	55
2,84E-03	21,7	6,70E-03	1,00E-02	55
2,25E-03	21,7	5,70E-03	1,00E-02	55
5,53E-03	21,7	1,17E-02	1,00E-02	55
9,10E-04	21,3	3,57E-03	1,00E-02	55
3,21E-03	16,5	5,79E-03	8,00E-04	55
3,13E-03	17,5	5,79E-03	8,00E-04	55

Removed moisture [kg/kg]	Outdoor temperature [C]	Outdoor moisture [kg/kg]	Indoor moisture [kg/kg]	Regeneration temperature [C]
3,04E-03	18,5	5,79E-03	8,00E-04	55
2,95E-03	19,5	5,79E-03	8,00E-04	55
2,86E-03	20,5	5,79E-03	8,00E-04	55
2,76E-03	21,5	5,79E-03	8,00E-04	55
2,65E-03	22,5	5,79E-03	8,00E-04	55
2,55E-03	23,5	5,79E-03	8,00E-04	55
2,46E-03	24,5	5,79E-03	8,00E-04	55
2,36E-03	25,5	5,79E-03	8,00E-04	55
2,26E-03	26,5	5,79E-03	8,00E-04	55
2,15E-03	27,5	5,79E-03	8,00E-04	55
2,05E-03	28,5	5,79E-03	8,00E-04	55
1,95E-03	29,5	5,79E-03	8,00E-04	55
1,84E-03	30,5	5,79E-03	8,00E-04	55
5,37E-03	21,7	1,07E-02	8,00E-04	55
4,87E-03	21,7	9,70E-03	8,00E-04	55
4,38E-03	21,7	8,70E-03	8,00E-04	55
3,85E-03	21,7	7,70E-03	8,00E-04	55
3,29E-03	21,7	6,70E-03	8,00E-04	55
2,69E-03	21,7	5,70E-03	8,00E-04	55
5,81E-03	21,7	1,17E-02	8,00E-04	55
1,30E-03	21,3	3,57E-03	8,00E-04	55
2,09E-03	16,5	5,79E-03	1,40E-02	55
1,98E-03	17,5	5,79E-03	1,40E-02	55
1,88E-03	18,5	5,79E-03	1,40E-02	55
1,77E-03	19,5	5,79E-03	1,40E-02	55
1,65E-03	20,5	5,79E-03	1,40E-02	55
1,54E-03	21,5	5,79E-03	1,40E-02	55
1,43E-03	22,5	5,79E-03	1,40E-02	55
1,31E-03	23,5	5,79E-03	1,40E-02	55
1,19E-03	24,5	5,79E-03	1,40E-02	55
1,08E-03	25,5	5,79E-03	1,40E-02	55
9,60E-04	26,5	5,79E-03	1,40E-02	55
8,40E-04	27,5	5,79E-03	1,40E-02	55
7,20E-04	28,5	5,79E-03	1,40E-02	55
5,90E-04	29,5	5,79E-03	1,40E-02	55
4,70E-04	30,5	5,79E-03	1,40E-02	55
4,02E-03	21,7	1,07E-02	1,40E-02	55
3,57E-03	21,7	9,70E-03	1,40E-02	55
3,09E-03	21,7	8,70E-03	1,40E-02	55

Removed moisture [kg/kg]	Outdoor temperature [C]	Outdoor moisture [kg/kg]	Indoor moisture [kg/kg]	Regeneration temperature [C]
2,58E-03	21,7	7,70E-03	1,40E-02	55
2,03E-03	21,7	6,70E-03	1,40E-02	55
1,46E-03	21,7	5,70E-03	1,40E-02	55
4,46E-03	21,7	1,17E-02	1,40E-02	55
1,90E-04	21,3	3,57E-03	1,40E-02	55
1,47E-03	16,5	5,79E-03	1,20E-02	45
1,36E-03	17,5	5,79E-03	1,20E-02	45
1,24E-03	18,5	5,79E-03	1,20E-02	45
1,12E-03	19,5	5,79E-03	1,20E-02	45
1,00E-03	20,5	5,79E-03	1,20E-02	45
8,70E-04	21,5	5,79E-03	1,20E-02	45
7,50E-04	22,5	5,79E-03	1,20E-02	45
6,20E-04	23,5	5,79E-03	1,20E-02	45
5,00E-04	24,5	5,79E-03	1,20E-02	45
3,70E-04	25,5	5,79E-03	1,20E-02	45
2,50E-04	26,5	5,79E-03	1,20E-02	45
1,20E-04	27,5	5,79E-03	1,20E-02	45
-1,00E-05	28,5	5,79E-03	1,20E-02	45
-1,40E-04	29,5	5,79E-03	1,20E-02	45
-2,60E-04	30,5	5,79E-03	1,20E-02	45
3,14E-03	21,7	1,07E-02	1,20E-02	45
2,73E-03	21,7	9,70E-03	1,20E-02	45
2,28E-03	21,7	8,70E-03	1,20E-02	45
1,81E-03	21,7	7,70E-03	1,20E-02	45
1,32E-03	21,7	6,70E-03	1,20E-02	45
8,00E-04	21,7	5,70E-03	1,20E-02	45
3,54E-03	21,7	1,17E-02	1,20E-02	45
-3,70E-04	21,3	3,57E-03	1,20E-02	45
1,92E-03	16,5	5,79E-03	1,00E-02	45
1,81E-03	17,5	5,79E-03	1,00E-02	45
1,70E-03	18,5	5,79E-03	1,00E-02	45
1,58E-03	19,5	5,79E-03	1,00E-02	45
1,46E-03	20,5	5,79E-03	1,00E-02	45
1,35E-03	21,5	5,79E-03	1,00E-02	45
1,23E-03	22,5	5,79E-03	1,00E-02	45
1,12E-03	23,5	5,79E-03	1,00E-02	45
9,90E-04	24,5	5,79E-03	1,00E-02	45
8,70E-04	25,5	5,79E-03	1,00E-02	45
7,50E-04	26,5	5,79E-03	1,00E-02	45

Removed moisture [kg/kg]	Outdoor temperature [C]	Outdoor moisture [kg/kg]	Indoor moisture [kg/kg]	Regeneration temperature [C]
6,30E-04	27,5	5,79E-03	1,00E-02	45
5,10E-04	28,5	5,79E-03	1,00E-02	45
3,90E-04	29,5	5,79E-03	1,00E-02	45
2,70E-04	30,5	5,79E-03	1,00E-02	45
3,66E-03	21,7	1,07E-02	1,00E-02	45
3,22E-03	21,7	9,70E-03	1,00E-02	45
2,78E-03	21,7	8,70E-03	1,00E-02	45
2,31E-03	21,7	7,70E-03	1,00E-02	45
1,81E-03	21,7	6,70E-03	1,00E-02	45
1,28E-03	21,7	5,70E-03	1,00E-02	45
4,06E-03	21,7	1,17E-02	1,00E-02	45
8,00E-05	21,3	3,57E-03	1,00E-02	45
2,41E-03	16,5	5,79E-03	8,00E-04	45
2,29E-03	17,5	5,79E-03	8,00E-04	45
2,19E-03	18,5	5,79E-03	8,00E-04	45
2,08E-03	19,5	5,79E-03	8,00E-04	45
1,98E-03	20,5	5,79E-03	8,00E-04	45
1,87E-03	21,5	5,79E-03	8,00E-04	45
1,75E-03	22,5	5,79E-03	8,00E-04	45
1,64E-03	23,5	5,79E-03	8,00E-04	45
1,53E-03	24,5	5,79E-03	8,00E-04	45
1,42E-03	25,5	5,79E-03	8,00E-04	45
1,30E-03	26,5	5,79E-03	8,00E-04	45
1,19E-03	27,5	5,79E-03	8,00E-04	45
1,08E-03	28,5	5,79E-03	8,00E-04	45
9,50E-04	29,5	5,79E-03	8,00E-04	45
8,40E-04	30,5	5,79E-03	8,00E-04	45
4,19E-03	21,7	1,07E-02	8,00E-04	45
3,77E-03	21,7	9,70E-03	8,00E-04	45
3,32E-03	21,7	8,70E-03	8,00E-04	45
2,85E-03	21,7	7,70E-03	8,00E-04	45
2,34E-03	21,7	6,70E-03	8,00E-04	45
1,80E-03	21,7	5,70E-03	8,00E-04	45
4,59E-03	21,7	1,17E-02	8,00E-04	45
5,60E-04	21,3	3,57E-03	8,00E-04	45
1,06E-03	16,5	5,79E-03	1,40E-02	45
9,30E-04	17,5	5,79E-03	1,40E-02	45
8,10E-04	18,5	5,79E-03	1,40E-02	45
6,80E-04	19,5	5,79E-03	1,40E-02	45

Removed moisture [kg/kg]	Outdoor temperature [C]	Outdoor moisture [kg/kg]	Indoor moisture [kg/kg]	Regeneration temperature [C]
5,60E-04	20,5	5,79E-03	1,40E-02	45
4,30E-04	21,5	5,79E-03	1,40E-02	45
3,00E-04	22,5	5,79E-03	1,40E-02	45
1,70E-04	23,5	5,79E-03	1,40E-02	45
4,00E-05	24,5	5,79E-03	1,40E-02	45
-9,00E-05	25,5	5,79E-03	1,40E-02	45
-2,30E-04	26,5	5,79E-03	1,40E-02	45
-3,50E-04	27,5	5,79E-03	1,40E-02	45
-4,90E-04	28,5	5,79E-03	1,40E-02	45
-6,20E-04	29,5	5,79E-03	1,40E-02	45
-7,50E-04	30,5	5,79E-03	1,40E-02	45
2,67E-03	21,7	1,07E-02	1,40E-02	45
2,25E-03	21,7	9,70E-03	1,40E-02	45
1,82E-03	21,7	8,70E-03	1,40E-02	45
1,36E-03	21,7	7,70E-03	1,40E-02	45
8,70E-04	21,7	6,70E-03	1,40E-02	45
3,60E-04	21,7	5,70E-03	1,40E-02	45
3,06E-03	21,7	1,17E-02	1,40E-02	45
-7,80E-04	21,3	3,57E-03	1,40E-02	45
3,00E-04	16,5	5,79E-03	1,20E-02	35
2,00E-04	17,5	5,79E-03	1,20E-02	35
-9,00E-05	19,5	5,79E-03	1,20E-02	35
-2,20E-04	20,5	5,79E-03	1,20E-02	35
-3,60E-04	21,5	5,79E-03	1,20E-02	35
-4,90E-04	22,5	5,79E-03	1,20E-02	35
-6,20E-04	23,5	5,79E-03	1,20E-02	35
-7,60E-04	24,5	5,79E-03	1,20E-02	35
-8,90E-04	25,5	5,79E-03	1,20E-02	35
-1,03E-03	26,5	5,79E-03	1,20E-02	35
-1,17E-03	27,5	5,79E-03	1,20E-02	35
-1,30E-03	28,5	5,79E-03	1,20E-02	35
-1,43E-03	29,5	5,79E-03	1,20E-02	35
-1,57E-03	30,5	5,79E-03	1,20E-02	35
1,68E-03	21,7	1,07E-02	1,20E-02	35
1,30E-03	21,7	9,70E-03	1,20E-02	35
9,00E-04	21,7	8,70E-03	1,20E-02	35
4,80E-04	21,7	7,70E-03	1,20E-02	35
4,00E-05	21,7	6,70E-03	1,20E-02	35
-4,30E-04	21,7	5,70E-03	1,20E-02	35

Removed moisture [kg/kg]	Outdoor temperature [C]	Outdoor moisture [kg/kg]	Indoor moisture [kg/kg]	Regeneration temperature [C]
2,04E-03	21,7	1,17E-02	1,20E-02	35
1,46E-03	21,3	3,57E-03	1,20E-02	35
8,20E-04	16,5	5,79E-03	1,00E-02	35
7,00E-04	17,5	5,79E-03	1,00E-02	35
5,70E-04	18,5	5,79E-03	1,00E-02	35
4,40E-04	19,5	5,79E-03	1,00E-02	35
3,20E-04	20,5	5,79E-03	1,00E-02	35
1,90E-04	21,5	5,79E-03	1,00E-02	35
6,00E-05	22,5	5,79E-03	1,00E-02	35
-7,00E-05	23,5	5,79E-03	1,00E-02	35
-2,00E-04	24,5	5,79E-03	1,00E-02	35
-3,30E-04	25,5	5,79E-03	1,00E-02	35
-4,60E-04	26,5	5,79E-03	1,00E-02	35
-5,90E-04	27,5	5,79E-03	1,00E-02	35
-7,10E-04	28,5	5,79E-03	1,00E-02	35
-8,40E-04	29,5	5,79E-03	1,00E-02	35
-9,70E-04	30,5	5,79E-03	1,00E-02	35
2,25E-03	21,7	1,07E-02	1,00E-02	35
1,87E-03	21,7	9,70E-03	1,00E-02	35
1,46E-03	21,7	8,70E-03	1,00E-02	35
1,04E-03	21,7	7,70E-03	1,00E-02	35
5,90E-04	21,7	6,70E-03	1,00E-02	35
1,20E-04	21,7	5,70E-03	1,00E-02	35
2,61E-03	21,7	1,17E-02	1,00E-02	35
-9,40E-04	21,3	3,57E-03	1,00E-02	35
1,38E-03	16,5	5,79E-03	8,00E-04	35
1,26E-03	17,5	5,79E-03	8,00E-04	35
1,14E-03	18,5	5,79E-03	8,00E-04	35
1,02E-03	19,5	5,79E-03	8,00E-04	35
9,00E-04	20,5	5,79E-03	8,00E-04	35
7,80E-04	21,5	5,79E-03	8,00E-04	35
6,60E-04	22,5	5,79E-03	8,00E-04	35
5,40E-04	23,5	5,79E-03	8,00E-04	35
4,20E-04	24,5	5,79E-03	8,00E-04	35
3,00E-04	25,5	5,79E-03	8,00E-04	35
1,70E-04	26,5	5,79E-03	8,00E-04	35
5,00E-05	27,5	5,79E-03	8,00E-04	35
-7,00E-05	28,5	5,79E-03	8,00E-04	35
-1,90E-04	29,5	5,79E-03	8,00E-04	35

Removed moisture [kg/kg]	Outdoor temperature [C]	Outdoor moisture [kg/kg]	Indoor moisture [kg/kg]	Regeneration temperature [C]
-3,10E-04	30,5	5,79E-03	8,00E-04	35
2,85E-03	21,7	1,07E-02	8,00E-04	35
2,47E-03	21,7	9,70E-03	8,00E-04	35
2,07E-03	21,7	8,70E-03	8,00E-04	35
1,64E-03	21,7	7,70E-03	8,00E-04	35
1,19E-03	21,7	6,70E-03	8,00E-04	35
7,20E-04	21,7	5,70E-03	8,00E-04	35
3,22E-03	21,7	1,17E-02	8,00E-04	35
-3,80E-04	21,3	3,57E-03	8,00E-04	35
-1,80E-04	16,5	5,79E-03	1,40E-02	35
-3,40E-04	17,5	5,79E-03	1,40E-02	35
-4,50E-04	18,5	5,79E-03	1,40E-02	35
-5,80E-04	19,5	5,79E-03	1,40E-02	35
-7,20E-04	20,5	5,79E-03	1,40E-02	35
-8,60E-04	21,5	5,79E-03	1,40E-02	35
-1,00E-03	22,5	5,79E-03	1,40E-02	35
-1,14E-03	23,5	5,79E-03	1,40E-02	35
-1,28E-03	24,5	5,79E-03	1,40E-02	35
-1,42E-03	25,5	5,79E-03	1,40E-02	35
-1,56E-03	26,5	5,79E-03	1,40E-02	35
-1,70E-03	27,5	5,79E-03	1,40E-02	35
-1,84E-03	28,5	5,79E-03	1,40E-02	35
-1,98E-03	29,5	5,79E-03	1,40E-02	35
-2,11E-03	30,5	5,79E-03	1,40E-02	35
1,15E-03	21,7	1,07E-02	1,40E-02	35
7,70E-04	21,7	9,70E-03	1,40E-02	35
3,80E-04	21,7	8,70E-03	1,40E-02	35
-4,00E-05	21,7	7,70E-03	1,40E-02	35
-4,70E-04	21,7	6,70E-03	1,40E-02	35
-9,30E-04	21,7	5,70E-03	1,40E-02	35
1,51E-03	21,7	1,17E-02	1,40E-02	35
-8,30E-04	21,3	3,57E-03	1,40E-02	35

Table A.1: Inputs and outputs from desiccant wheel simulation.

The regression equation ends up being:

$$Y' = -3.21 \cdot 10^{-3} + (-1,21 \cdot 10^{-4}) \cdot X_1 + (4.70 \cdot 10^{-1}) \cdot X_2 + (-9.90 \cdot 10^{-2}) \cdot X_3 + (1.13 \cdot 10^{-4}) \cdot X_4$$

where:

Y' : Removed moisture content [kg_w/kg_{da}]

X_1 : Outdoor temperature [°C]

X_2 : Outdoor moisture content [kg_w/kg_{da}]

X_3 : Indoor moisture content [kg_w/kg_{da}]

X_4 : Regeneration temperature [°C]

Plotting the actual values vs. the predicted values gives the following graph.

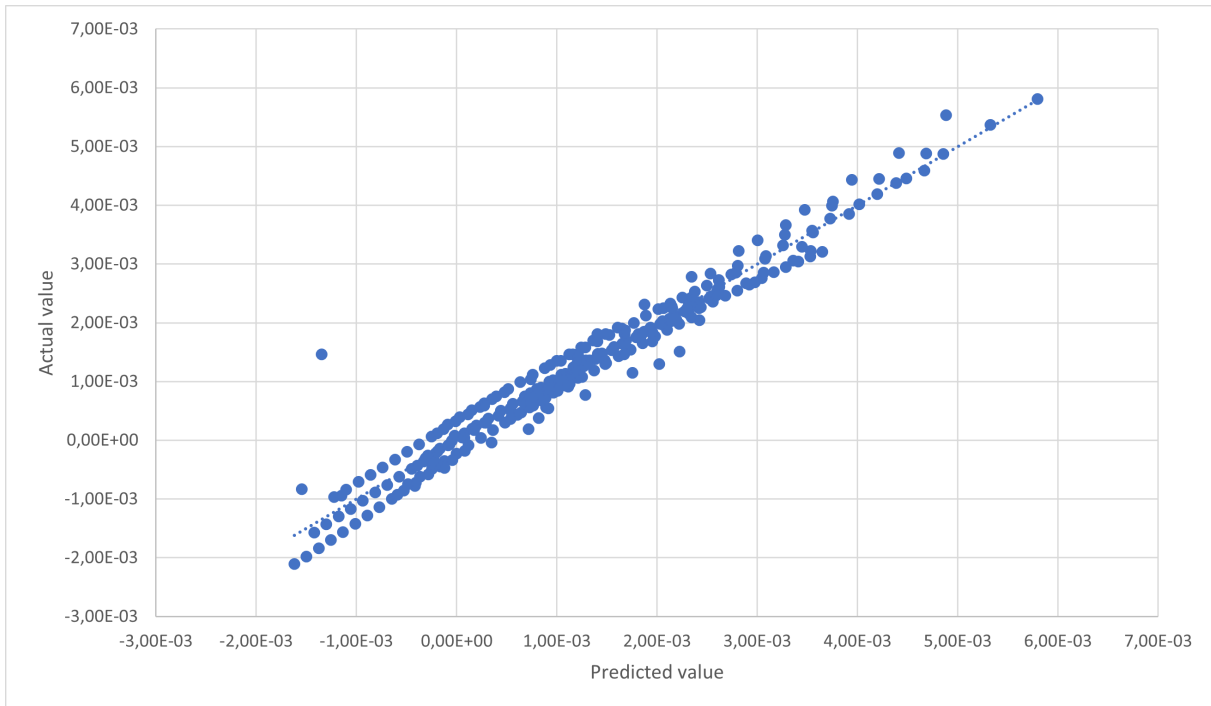


Figure A.1: Scatterplot of predicted vs. actual values

Statistics	
Multiple R	0,980
R square	0,961
Adjusted R square	0,960
Standard error	0,000299

Table A.2: Statistics from regression analysis.

